Gasification, Liquefaction and Deoxy-Liquefaction of Switchgrass using Sub- and Supercritical Water

by

Hema Ramsurn

A dissertation submitted to the Graduate Faculty of
Auburn University
in partial fulfillment of the
requirements for the Degree of
Doctor of Philosophy

Auburn, Alabama
August 03, 2013

Keywords:biomass, hydrothermal, gasification, liquefaction, hydrogen, deoxygenation

Approved by

Ram B. Gupta, Chair, Professor of Chemical Engineering
Yoon Y. Lee, Professor of Chemical Engineering
Steve R. Duke, Associate Professor of Chemical Engineering
Oladiran Fasina, Associate Professor of Biosystem Engineering

Abstract

Increased demand in transportation fuels, environmental concerns and depletion of fossil fuel require development of efficient conversion technologies for second-generation biofuels. In this dissertation, sub- and supercritical water have been used as the medium to transform biomass (here, switchgrass) into biochar, syngas, and biocrude through carbonization, gasification, liquefaction and deoxy-liquefaction. The challenges with thermal gasification of biomass to produce syngas include high transportation and drying costs of biomass, the need for high temperature (700-1000 ^{o}C) gasifiers and conditioning of the produced gases. Some of these challenges can be addressed by first converting biomass into high-energy-density biochar before transportation, and then hydrothermal gasification of biochar at the site of Fischer-Tropsch plant for liquid fuels synthesis. In the first part of this work (Chapter 2), a high-energy density (> 27 MJ/kg) biochar is first produced via hydrothermal carbonization of switchgrass at 300 ^{o}C, and then the biochar is gasified in hydrothermal medium at 400-650 °C. The carbon gasification efficiency in hydrothermal medium is much better than that in the thermal medium. For example, at 550 °C, only 5.9% carbon gasification is achieved in the thermal medium as compared to 23.8% in hydrothermal medium. The addition of 25 wt% K_2CO_3 catalyst enhances the hydrothermal gasification to 43.8%. The gasification can be further enhanced if the biochar is passivated with a small amount of $Ca(OH)_2$ when producing from biomass. The use of $Ca(OH)_2$ passivation during hydrothermal

carbonization coupled with the use of K_2CO_3 catalysis during hydrothermal gasification with short reaction times of 5 and 30 minutes, respectively result in a high carbon gasification efficiency of 75% at 600 °C. The heating value of the syngas obtained increased with passivation (due to enhanced gasification) and was comparable to that obtained from low-grade coal gasification.

Apart from producing syngas, biomass can also be liquefied into energy-dense biocrude. In Chapter 3, a novel two-step process is proposed in which acidic subcritical-water followed by alkaline supercritical-water media are utilized for the liquefaction. The concept is tested with switchgrass. The first step is carried out at 200 °C in acidic subcritical water to liquefy hemicelluloses to biocrude. In the second step, the remaining un-liquefied biomass (biomass-H) is subjected to supercritical water at 380 °C with $Ca(OH)_2$ as catalyst for minimizing the formation of char, enhancing lignin solubilization and therefore increasing liquefaction of the remaining polysaccharides toward biocrude. The extraction of biocrude from the first step before subjecting the unliquefied biomass to the second step is very crucial. It avoids repolymerisation reactions between the hemicelluloses degradation products and lignin degradation products which would have resulted in char. The proposed two-step liquefaction produces significantly higher amount of biocrude as compared to the traditional one-step process. The yield of biocrude from the proposed process is 40% on mass basis and 67% on energy basis of the feedstock biomass.

The biocrude obtained from hydrothermal liquefaction has to be upgraded to be able to be used as a “drop-in” fuel. In the last part of this work, switchgrass was liquefied in supercritical water (SCW) using calcium formate as an *in-situ* source of hydrogen to

enhance its deoxygenation and hence improve the quality of the biocrude obtained. In supercritical water, calcium formate produces hydrogen via decomposition and hydrolysis reactions, and simultaneously switchgrass hydrolyzes to form oxygenated hydrocarbon compounds from cellulose, hemicelluloses, and lignin. Because of the close proximity of the newly-formed hydrogen and active oxygenated hydrocarbons, hydrodeoxygenation occurs whereby some of the oxygenated compounds are upgraded by the removal of oxygen in the form of water. The analysis of the biocrude, obtained in the presence of calcium formate, shows the presence of benzene, polyaromatic hydrocarbons, and alkyl phenolics as opposed to alkoxy phenolic compounds (obtained without formate addition). The benzene formation is attributed to the hydrogenation of phenols (from lignin decomposition) but also due to the Diels-Alder alkene addition (alkenes formed by liquefaction of unsaturated triglycerides), followed by dehydrogenation. The addition of calcium formate doubles the yield of oily biocrude to about 10 wt% and increases the heating value from 28 to 34 kJ/g. The content of formic acid increases in the aqueous biocrude (biocrude-W) due to the enhanced decomposition of xylose and glucose. This study has therefore used a low-value catalyst to increase the energy content of the upgraded biocrude by 20% in a simple one-pot reaction.

Acknowledgments

I would like to thank, my advisor, Dr. Ram B. Gupta for his guidance and support during my dissertation work. I would like to express my sincere thanks to the committee members: Dr. Yoon Y. Lee, Dr. Steve R. Duke and Dr. Oladiran Fasina, for their valuable comments and suggestions and Dr Sushil Adhikari for having graciously accepted to be my outside reader.

A special thanks to the chemical engineering staff, Karen Cochran, Sue Allen, Georgetta Dennis, and Jennifer Harris for helping me with logistic, academic and financial matters. I would also like to acknowledge Brian Schwieker, our engineering technician, who has always gone out of his way to help me.

My group colleagues Dr. Courtney Ann Ober, Shaima Nahreen, Emmanuel Nyankson and Richard Cullum deserve special appreciation for their assistance and cooperation in making our experience in the laboratory enjoyable but fruitful. I would like to acknowledge Dr. Sandeep Kumar for the collaborative work presented in Chapter 2 as well as my former lab group members, Dr. Lingzhao Kong and Dr. Adam Byrd, for their assistance in the laboratory. I would also like to thank the “Roberts” group, especially Jennifer Duggan, for their friendship that made my journey here so enjoyable.

My gratitude goes to my husband, Nishal, my parents and family who have always believed in me and supported me in all my endeavors. My son Nikhil, whose smile and silly jokes, has kept me going through some tough times. Finally, a special

dedication to Prof Subhash Sinha for having introduced me to Auburn University and encouraged me through my years here at Auburn.

Last but not least, I want to thank the National Science Foundation (NSF-CBET-0828269), Alabama Center for Paper and Bioresource Engineering, and the U.S. Department of Energy (DE-FC26-05NT42456) for funding this research.

Table of Contents

List of Tables

List of Figures

List of Abbreviations

1,2-PDO	1,2-propanediol
APR	Aqueous Phase Reforming
DMF	Dimethylfuran
DP	Deposition-Precipitation
EPAct	Energy Policy Act
FA	Formic Acid
FAEEs	Fatty Acid Ethyl Esters
FCC	Fluid Catalytic Cracking
FFA	Furan and Furfuryl Alcohol
FT	Fischer-Tropsch
FTIR	Fourier Transform Infrared
GC	Gas Chromatography
GC-MS	Gas Chromatograph Mass Spectrometer
GUAs	Guaiacols
GBL	γ-butyrolactone
GVL	ɤ-valerolactone
HDM	Hydrodemetallization
HDN	Hydrodenitrogenation

HDO	Hydrodeoxygenation
HDS	Hydrodesulphurization
HHV	High Heating Value
HMF	5-(Hydroxymethyl)furfural
HPLC	High-Pressure Liquid Chromatography
HTU	Hydrothermal Upgrading
HYD	Hydrogenation
HZSM-5	The zeolite (see ZSM-5) ion exchange sites are occupied by H^+ ions
ID	Identity
m/z	mass per charge
MCM-41	Mesoporous molecular sieves
NMR	Nuclear Magnetic Resonance
NPs	Nanoparticles
PAHs	Polycyclic Aromatic Hydrocarbons
PNL/PNNL	Pacific Northwest National Laboratory
PVP	Poly(vinylpyrrolidone)
R&D	Research & Development
SA	Succinic Acid
SBA-15	ordered mesoporous silica
SCW	Supercritical Water
SCWG	Supercritical Water Gasification
SEM	Scanning Electron Microscope
SMNPs	Supported Metal Nanoparticles

TGA	Thermogravimetric Analysis
THF	Tetrahydrofuran
TOC	Total Organic Carbon
TORs	Turnover Rates
WGS	Water Gas Shift
WHSV	Weight Hourly Space Velocity
XAS	X-ray Absorption Spectroscopy
XPS	X-ray Photoelectron Spectroscopy
XRD	X-Ray Diffractometer
ZSM-5	Zeolite Socony Mobil–5

Chapter 1

Introduction

1.1 Biofuels: the Future of Transportation

Considerable effort has been directed to develop processes producing liquid fuels from biomass since global energy consumption is on the rise and the limited fossil fuel reserves are being exhausted. With the haphazard price fluctuations of fossil fuels, the question of fossil oil dependability as the primary energy fuel is also being raised.[1] According to the annual review from the US Energy Information Administration,[2] in 2012, transportation sector accounted for about 30% of the total energy consumption in the US . According to the same source, almost 20% of the world's total delivered energy is used in the transportation sector, where liquid fuels are the dominant source. Transportation alone accounts for more than 50% of the world's consumption of liquid fuels, and its share will increase over the projection period as shown in the Figure 1.1. It is predicted that the transportation share of total liquid fuels consumption will account to 61 % in 2035, while the share of other end-use sectors will be on the decline.

Biomass, one of the largest primary energy resources, is therefore regarded as one of the alternatives for the production of transportation fuels. Biomass is considered "clean" due to its negligible sulphur, nitrogen and ash content resulting in lower SO_x, NO_x and soot emissions when compared to conventional fuels.[3] Furthermore, since the

released CO_2 will be recycled into plants by photosynthesis, the use of biomass results in zero net emission of CO_2 and hence less greenhouse effect.

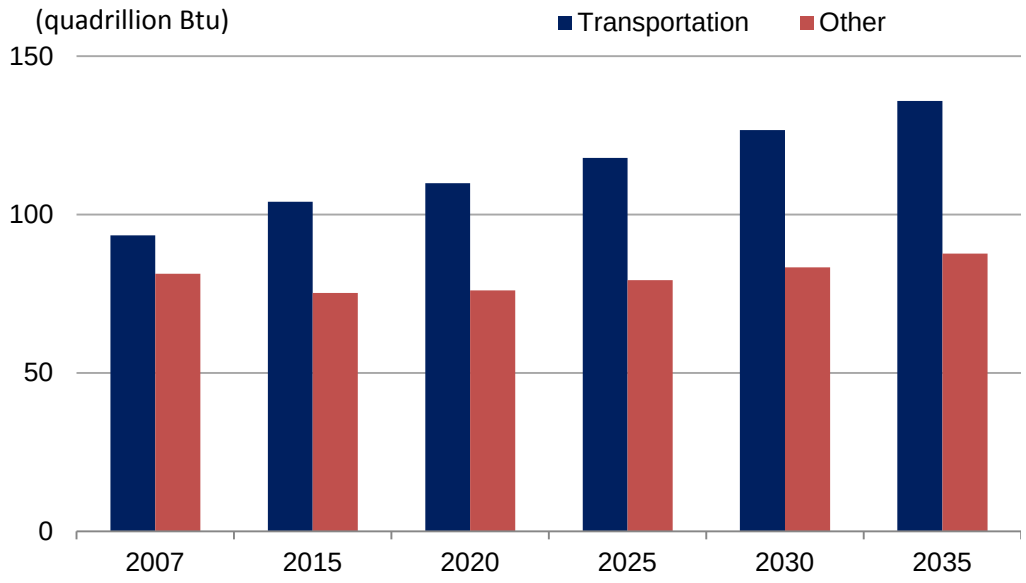

Figure 1.1 World liquid fuels consumption, 2007-2035 (quadrillion Btu)[4]

The use of biomass as an energy source would not only reduce the dependency on fossil fuels but also reduce the amount of CO_2 emissions to the atmosphere, promote regional engineering, increase R&D and create employment, among other benefits. Furthermore, according to the Renewable Fuel Standard program, created under the Energy Policy Act (EPAct) of 2005, the United States is mandated to blend 36 billion gallons of renewable fuels into transportation fuel by 2022.[5] It is hence imperative to explore means and ways to convert biomass to biofuels whose demand is already on the rise.

1.2 Structure of Biomass

The term 'biofuel' usually refers to any solid, liquid or gaseous fuel predominantly produced from biomass. Liquid biofuel includes bioalcohols, vegetable

oils, biodiesels, biocrude and synthetic oils.[6] In order to transform biomass into biofuels, the complex structure of biomass has to be studied so that the challenges of converting biomass to fuel can be better understood and overcome. Lignocellulose refers to the structure of biomass. The main constituents of biomass are the biopolymers cellulose, hemicelluloses and lignin with a number of inorganic compounds (major source of ash). The wall of the lignocellulotic plant cells typically consists of 30-35 wt% cellulose, 15-35 wt% hemicellulose and 18-35 wt% lignin. Softwood tends to have more lignin than hardwood which, in turn, has relatively more hemicellulose.[7] Figure 1.2 summarizes the general components of lignocellulosic biomass.

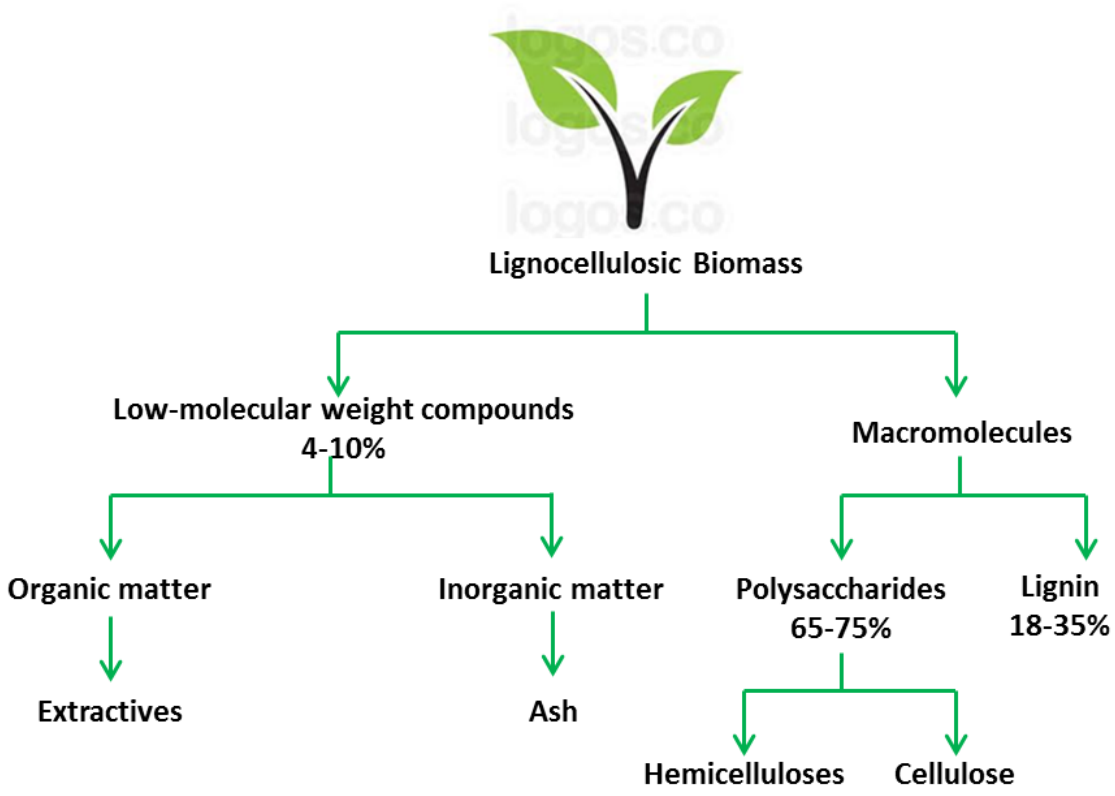

Figure 1.2 Composition of lignocellulosic biomass

The most abundant carbohydrates in biomass are cellulose and hemicellulose while lignin is an aromatic heteropolymer (a compound formed from subunits that are not all the same). The biopolymers interact in a very complex structure, as depicted in Figure 1.3, which consists of cellulose surrounded by a monolayer of hemicellulose and embedded in a matrix of hemicellulose and lignin.

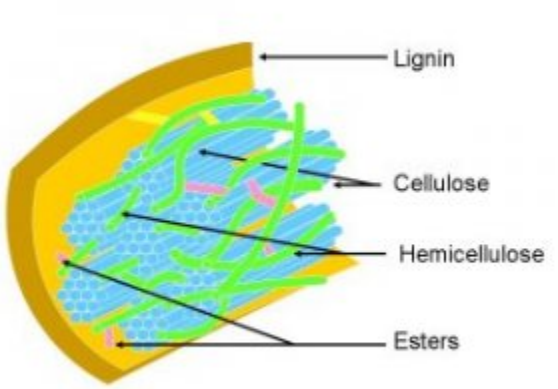

Figure 1.3 Complex structure of biomass[8]

1.2.1 Cellulose

Cellulose is a glucose polymer, consisting of linear chains of (1,4)-D-glucopyranose units, with an average molecular weight of around 10^6 or more. The removal of water from glucose forms glucose anhydride which polymerizes into long cellulose chains with 5000-10000 glucose units linked by β-(1→4)-glycosidic bonds (Figure 1.4).[9] The straight chains enable the formation of strong intra- and inter-molecule hydrogen bonds which hold the network flat and allow the hydrophobic ribbon faces to stack.[10] Cellulose's tendency to form crystals using those hydrogen bonds renders it insoluble in water, hence resistant to enzymatic attacks. The crystalline structure makes cellulose resist thermal decomposition better than hemicellulose with a

degradation temperature of around 240-350 °C to produce anhydrocellulose and levoglucosan.[9]

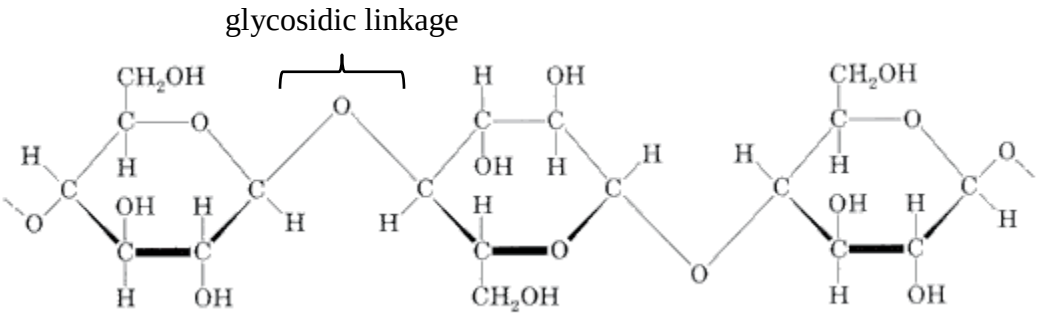

Figure 1.4 Cellulose structure

1.2.2 Hemicellulose

Hemicellulose (also known as polyose) is a mixture of polysaccharides, composed almost entirely of sugars (monosaccharides) such as glucose, mannose, xylose and arabinose and 4-*O*-methyl glucuronic and galacturonic acid residues (Figure 1.5). Hemicellulose has an average molecular weight of < 30,000[11] (which is less than cellulose) since the number of repeating saccharide monomers is only about 150. Depending on the plant type, the composition of hemicellulose varies for e.g. grass hemicellulose has more xylan while wood hemicellulose is rich in mannan, glucan and galactan.[10a] In contrast to cellulose, hemicellulose is a heterogeneous branched polysaccharide that binds tightly, but non-covalently, to the surface of each cellulose microfibril. This abundance of side-groups and the less uniform structure makes hemicellulose less crystalline than cellulose and it is hence more readily soluble in water at temperatures above 180 °C.

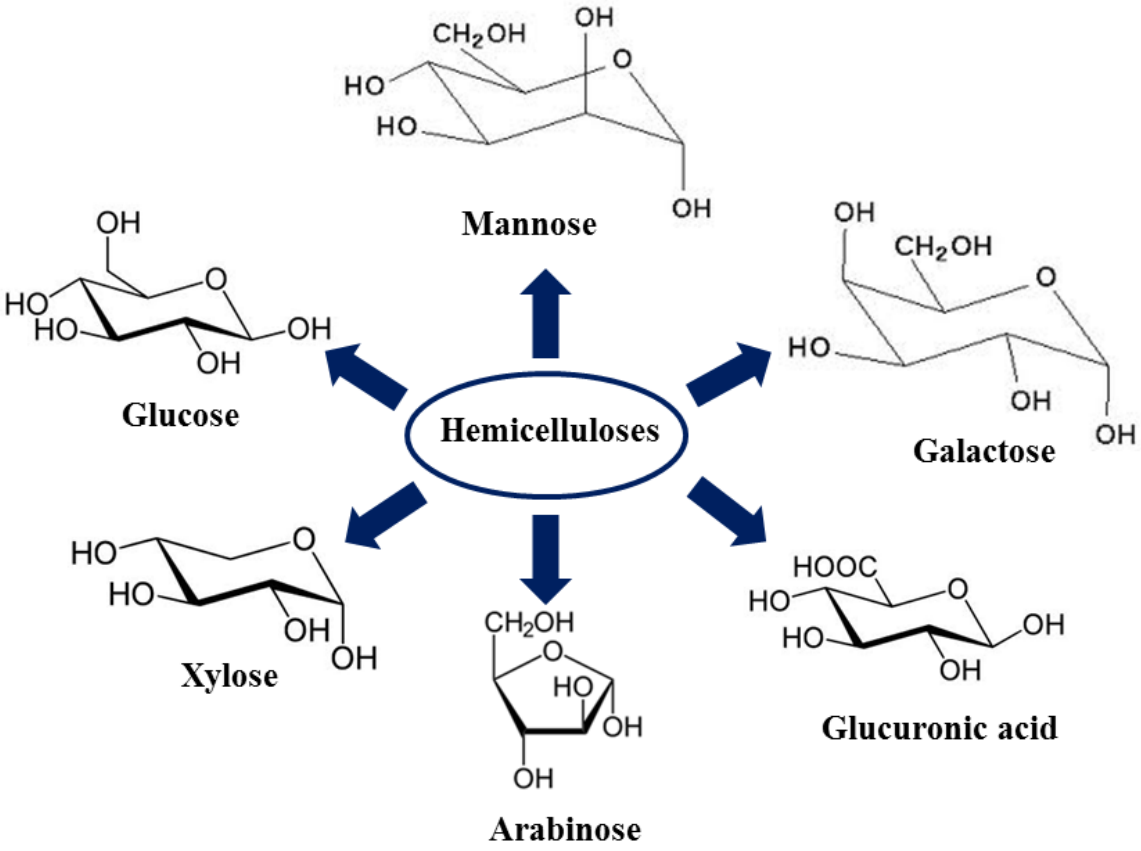

Figure 1.5 Main components of hemicelluloses

1.2.3 Lignin

Lignin can be regarded as a group of amorphous, high molecular-weight, chemically related compounds with no exact structure. The building blocks of lignin are believed to be a three carbon chain attached to rings of six carbon atoms, called phenyl-propanes with zero, one or two methoxyl groups attached to the rings. This aromatic heteropolymer consists of p-hydroxyphenylpropanoid units held together by C-C or C-O-C bonds. The main buiding blocks are p-coumaryl alcohol, coniferyl alcohol and sinapyl alcohol (Figure 1.6).[10a] These units undergo radical dimerization and further oligomerization to polymerize and cross-link. Lignin is the main binder for the

agglomeration of fibrous cellulosic components and is also a shield against microbial/fungal attack. Lignin structures are different in hardwood and softwood.

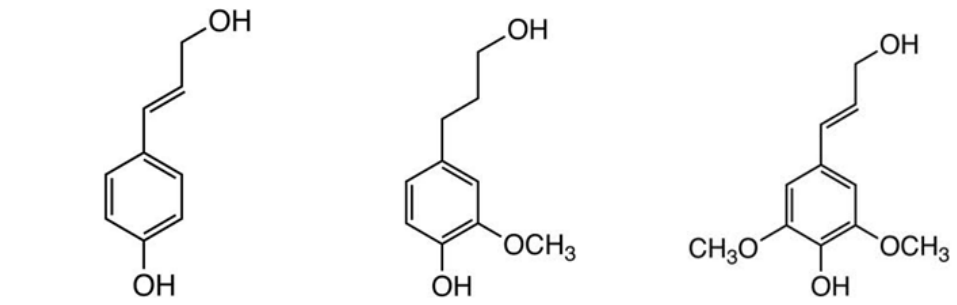

Figure 1.6 Main building blocks of lignin

In softwoods, guaiacyl lignin from polymerization of coniferyl phenylpropane units, is predominant while in hardwoods, guaicyl-syringyl, a copolymer of both coniferyl and sinapyl phenylpropane units, is predominant.[12] The decomposition temperature of lignin is around 280-500 °C and its liquefaction or pyrolysis yields phenols via the cleavage of ether and carbon-carbon linkages. However, lignin is tougher to dehydrate compared to cellulose and hemicellulose and produces more char.[13]

1.2.4 Inorganic Minerals and Organic Extractives

The ash content of the biomass constitutes of the mineral content with typical components like potassium, sodium, phosphorous, calcium and magnesium while the organic extractives include among others, fats, waxes, proteins, pectins, essential oils, gums, resins, starches, etc.

1.3 Biomass Upgrading to Liquid Fuel

The highly crystalline structure of cellulose makes it insoluble in water while the amorphous hemicellulose and lignin create a protective sheath around the cellulose and hinders enzymatic attack. Processing of lignocellulose is therefore essential for the conversion of lignocellulosic biomass to biofuels.[8] According to Zhang et al.,[14] upgrading of biomass to liquid fuel is a two-step process: upgrading biomass to a liquid product (bio-oil or biocrude) mainly through pyrolysis or hydrothermal liquefaction and then upgrading the bio-oil/biocrude usually via catalytic cracking or catalytic hydrotreatment. Figure 1.7 below depicts the main conversion processes required to upgrade bio-oil/biocrude.

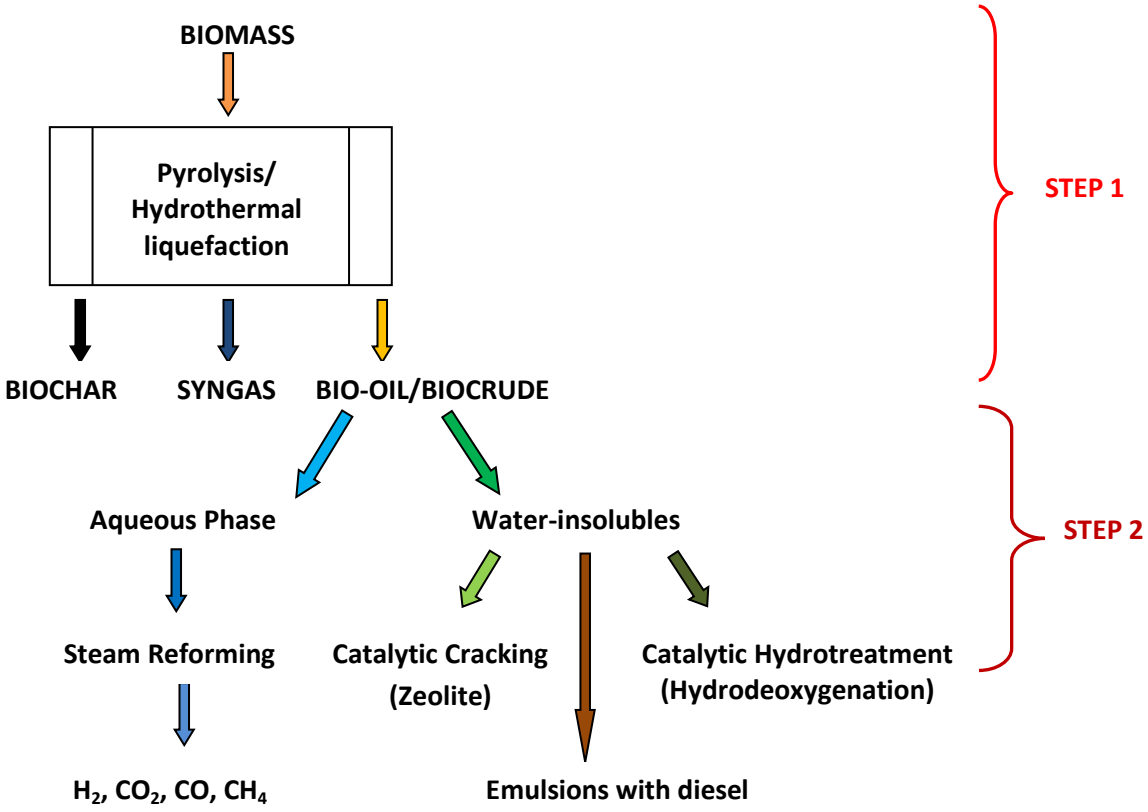

Figure 1.7 Conversion routes for bio-oil/biocrude upgrading

1.3.1 Bio-oil / Biocrude Production (Step 1)

The first step in biocrude/bio-oil production is to either pyrolyze or hydrothermally liquefy the biomass (Figure 1.7). For convenience and ease of reference, the term 'bio-oil' will be referred to as the liquid product from pyrolysis of biomass while the term 'biocrude' will refer to the liquid product from hydrothermal liquefaction. During pyrolysis, the biomass is heated in the absence of air and the gaseous product formed is then condensed to obtain bio-oil. However, the biomass needs to be dried first before grinding for optimal heat transfer. Grinding specification depends on the reactor technology used and the smaller the particles, the higher the cost of grinding. The four main pyrolysis technologies available for commercialization are (1) fluidized beds, (2) circulating fluid beds, (3) ablative pyrolysers and (4) vacuum pyrolysers.[15] The essential design parameters for pyrolysis include a very high heating and heat transfer rate (with finely ground biomass), carefully controlled temperatures (around 450-550 °C) and rapid cooling of the pyrolysis vapors (residence time < 1 s). Following the pyrolysis reactor, a cyclone separates the solid char to prevent its collection in the liquid products. The liquid-gas products are separated and the liquid is rapidly condensed to avoid cracking at higher temperatures.[15]

On the other hand, liquefaction of biomass usually occurs at high pressures (50-200 bar) and low temperatures (250-450 °C) to produce a water-insoluble biocrude. The reactor feed consists of a slurry of biomass and solvent, reducing gases and catalyst (including alkali, metals and Ni/Ru heterogeneous catalysts), if required. The main types of liquefaction processes are hydrothermal processing (water or aqueous solvent), hydropyrolysis (no carrier liquid solvent) and solvolysis (reactive liquid solvent).[15] In

this study, hydrothermal treatment has been used to liquefy and gasify biomass. Section 1.4 gives more details about this particular biomass converting technology.

1.3.2 Characteristics of Bio-oil and Biocrude

Bio-oil/biocrude produced via different methods including pyrolysis and liquefaction of biomass, is a promising second-generation renewable energy carrier.[16] However, due to depolymerization and fragmentation of cellulose, hemicellulose and lignin present in the biomass, bio-oils and biocrude are multi-component mixtures of different size molecules, hence the difference between the elemental composition of bio-oil, biocrude and petroleum derived fuel.[3] Table 1.1 compares biocrude and bio-oil obtained respectively from hydrothermal treatment and pyrolysis, with petroleum.

Because of the original moisture content in the feedstock, bio-oil and biocrude have a high moisture content especially when derived from fast pyrolysis whereby water is a product of dehydration reactions.[17] This leads to a low heating value and flame temperature but however water does enhance fluidity and decrease viscosity, which is beneficial for combustion of bio-oil in the engine.[3] Bio-oil and biocrude usually contain various oxygen compounds such as carboxyl, carbonyl, hydroxyl and methoxy groups[18] but the type of biomass and reaction conditions influence the composition of the bio-oil/biocrude. Compared to conventional crudes which contain only about 1-2 wt% oxygen, biomass-derived synthetic crudes may contain up to 50 wt% of O_2,[19] as shown in Table 1.1. This leads to thermal and chemical instability and adversely affects the biocrude's and bio-oil's miscibility with hydrocarbons[16, 18] while also lowering the energy density by 50%. Because of their high distillation residues due to their complex

compositions and their wide range of boiling point temperatures, bio-oil/biocrude cannot be used in the instance of complete evaporation before combustion.[3]

Table 1.1 Comparison between biocrude, bio-oil and petroleum fuel [20]

Characteristic	Hydrothermal Biocrude		Fast Pyrolysis Bio-oil	Heavy petroleum fuel
	Wet	Dry		
Water content, wt%	3.5	0	15-25	0.1
Insoluble solids, wt%	1		0.5-0.8	0.01
Carbon, wt%	72.6-74.8	76.5-77.5	39.5-55.8	85.2
Hydrogen, wt%	8.0	7.8	6.1-7.5	11.1
Oxygen, wt%	16.3-16.6	12.5-14.1	37.9-52.6	1.0
Nitrogen, wt%	<0.1		<0.1	0.3
Sulfur, wt%	<0.05		<0.05	2.3
Ash, wt%	0.3-0.5		0.2-0.3	-
HHV, MJ/kg	34[15]		16.5-17.5	40
Density, g/ml	1.10		1.23	0.94
Viscosity, cp	3,000-17,000 @ 60°C		10-150 @ 50°C	180 @ 50°C
Distillation residue[15]	Up to 50			1
pH[3]	2-3			-

From Table 1.1, it can also be noticed that both biocrude and bio-oil have a large range of viscosity which varies with the biomass type and conversion processes used. Though for pyrolysis bio-oil, there is a need to increase the viscosity (e.g. via methanol addition), for biocrude from hydrothermal treatment, the opposite is required and can be

achieved by either water or a suitable solvent addition. The low pH values of the bio-oils are due to the substantial presence of carboxylic acids such as acetic and formic acids which lead to corrosion, especially at elevated temperatures. It is therefore important to consider the materials of construction like stainless steel during any upgrading process.[17] Ash content is also a major concern since its presence can cause erosion, corrosion and kicking problems in the engines and the valves. The alkali metals like calcium (responsible for hard deposits), sodium, potassium and vanadium (responsible for high temperature corrosion and deposition) can be tackled by biomass pretreatment, hot gas filtration and catalytic upgrading.[3, 20]

More than 400 compounds have been found in bio-oil/biocrude but usually they contain acids (acetic, propanoic), esters (methyl formate, butyrolactone), alcohols (methanol, ethylene glycol, ethanol), ketones (acetone), aldehydes (acetaldehyde, formaldehyde), miscellaneous oxygenates (glycolaldehyde, acetol), sugars, furans (furfurans, HMF), phenols, guaiacols and syringols.[15] Bio-oil/biocrude is therefore a complex mixture, highly-oxygenated with large size molecules whose composition varies greatly[21] as illustrated in Figure 1.8.

1.3.3 Bio-oil / Biocrude Upgrading (Step 2)

Since the direct use of bio-oil/biocrude is not feasible, they require chemical transformation to increase their volatility, thermal stability, heating value and to reduce their viscosity through oxygen removal and molecular weight reduction.[22] As illustrated in Figure 1.7, the three main routes used for upgrading are (1) hydrodeoxygenation (HDO) with typical hydrotreating catalysts (sulfided CoMo or NiMo), (2) catalytic

cracking e.g. zeolite upgrading and (3) forming emulsions with diesel fuel. It is to be noted that the aqueous phase of bio-oil/biocrude can be converted to hydrogen or syn-gas by (4) steam-reforming.

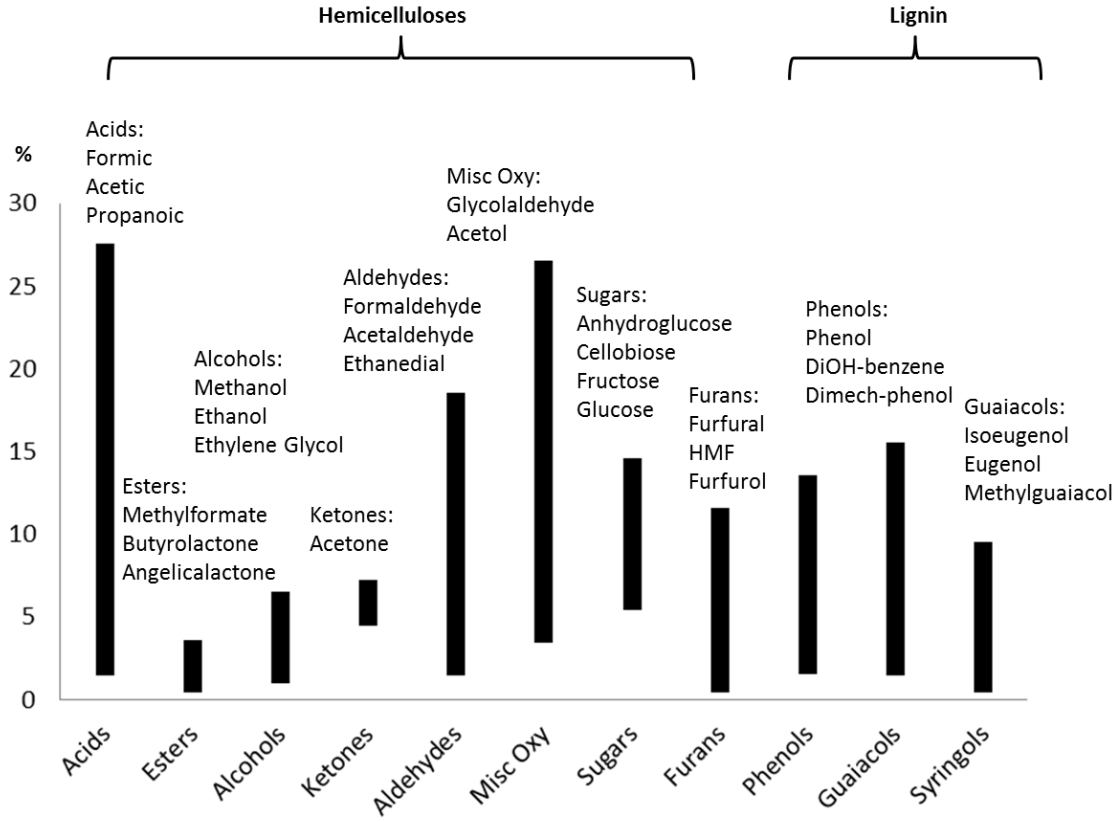

Figure 1.8 Composition range of the compounds to be upgraded in bio-oil[21]

1.3.3.1 Hydrodeoxygenation, HDO

HDO entails the removal of oxygen by conversion to H_2O and hence the reduction in molecular weight and the formation of saturated C-C bonds. Usually, HDO involves treatment of bio-oils at 300-600 °C with high pressure H_2 (10-20 MPa) in the presence of heterogeneous catalysts.[15] The block diagram (Figure 1.9) illustrates a typical bio-oil/biocrude upgrading process flow via HDO. Typically, an oil phase and a separate

aqueous phase would be produced during hydroprocessing. In order to minimize hydrogen consumption, HDO must be emphasized without saturation of the aromatic rings[22] with the use of an active catalyst to achieve high conversions and avoid hydrogenation of aromatics to conserve the octane number. Before the final elimination of oxygen (O), several bonds have to be broken and bond strengths therefore come into play in HDO.

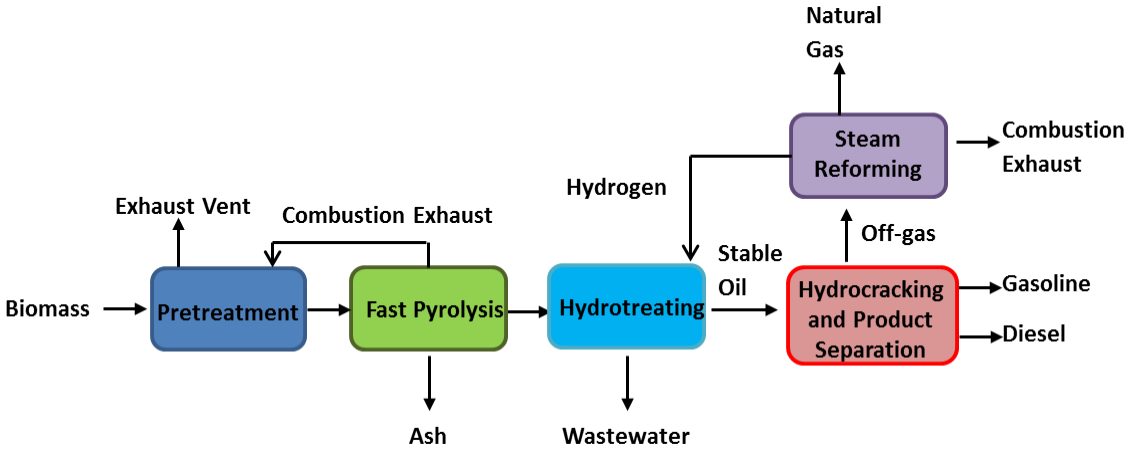

Figure 1.9 Schematic diagram of current HDO process to upgrade bio-oil

The bond dissociation energy of O attached to an aromatic carbon is 422 kJ/mol while that attached to an aliphatic carbon is 339 kJ/mol,[19] implying that elimination of O from phenols and aromatic ethers are more challenging than from alcohols and aliphatic ethers. Hence after hydrogenation of an aromatic ring to its corresponding cycloalkane, it would be much easier to break the aliphatic-O bonds, suggesting that H_2 pressure may be an important factor influencing HDO. The main process reaction on a model compound via HDO is as follows[1]:

H_2 + -(CH_2O)- → -(CH_2)- + H_2O where -(CH_2O)- represents the bio-oil.

Figure 1.10 shows some typical structures of O-compounds in bio-oils from pyrolysis. Compounds containing two or more O-groups, i.e., hydroxylic and etheric groups, are quite common. Examples of such structures are guaiacols (GUAs), eugenol, vanillin and biphenols. Two steps might be required to achieve a complete conversion of such compounds to hydrocarbons. Additional phenols and dihydroxyphenols are important products of the first step, the so-called stabilizing step.

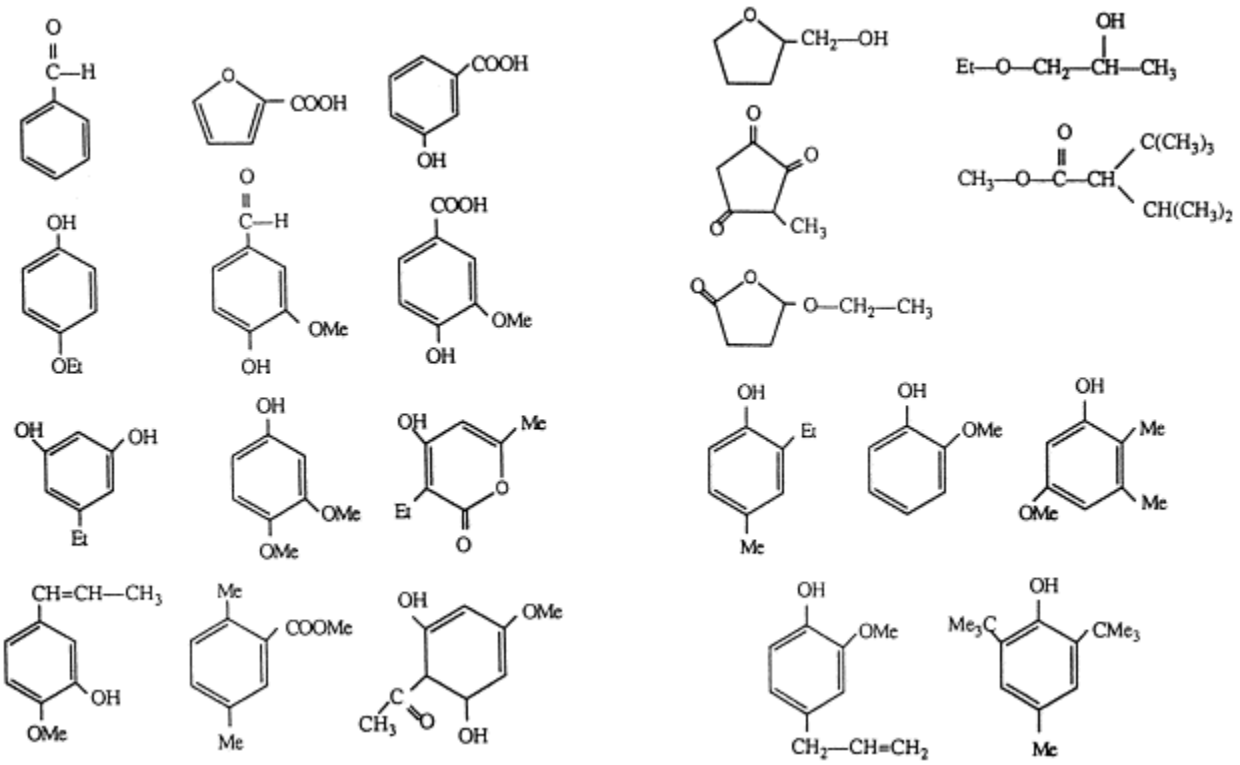

Figure 1.10 Typical O-compounds usually found in bio-oil[19]

Therefore, the HDO of such a species is an important part in the final step. Since phenol (can be present in the feed or formed as intermediates during HDO of furans) and its derivatives are chemically very stable, they are more resistant to oxygen removal. Guaiacol and substituted GUA on the other hand are chemically very reactive, hence one

of the causes of bio-oil's instability. This is the reason why studies have been conducted on both phenols and GUA as model compounds to represent the lignin fraction of wood-based bio-oils.

Usually, a multi-stage operation is required for bio-oil conversion to commercial fuels with a first stabilization stage performed below 573 K to remove O-compounds[19] where primary reactants like methoxyphenols, biphenols and ethers are converted to phenols. The latter are removed in a second stage at 623 K whereby other O-compounds like ketones, carboxylic acids, esters, etc. may also be involved. It is to be noted that because of their resistance to HDO, phenols and furans are perhaps the most-important O-compounds. Usually, bio-oil from pyrolysis contain phenols which account for a quarter of the liquids derived from lignocellulosic biomass and also other O-compounds like ketones, aldehydes, carboxylic acids, esters, alcohols and ethers.[19] In fact, a relatively high content of GUAs are found in bio-oils and it usually forms coke from the interaction of GUA with the γ-Al_2O_3 support. Using carbon-supported CoMo catalyst, the phenol/catehol (primary product from HDO of GUA) ratio was found to be seven times higher than when using γ-Al_2O_3.

Numerous studies have been conducted involving HDO on model O-compounds like furans and phenols as well as mixtures and real feeds. Usually, HDO occurs simultaneously with other reactions such as hydrodesulphurization (HDS), hydrodenitrogenation (HDN), hydrodemetallization (HDM) and hydrogenation (HYD), which influence the HDO reaction and therefore reaction conditions, feed and the catalyst used dictate the overall mechanism.[19] Products from HDO of liquids from high-pressure liquefaction system are primarily phenolic with cyclic ketones, methoxyphenols and

naphtols in lesser concentration while wood pyrolysis liquids contain large quantities of low-molecular weight organic acids, ketones, aldehydes and furans with phenols in methoxy or dimethoxy forms.[23] The latter is thermally less stable and a more active catalyst at lower temperatures would probably be needed. Hence, high-pressure liquefaction products have better commercial application.

The upgrading of hydrothermal liquefaction product was investigated by the Pacific Northwest National Laboratory (PNL/PNNL) whereby initially, batch reactions of model phenolic compounds were tested using various catalysts[24] including CoMo, NiMo, NiW, Ni, Co, Pd and CuCrO to hydrogenate phenol at 300/400 °C for 1 hour. It was found that the sulfided form of CoMo was the most active catalyst at 400 °C with a yield of 33.8% benzene and 3.6% cyclohexane. In a second step, high-pressure liquefaction oil (biocrude) from the Albany Biomass Liquefaction pilot plant was hydrotreated in an attempt to make gasoline. Nickel and sulfided cobalt-molybdenum catalysts were used in a continuous-flow, fixed catalyst bed reactor system operated in an upflow configuration.[23] A suite of 22 different catalyst combinations were used to treat a light oil fraction and the sulfide form of the CoMo catalyst was found to be more active than its oxide form. In the same study, hydrocracking of whole oil using nickel catalyst yielded similar results as with CoMo except for the higher gas yield and hydrogen consumption. However, Ni catalyst lost its activity over the several hours of operation. After distillation of the products, GC-MS analysis revealed the presence of cyclic alkanes and aromatics from the cyclic ketones and phenolics in the liquefaction product.

Other studies have also demonstrated that high yields of high-quality gasoline can be produced from biomass-derived oils but with low space velocities.[22] The rate-limiting

steps in upgrading bio-oils are cracking and hydrogenation of the higher molecular weight components. A patent filed by Baker et al.[25] looked into a multistep process including hydrotreating for oxygen reduction, separation of aqueous, gasoline and gas phases and hydrocracking of heavy components in order to get a better yield of aromatic gasoline. This was achieved by removing a fraction from the system before the rings became saturated and hydrogen consumption was also minimized by 13% as opposed to the single-stage concept. Detailed analysis of the distillates obtained from HDO of the bio-oils revealed the primary components of the aromatic and aliphatic portions.

At the Chalmers Institute of Technology,[26] the oil was preprocessed to facilitate cracking. The light oil was separated from the heavier components by means of solvent extraction with a yield of 74% with acetone. A test was performed on decalin extract (2.5% naphta, 38.2% atmospheric gas oil, 39.5% vacuum gas oil and 19.8% vacuum residue) of bio-oil at 300-390 °C and 50-150 bar for 20 min to 5 hours with yields of 1% gas, 16% naphta, 41% atmospheric gas oil, 34% vacuum gas oil and 8% vacuum residue at 350 °C and 100 bar. Between 350-375 °C, there was minimum coke laydown and deposition on catalyst was about 2-4 wt% and occurred during the first 2.5 hours. It was concluded by extrapolation that at 410 °C, residue would be eliminated since the heavier components would be converted to lighter ones. In other tests, the wood oil was desalted before hydroprocessing and from the results, the authors concluded that desalting was sufficient and solvent extraction was not needed to get a good yield.

For slow pyrolysis bio-oil upgrading, research conducted at Texas A&M University[27] revealed that using a batch reactor at 400 °C for 1 h with Pd on alumina catalyst, produced the highest liquid yield while Pt or Re on alumina and Raney nickel

were nearly as useful but had higher gas yields. Using carbon support caused more gas yield while sulfided CoMo, NiMo and NiW catalysts had lower activity compared to the precious metal catalysts. When using a continous process, the researchers found that 5% Pt on alumina (reaction temperature range of 350-400 °C) was more active for oxygen removal (27-45%) when compared with the commercial CoMo, NiMo and NiW catalysts which achieved only 15-39% oxygen removal.

Upgrading fast pyrolysis bio-oil is more demanding due to its high reactivity and instability. Research conducted at the PNL/PNNL[22, 28] focused on catalytic hydroprocessing with a two-stage hydrotreatment: catalytic hydrotreatment below 300 °C with Ni or sulfided CoMo catalyst to produce a stabilized bio-oil and then from the low-temperature hydrotreated bio-oil, gasoline-range hydrocarbons were produced at 350 °C and 13.8 MPa using sulfide CoMo. DMT FuelTec[29] performed a pilot-scale test whereby the bio-oil was processed with powdered NiMo catalyst at 30 MPa, 380 °C in a 2x10 m reactor tube. There were subsequent separation steps to yield three product streams. The analysis of the lightest product (33.9% yield) showed highly deoxygenated product but no information on cost and size of the fixed-bed reactors were provided. Universite Catholique de Louvain in Belgium[22] used sulfide CoMo and NiMo catalyst on alumina and dimethyldisulfide was also added to maintain a reasonable H_2S partial pressure at 300-400 °C and 12 MPa. The authors claimed that supported noble metal catalysts would be readily deactivated. They concluded that the lowest oxygen-content product was produced at 300 °C. At Universite Laval[30] a two-step concept was devised using Ru catalyst at very low temperature (80°C) and then hydrotreating by NiW at about 325 °C to yield a product with less than 10% oxygen content. Some other studies[22] have found

that reaction temperatures above 80 °C are unsuitable for hydrogenation of bio-oils because of separation of product phases. Furthermore, it was concluded that palladium was inactive at 60 °C, raney nickel resulted in reduced viscosity at 80 °C while copper chromite resulted in a more viscous oil at the same temperature. HDO therefore proceeds through a complex set of reactions and a number of postulated mechanisms are found in literature.[1, 19] The overall reactions of model compounds are shown in Table 1.2.

Table 1.2[1] Overall process reactions of model compounds

Model compounds	Reaction
Guaiacol→catechol	$C_6H_4(OH)(OCH_3)+H_2 \rightarrow C_6H_4(OH)(OH)+CH_4$
Catechol→phenol	$C_6H_4(OH)(OH)+H_2 \rightarrow C_6H_5(OH)+H_2O$
Phenols→benzene	$C_6H_5(OH)+H_2 \rightarrow C_6H_6+H_2O$
Phenols→cyclohexanone	$C_6H_5(OH)+2H_2 \rightarrow C_6H_{10}O$
Cyclohexanone→cyclohexanol	$C_6H_{10}O+H_2 \rightarrow C_6H_{11}(OH)$
Cyclohexanol→cyclohexene	$C_6H_{11}(OH) \rightarrow C_6H_{10}+H_2O$
Cyclohexene→cyclohexane	$C_6H_{10}+H_2 \rightarrow C_6H_{12}$

1.3.3.2 Catalytic Cracking

In oil refining and production of fine chemicals, zeolite, crystalline microporous materials with well-defined pore structures, are usually used as catalysts due to their active acid sites. Zeolites can therefore be used to upgrade bio-oils by reducing their oxygen content and improve their thermal stability (Figure 1.11).

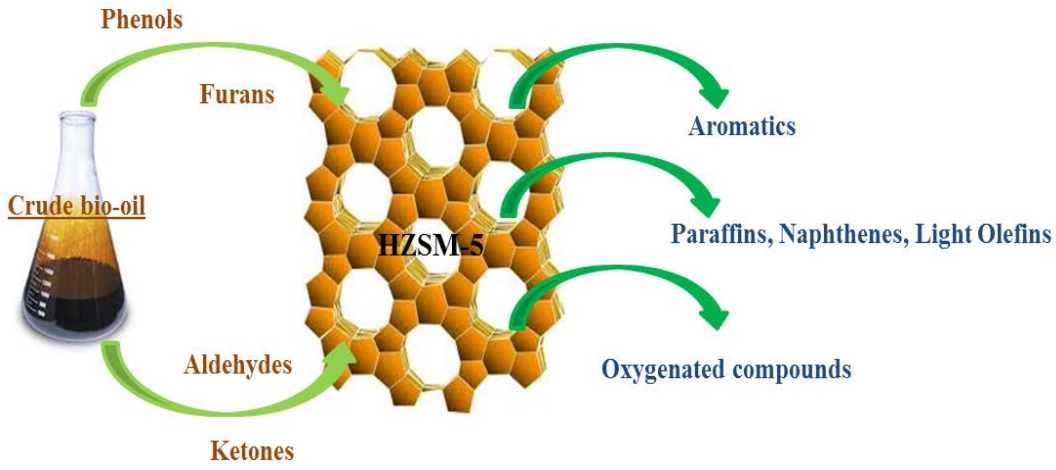

Figure 1.11 Bio-oil upgrading using zeolite catalyst

Usually, the reaction conditions are 350-500 °C, atmospheric pressure and gas hourly space velocities of around 2.[15] Zeolite cracking is however not as well developed as HDO since the product is a low grade fuel due to high carbon formation (20–40 wt%) which results in rapid deactivation of the catalyst.[31]

Adjaye et al.[32] observed between 30-40 wt% of bio-oil depositing on the catalyst as coke or as char in the reactor with the ZSM-5 catalyst. Usually, the products from zeolite upgrading include hydrocarbons, water-soluble and oil-soluble organics, water, gases and coke.[15] Others[3] have used ZnO, AL-MCM-41, Cu/Al-MCM-41 and Al-MCM-41 to catalytically crack the pyrolysis vapours. Although catalytic cracking is considered to be cheaper, low hydrocarbon yields and high coke yields usually limit this upgrading process. One study[33] attempted to upgrade pyrolysis bio-oil from rice husk using sub- and super-critical ethanol in the presence of an HZSM-5 catalyst for esterification of the acids. Supercritical upgrading was more effective than subcritical upgrading process: HZSM-5 was found to facilitate cracking of heavy components of crude bio-oil more

effectively and there was a decrease in the residue of distillated upgraded bio-oil. Adam et al.[34] compared seven mesoporous catalysts (four Al-MCM-41 type catalysts with a Si/Al ratio of 20, a commercial FCC catalyst, a pure siliceous SBA-15 and an aluminum incorporated SBA-15 material) used to convert pyrolysis vapors of spruce wood to improved bio-oil. All the catalysts exhibited an increase in the hydrocarbon and acid yields and a decrease in the carbonyl yields. The FCC was the best performing catalyst. A recent study[35] investigated the effect of temperature and bio-oil/methanol ratio in the feed on HZSM-5 catalysts deactivation during the production of hydrocarbons from crude bio-oil. A direct relationship between coke deposition and deactivation and the concentration of bio-oil oxygenates in the reaction medium was found. To prevent coke deposition, a HZSM-5 zeolite catalyst with a reduced SiO_2/Al_2O_3 ratio, high reaction temperature (at least in the 450–550 °C range) and high methanol/bio-oil ratio in the feed were used. The acidity of the catalyst not only increased conversion but also favored formation of polycondensed aromatic structured-coke.

1.3.3.3 Emulsions with Diesel Fuel

Due to their high moisture content, pyrolysis bio-oils are not soluble in petroleum-derived fuels but however, they can be emuilsified by using a surfactant. Chiaramonti et al.[36] found emulsions to be more stable when using different ratios with diesel but the viscosity was higher with high bio-oil content. The emulsifier should be between 0.5-2% for acceptable viscosity. Ikura et al.[37] centrifugated and emulsified bio-oil in no.2 diesel by CANMET surfactant and reported the cost of production to be 2.6 cents/L for 10% emulsion, 3.4 cents/L for 20% and 4.1c/L for 30%. Even though

emulsification does not require redundant chemical transformations, high cost due to surfactant addition and high energy cost due to emulsification cannot be overlooked. Furthermore, corrosiveness to the engine is serious when using this upgrading technique. One group[38] studied the corrosiveness of two bio-oil/diesel emulsions with bio-oil concentrations of 10 wt% and 30 wt%. The corrosion properties to four metals namely aluminum, brass, mild steel and stainless steel at different temperatures were investigated through weight loss of the metals immersed in the oil samples. X-ray photoelectron spectroscopy (XPS) was also used to study the chemical states of the elements on the metal surface. Stainless steel was the least affected while mild steel was the least resistant to corrosion. Furthermore, organic deposits were formed on aluminum and brass, but not on stainless steel. However, bio-oil was found to be more corrosive than the two emulsions since the diesel limited the contact area between bio-oil and metals.

1.3.3.4 Steam Reforming

Another route of producing a range of fuels is by steam reforming the aqueous fraction of bio-oil/biocrude to produce syngas. Steam reforming reactions usually require high temperatures, 600-800 °C, and high space velocities with a Ni-based catalyst.[15]. Because bio-oil/biocrude components are thermally unstable and hence decompose on heating, steam reforming is not easy and coking also causes deactivation of the catalysts. Czernik et al.[39] used a fluidized bed reactor to reform bio-oils with a yield of 6 kg of hydrogen per 100 kg of wood used for pyrolysis. This study concluded that fluidized bed was more stable than fixed bed but the commercial catalysts designed for fixed bed, were susceptible to attrition in the fluidized bed. Garcia et al.[40] used magnesium and

lanthanum to enhance steam adsorption to facilitate carbon gasification. They also used cobalt and chromium as additives to reduce coking by modifying the metal sites forming alloys with nickel. Byrd et al.[41] gasified liquefied switchgrass biocrude over nickel, cobalt, and ruthenium catalysts supported on TiO_2, ZrO_2, and $MgAl_2O_4$ at 600°C and 250 bar with a WHSV of 9 h^{-1}. Catalysts supported on $MgAl_2O_4$ charred immediately and any given metal supported on ZrO_2 gave a higher conversion of bio-oil than when supported on TiO_2. The highest hydrogen yield was obtained with Ni/ZrO_2, while the lowest was with Ru/ZrO_2, which gave a product gas composed of mostly methane and CO_2.

1.4 Hydrothermal Treatment

Biomass can be transformed into renewable fuels through a number of conversion methods including biochemical methods (using enzymes) and thermochemical methods like pyrolysis, liquefaction, gasification, etc. In this dissertation, hydrothermal liquefaction and gasification are used as a means to convert biomass. Water as reaction medium is safe, non-toxic, inexpensive and readily available. Liquefaction usually requires a temperature of 280-370 °C and 100-250 bars of pressure where the water is still in the liquid form, as seen on the phase diagram of water (Figure 1.12). During biomass liquefaction, water acts as a reactant and a catalyst to produce biocrude (oily phase), a water-soluble phase, gas and biochar. As temperature and pressure are increased, gasification becomes more dominant especially in the supercritical environment (above the critical point of 374 °C and 220 bar) to form H_2, CO_2 and CH_4.

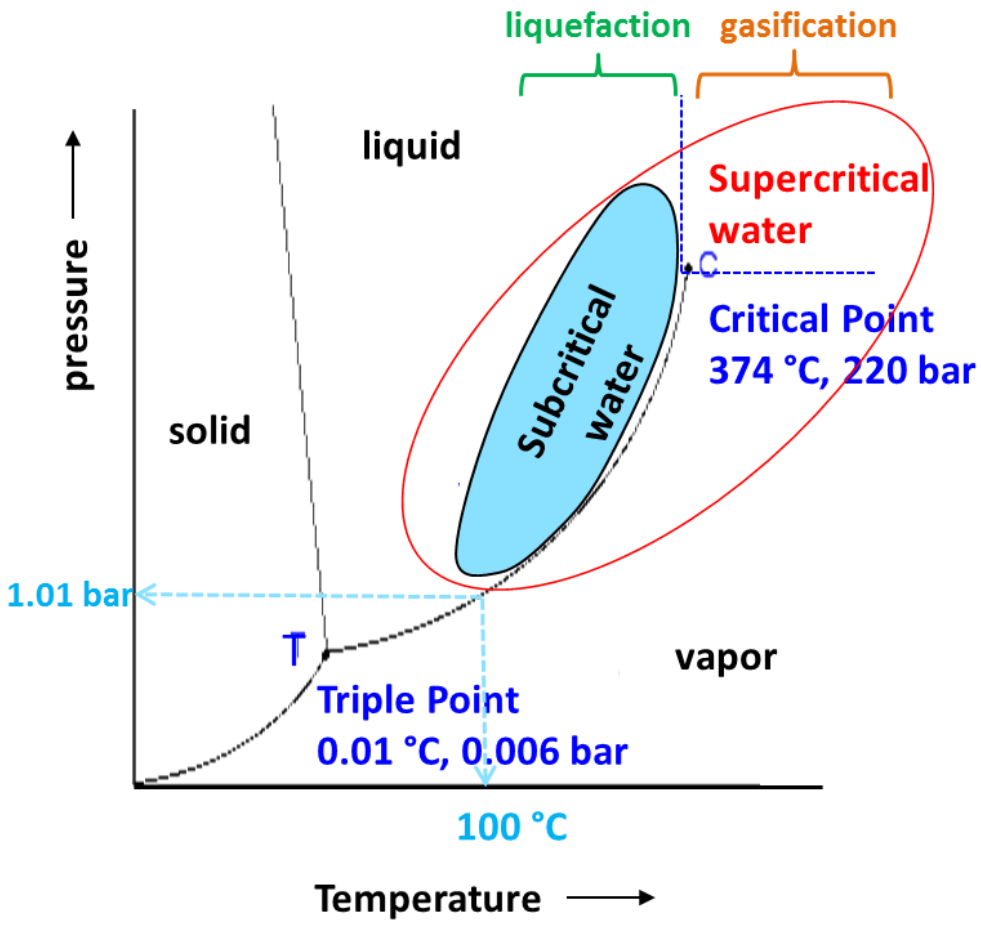

Figure 1.12 Phase diagram of water

The industrial application of this technology however faces a number of challenges namely corrosion which requires use of expensive materials and high operating conditions which has tough requirements for the process components like feed pumps. However, hydrothermal liquefaction can be promising from the standpoint of energy consumption and process integration. Even though the yield from lignocellulosic biomass liquefaction is not too high (about 30%) when compared to pyrolysis, the biocrude so-produced is more stable and the process eliminates the cost of biomass drying.[10a] The high energy requirements can be tackled through energy recirculation for

e.g. by preheating the substrate with the reactor effluent stream. Hydrothermal liquefaction has the potential to produce fuels that can blend with or replace transportation fuels and value-added compounds that can be further converted to platform chemicals. In this context, research and development has to address the technological challenges so that an integrated bio-refinery approach can be adopted to enhance the economy of this process.

1.4.1 Properties of Sub- and Supercritical Water

The properties of water change with temperature and pressure, as illustrated in Figure 1.13. For example, as the temperature of the water is increased, it becomes less dense due to thermal expansion. Above the critical temperature of 374 °C, the density decreases very rapidly up to about 410 °C, after which the rate of decrease slows down. Water can act as an acid/base catalyst precursor below the critical point and at high pressures since the ionic product is up to three orders of magnitude higher than under ambient conditions. In the subcritical region, the relatively low dielectric constant enhances ionic reactions which promote biomass liquefaction.[42] In the supercritical state, water behaves as a non-polar solvent which can dissolve compounds like alkanes, aromatics etc., since these organics are completely miscible in supercritical water (SCW). Furthermore, oxygen is completely miscible in SCW while inorganics are practically insoluble.[43] If the temperature is not too elevated, C-C bond formation and organometallic-catalyzed reactions are enhanced in SCW since the water molecule structure is unchanged and it is still polar and can interact with ions.[42] This means that

depending on the temperature and pressure, water can either support free radical or polar and ionic reactions, making it an adjustable solvent.

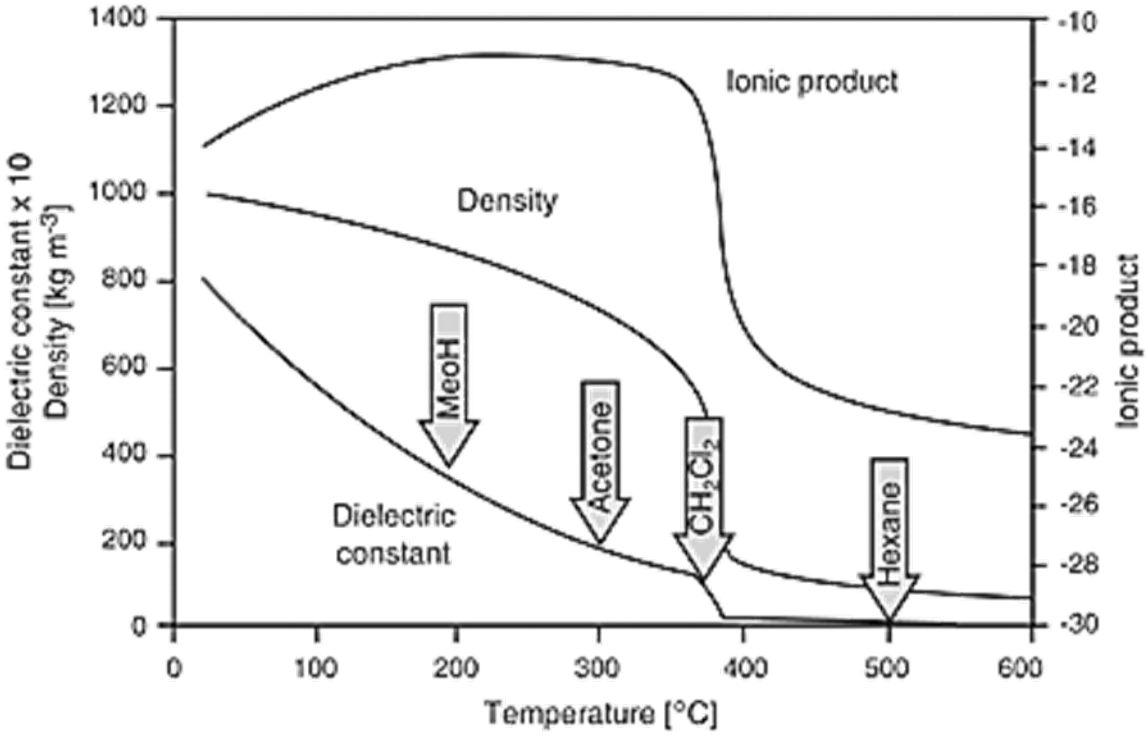

1.13 Physical properties of water vs. temperature at 24 MPa[44]

(Dielectric constants of typical organic solvents at room temperature are also indicated)

From Figure 1.13, it can be observed that the dielectric constant of water decreases with density. The rates of chemical reactions during biomass liquefaction and gasification depend on the properties of water as a solvent. The dielectric constant drops from 80 to 20 from room temperature to 300 °C and is less than 5 above the critical temperature. This reduction is due to the disruption in the hydrogen-bonding network which decreases with temperature. The solubility of small organic compounds is

enhanced due to low dielectric constant of water which provides a homogeneous single-phase medium.[45] From 200-300 °C, there is a slight increase in the ionic product ($K_w = [H^+][OH^-]$) of water which reduces sharply above the critical temperature. The increase is due to the fact that self-dissociation of water is endothermic but at higher temperatures above critical point, the dielectric constant and density drop drastically. This means that the solvation and stabilization power of ionic species decrease, leading to the decrease in the ionic product.[42] High temperature and high H^+ and OH^- concentrations coupled with catalysis by water molecules drive the increase in reactivity even in the absence of added alkali or base. Supercritical water has high diffusion rates and miscibility and low viscosity which influence the reaction rates. High diffusion rate actually avoids mass transfer limitations and good solubility prevents coke formation so that SCW is an excellent medium for heterogeneous catalysis.[42] High temperature and low density also leads to the breakdown of the wide-range hydrogen network present in water into clusters. As a result, both the average number of water molecules attached to clusters by hydrogen bonds and the lifetime of a hydrogen bond decrease but the mobility of single water molecules increases. Translational and rotational motions are no longer hindered and this leads to an increase self-diffusivity and enhances energy transfer between fast reacting solutes and solvents.[46] The network breakdown also leads to a high local concentration of H^+ and OH^- ions moving very fast inside the clusters, hence increasing reactivity.

1.5 References

1. Ahmad, M. M.; Nordin, M. F.; Azizan, M. T., Upgrading of Bio-oil into High-Value Hydrocarbons via Hydrodeoxygenation. *American Journal of Applied Sciences* **2010,** *7* (6), 746-755.

2. EIA, Energy Consumption by Sector. In *Annual Energy Outlook 2013 Early Release Overview*, U.S. Energy Information Administration: 2013.

3. Zhang, Q.; Chang, J.; Wang, T.; Xu, Y., Review of biomass pyrolysis oil properties and upgrading research. *Energy Conversion and Management* **2007,** *48* (1), 87-92.

4. DOE, Transportation sector energy consumption. In *International Energy Outlook 2011*, US Department of Energy, Energy Information Administration: 2011.

5. Sissine, F. In *Energy Independence and Security Act of 2007: a summary of major provisions*, DTIC Document: 2007.

6. Demirbas, A., Biofuels securing the planet's future energy needs. *Energy Conversion and Management* **2009,** *50* (9), 2239-2249.

7. Behrendt, F.; Neubauer, Y.; Oevermann, M.; Wilmes, B.; Zobel, N., Direct Liquefaction of Biomass. *Chemical Engineering & Technology* **2008,** *31* (5), 667-677.

8. McIntosh, P. What is Lignocellulose? http://lignofuel.wordpress.com/2010/09/15/lignocellulose/.

9. Mohan, D.; Pittman, C. U.; Steele, P. H., Pyrolysis of Wood/Biomass for Bio-oil: A Critical Review. *Energy & Fuels* **2006,** *20* (3), 848-889.

10. (a) Toor, S. S.; Rosendahl, L.; Rudolf, A., Hydrothermal liquefaction of biomass: A review of subcritical water technologies. *Energy* **2011,** *36* (5), 2328-2342; (b)

Zugenmaier, P., Conformation and packing of various crystalline cellulose fibers. *Progress in Polymer Science* **2001,** *26* (9), 1341-1417.

11. McKendry, P., Energy production from biomass (part 1): overview of biomass. *Bioresource Technology* **2002,** *83* (1), 37-46.

12. McCarthy, J. L.; Islam, A. In *Lignin chemistry, technology, and utilization: a brief history*, ACS Symposium Series, ACS Publications: 2000; pp 2-99.

13. Goldstein, I. S., Organic chemicals from biomass. **1981**.

14. Zhang, S.; Yan, Y.; Li, T.; Ren, Z., Upgrading of liquid fuel from the pyrolysis of biomass. *Bioresource Technology* **2005,** *96* (5), 545-550.

15. Huber, G. W.; Iborra, S.; Corma, A., Synthesis of Transportation Fuels from Biomass:Chemistry, Catalysts, and Engineering. *Chemical Reviews* **2006,** *106* (9), 4044-4098.

16. Zhao, C.; Kou, Y.; Lemonidou, A. A.; Li, X.; Lercher, J. A., Highly Selective Catalytic Conversion of Phenolic Bio-Oil to Alkanes. *Angewandte Chemie International Edition* **2009,** *48* (22), 3987-3990.

17. Oasmaa, A.; Czernik, S., Fuel Oil Quality of Biomass Pyrolysis Oils-State of the Art for the End Users. *Energy & Fuels* **1999,** *13* (4), 914-921.

18. Senol, O. I.; Viljava, T. R.; Krause, A. O. I., Effect of sulphiding agents on the hydrodeoxygenation of aliphatic esters on sulphided catalysts. *Applied Catalysis A: General* **2007,** *326* (2), 236-244.

19. Furimsky, E., Catalytic hydrodeoxygenation. *Applied Catalysis A: General* **2000,** *199* (2), 147-190.

20. Laboratory, P. N. N., Hydroprocessing of pyrolysis bio-oil to fuels and chemicals. Energy, U. S. D. o., Ed. Madison, Wisconsin, 2008.

21. Milne, T. A.; Agblevor, F.; Davis, M.; Deutch, S.; Johnson, D., *Developments in Thermal Biomass Conversion*. Blackie Academic and Prefessional: London, UK, 1997.

22. Elliott, D. C., Historical Developments in Hydroprocessing Bio-oils. *Energy & Fuels* **2007,** *21* (3), 1792-1815.

23. Elliott, D. C.; Baker, E. *Upgrading biomass liquefaction products through hydrodeoxygenation*; Pacific Northwest Lab., Richland, WA (USA): 1984.

24. Elliott, D. C., Hydrodeoxygenation of phenolic components of wood-derived oil. *Preprints-American Chemical Society. Division of Petroleum Chemistry* **1983,** *28* (3), 667-674.

25. Baker, E. G.; Elliott, D. C., Method of upgrading oils containing hydroxyaromatic hydrocarbon compounds to highly aromatic gasoline. Google Patents: 1993.

26. (a) Gevert, B. S.; Otterstedt, J. E., Upgrading of directly liquefied biomass to transportation fuels — hydroprocessing. *Biomass* **1987,** *13* (2), 105-115; (b) Gevert, B.; Andersson, P.; Jaeras, S.; Sandqvist, S., Hydroprocessing of desalted directly liquefied biomass. *Prepr. Pap., Am. Chem. Soc., Div. Fuel Chem.;(United States)* **1988,** *33* (CONF-8809228-).

27. Soltes, E.; Lin, S., Catalyst Specificities in High Pressure hydroprocessing of Pyrolysis and Gasification Tars. *screening* **1987,** *2*, 31.

28. (a) Elliott, D.; Baker, E. *Hydrotreating biomass liquids to produce hydrocarbon fuels*; Pacific Northwest Lab., Richland, WA (USA): 1986; (b) Baker, E.; Elliott, D.,

Catalytic upgrading of biomass pyrolysis oils. In *Research in thermochemical biomass conversion*, Springer: 1988; pp 883-895.

29. Kaiser, M., Upgrading of fast pyrolysis liquids by DMT. *Biomass gasification & pyrolysis: state of the art and future prospects* **1997**, 399-406.

30. Gagnon, J.; Kaliaguine, S., Catalytic hydrotreatment of vacuum pyrolysis oils from wood. *Industrial & engineering chemistry research* **1988,** *27* (10), 1783-1788.

31. Mortensen, P. M.; Grunwaldt, J. D.; Jensen, P. A.; Knudsen, K. G.; Jensen, A. D., A review of catalytic upgrading of bio-oil to engine fuels. *Applied Catalysis A: General* **2011,** *407* (1–2), 1-19.

32. (a) Adjaye, J. D.; Bakhshi, N. N., Production of hydrocarbons by catalytic upgrading of a fast pyrolysis bio-oil. Part I: Conversion over various catalysts. *Fuel Processing Technology* **1995,** *45* (3), 161-183; (b) Adjaye, J. D.; Bakhshi, N. N., Production of hydrocarbons by catalytic upgrading of a fast pyrolysis bio-oil. Part II: Comparative catalyst performance and reaction pathways. *Fuel Processing Technology* **1995,** *45* (3), 185-202.

33. Peng, J.; Chen, P.; Lou, H.; Zheng, X., Catalytic upgrading of bio-oil by HZSM-5 in sub- and super-critical ethanol. *Bioresource Technology* **2009,** *100* (13), 3415-3418.

34. Adam, J.; Antonakou, E.; Lappas, A.; Stöcker, M.; Nilsen, M. H.; Bouzga, A.; Hustad, J. E.; Oye, G., In situ catalytic upgrading of biomass derived fast pyrolysis vapours in a fixed bed reactor using mesoporous materials. *Microporous and Mesoporous Materials* **2006,** *96* (1–3), 93-101.

35. Ibáñez, M.; Valle, B.; Bilbao, J.; Gayubo, A. G.; Castaño, P., Effect of operating conditions on the coke nature and HZSM-5 catalysts deactivation in the transformation of crude bio-oil into hydrocarbons. *Catalysis Today* **2012,** *195* (1), 106-113.

36. (a) Chiaramonti, D.; Bonini, M.; Fratini, E.; Tondi, G.; Gartner, K.; Bridgwater, A. V.; Grimm, H. P.; Soldaini, I.; Webster, A.; Baglioni, P., Development of emulsions from biomass pyrolysis liquid and diesel and their use in engines--Part 2: tests in diesel engines. *Biomass and Bioenergy* **2003,** *25* (1), 101-111; (b) Chiaramonti, D.; Bonini, M.; Fratini, E.; Tondi, G.; Gartner, K.; Bridgwater, A. V.; Grimm, H. P.; Soldaini, I.; Webster, A.; Baglioni, P., Development of emulsions from biomass pyrolysis liquid and diesel and their use in engines--Part 1 : emulsion production. *Biomass and Bioenergy* **2003,** *25* (1), 85-99.

37. Ikura, M.; Stanciulescu, M.; Hogan, E., Emulsification of pyrolysis derived bio-oil in diesel fuel. *Biomass and Bioenergy* **2003,** *24* (3), 221-232.

38. Lu, Q.; Zhang, J.; Zhu, X., Corrosion properties of bio-oil and its emulsions with diesel. *Chin. Sci. Bull.* **2008,** *53* (23), 3726-3734.

39. Czernik, S.; French, R.; Feik, C.; Chornet, E., Hydrogen by Catalytic Steam Reforming of Liquid Byproducts from Biomass Thermoconversion Processes. *Industrial & Engineering Chemistry Research* **2002,** *41* (17), 4209-4215.

40. Garcia, L.; French, R.; Czernik, S.; Chornet, E., Catalytic steam reforming of bio-oils for the production of hydrogen: effects of catalyst composition. *Applied Catalysis A: General* **2000,** *201* (2), 225-239.

41. Byrd, A. J.; Kumar, S.; Kong, L.; Ramsurn, H.; Gupta, R. B., Hydrogen production from catalytic gasification of switchgrass biocrude in supercritical water. *International Journal of Hydrogen Energy* **2011,** *36* (5), 3426-3433.

42. Kruse, A.; Dinjus, E., Hot compressed water as reaction medium and reactant: Properties and synthesis reactions. *The Journal of Supercritical Fluids* **2007,** *39* (3), 362-380.

43. Shaw, R. W.; Brill, T. B.; Clifford, A. A.; Eckert, C. A.; Franck, E. U., Supercritical water: A medium for chemistry. *Chem. Eng. News* **1991,** *69* (51), 26-39.

44. Gupta, R. B., Supercritical Water Oxidation. *Encyclopedia of Chemical Processing* **2006,** *5*, 2927-2943.

45. Savage, P. E., A perspective on catalysis in sub- and supercritical water. *The Journal of Supercritical Fluids* **2009,** *47* (3), 407-414.

46. (a) Beta, I.; Li, J.-C.; Bellissent-Funel, M.-C., A quasi-elastic neutron scattering study of the dynamics of supercritical water. *Chemical physics* **2003,** *292* (2), 229-234; (b) Svishchev, I. M.; Plugatyr, A. Y., Hydroxyl radical in aqueous solution: computer simulation. *The Journal of Physical Chemistry B* **2005,** *109* (9), 4123-4128.

Chapter 2

Syngas Production by Hydrothermal Carbonization and Gasification of Biomass

2.1 Introduction

Gasification converts carbon-containing feedstock into a synthetic gas comprising of hydrogen, carbon monoxide, etc.[1] Gasification of biomass into fuel gases, such as synthesis gas or producer gas, is a promising route to produce renewable fuels, which is commonly accomplished via partial oxidation of the feedstock using sub-stoichiometric air or oxygen or by indirect heating with or without steam. Typically, gasification is performed using relatively dry feedstock with moisture < 10 wt% at 700-1000 °C and near ambient pressures. Steam gasification is less costly than oxygen gasification and yields a better quality gas than air gasification with a medium heating value of 15-20 MJm^{-3}.[1] Among the multitude number of uses, the synthesis gas or "syngas" can be utilized to produce liquid fuels by Fischer-Tropsch synthesis. Figure 2.1 illustrates the different possible uses of the syngas produced after biomass gasification.

The use of sub- and super- critical water (SCW) for gasification in lieu of organic solvents has several environmental advantages.[2] Compared to ambient water, SCW, above its critical point at 374 °C and 220 bar, has unique physical and chemical properties that make it suitable to use as a medium for organic chemistry. Section 1.4

gives more details about the unique properties of supercritical water but the most relevant ones are highlighted in this paragraph. Due to its significantly low dielectric constant and hydrogen bonding, SCW in high-temperature and low-density environment is more suitable for free radical reactions as compared to ionic reactions.

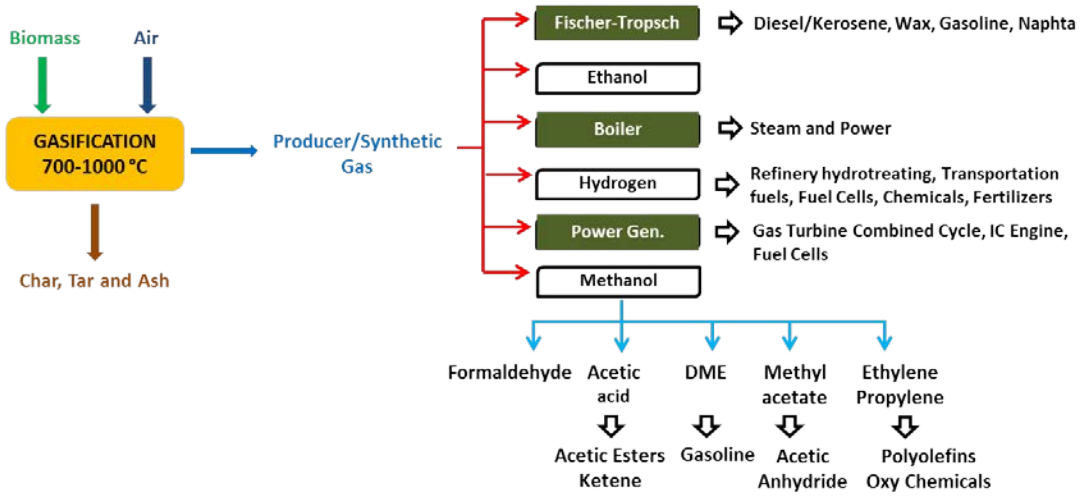

Figure 2.1 Possible uses of synthetic gas produced from biomass gasification

Interestingly, both the ionic product and the dielectric constant can be regulated by varying pressure and/or temperature.[3] SCW exhibits high diffusion rates, low viscosity and is miscible with light gases, hydrocarbons and aromatics.[4] Also, SCW has a higher density than low pressure steam, resulting in a high space-time yield.[5] In SCW medium, reactions can take place in a single phase as opposed to multiphase if conventional conditions are to be used.[2] Furthermore, the homogeneous reaction medium with a minimal mass transfer resistance favors decomposition of organic compounds into gases, decreasing formation of tar and char. This is a significant benefit over the conventional gasification of biomass.[6]

2.1.1 Supercritical Water Gasification of Biomass

Supercritical water gasification (SCWG) can utilize wet feedstock and has high gasification efficiency at comparatively low temperatures (e.g., 400-700 °C). There are two types of SCWG operations: (a) low-temperature ranging from 350 to 600 °C in the presence of metal catalysts, and (b) high-temperature ranging from 500 to 750 °C without catalyst or using non-metallic catalysts.[7] For example, for hydrogen formation from biomass, Watanabe et al.[8] used zirconia (ZrO_2) to catalyze the reaction while Elliott et al.[9] and Byrd et al.[10] demonstrated the significant activity of Ru, Rh and Ni as catalysts. Most of the gasification experiments usually yield a combination of liquid biocrude, syngas, and solid biochar products. Compared to atmospheric gasification, SCW gasification has a number of advantages. The homogeneous SCW medium lowers resistance to transport of the reactants and there is less residual tars and chars due to high solid conversion. The operating conditions produce hydrogen at thermodynamic equilibrium, meaning that the gas yields are high with higher hydrogen content. Also, the so produced hydrogen is at high pressure and allows for smaller reactors and lower energy requirements for subsequent pressurization.[11]

Gasification valorizes the low or negative-value feedstocks through their conversion to marketable fuels and products. Mimicking the commercial manufacture of hydrogen from catalytic steam reforming of methane, steam reforming of biomass (using cellulose as the model compound) was proposed as an alternative means to produce H_2 at a competitive price. The steam reforming of levoglucosan, formed by the pyrolysis of cellulose, is represented by the equation below:[7]

$$C_6H_{10}O_5 + 7H_2O \rightarrow 6CO_2 + 12H_2 \quad (2.1)$$

In the 1970s, Antal[12] predicted the thermodynamic equilibrium of the temperature and pressure effects on the cellulose steam reforming reaction and it was reported that above 600 °C, there would be no carbon residues with a gas rich in hydrogen with CH_4, CO and CO_2. However, as predicted by other studies,[13] at atmospheric conditions biomass does not react with steam to produce the desired synthesis gas due to the formation of char, tar, and higher hydrocarbons in the produced gas. The experiments performed by Modell[14] by immersing maple wood sawdust in SCW solved some of these problems. He found that the sawdust decomposed very quickly to tars and gases without char formation. Even though cellulose is the most stable biomass component, it undergoes rapid decomposition above the critical temperature of water.[15] Hot liquid water of around 190 °C partly decomposes lignin and hemicelluloses to form solvolysis products which undergo a variety of isomerization, dehydration, fragmentation and condensation reactions to ultimately form gas and tars if the temperature is increased.[16] But above 600 °C and the critical pressure of 220 bar, hydrothermolysis of the lignocellulosic biomass yields a gas composed mainly of H_2, CH_4, CO and CO_2 with some tar, implying that char formation has been suppressed while tar gasification is the main hurdle towards complete biomass gasification.[17]

The use of reduced nickel catalysts in sub and SCW gasification resulted in methane rich gas.[18] Minowa et al.[19] also used reduced Ni and some other alkali salts as their catalysts to liquefy/gasify cellulose at 200-400 °C and 80-220 bar. At 400 °C, the gas produced composed mainly of CH_4 and CO_2 with a reduction in residual chars and tars and conversion yields of up to 70%. For the operating conditions used, they concluded that hydrolysis reactions were crucial in biomass decomposition. The use of

Ni and Ru catalysts was investigated by the Pacific Northwest Laboratory by Elliot's group.[9, 20] Organic wastes were gasified in both sub- and SCW in a batch reactor at 350 °C and 200 bar for 2 hours to obtain conversion yields of 85%. The study highlighted the transformation of aromatic and aliphatic hydrocarbons into methane gas due to the presence of the hydrogenation catalysts. Corella et al.[21] investigated the effect of magnesium and calcium oxides on tar and char formation as well as on the gas yields. The catalysts studied were dolomite (MgO-CaO), pure calcite (CaO) and pure magnesite (MgO) at temperatures ranging from 780-910 °C with different contact times and catalyst particle sizes. In another study, several feedstocks[22] including corn- and potato-starch gels, wood sawdust suspended in a cornstarch gel, and potato wastes, were gasified in SCW (650 °C and 220 bar) in tubular flow reactors. A packed bed of carbon was used as the catalyst and it was observed that the organic content of these feedstocks vaporized to give a clean water effluent. Very high yields (>2 L/g) of gas with 57 mol% hydrogen were obtained but the reactors plugged after 1-2 hours of operation due to ash content and some char formation.

2.1.2 Rationale for Supercritical Water Gasification of Biochar instead of Biomass

The direct gasification of biomass has several drawbacks due to high moisture content, low mass and energy densities, and feeding challenges due to fibrous nature.[23] High transportation and storage costs and poor grindability also contribute to the disadvantages of gasifying biomass directly. Poor grindabililty leads to coarse biomass particles resulting in incomplete burnout, sedimentation and poor mixing.[24] On the other hand, biochar has low moisture retention, high heating value, is not perishable and is

easily compacted or fluidized.[25] Biochar is hence a more attractive option for gasification. Also, the use of biochar for gasification would provide another opportunity to use solid biochar produced from any biomass conversion process, and hence improving the overall carbon and energy recovery from the biomass. In industrial application, biochar can be produced at a remote site where biomass is available, and after pelletization and transportation, biochar can be used at the centralized facility to either produce syngas for FT fuels or as a feedstock for other products (Figure 2.1).

In this study, biochar refers to the carbon-rich solid product obtained after the carbonization of biomass in hydrothermal (subcritical water) medium.[26] The resulting biochar may be a valuable feedstock for gasification since the product has uniform carbon content of about 70 wt%, and a relatively high heating value (HHV) of about 28-29 kJ/g comparable to 33-34 kJ/g for coal. Even though biochar has a high potential as a fuel or carbon-rich material, very few studies have explored its gasification.[23] Mostly, research on biochar has been geared towards applying it as a soil additive as a means to sequester atmospheric CO_2[26] or as a way to immobilize soil contaminants like heavy metals and releasing essential nutrients like sulfur.[27] However, some studies[23, 28] have demonstrated that the inherent alkali and alkaline earth metallic species (i.e., K, Na and Ca) in the mallee biochar played an important role in the biochar steam gasification and concluded that the biochar was an attractive option as a possible source of energy. One recent study[29] gasified biochar from empty fruit bunches (EFB) in a fluidized bed using air at 500–850 °C. High temperature promoted H_2 production which increased from 5.53% (500 °C) to 27.97% (850 °C) (v/v), with a heating value of 30 kJ/g. At the same time, carbon conversion increased from 76% to 84%. Therefore, the use of biochar as a

renewable energy source providing an alternative path to biofuels is promising. Since not much literature is available for biochar gasification in hydrothermal medium, work done in the field of coal SCWG will be used as reference.

2.1.3 Supercritical Water Gasification of Coal

SCW has been utilized to gasify coal. For example, Hui[4] obtained gas containing 70% hydrogen from gasification of a 24 wt% coal-water-slurry with 2 wt% sodium carboxymethyl cellulose and 1 wt% K_2CO_3 at 580 °C and 250 bar using a fluidized bed reactor. Upon co-liquefaction with cellulose, Matsumara[30] observed an increase in hydrogen to carbon and oxygen to carbon ratios in the water-soluble product. Yamaguchi[31], for SCW gasification of Victorian brown coal without any catalyst, concluded that temperature and feed concentration had a significant effect on hydrogen yield which can be increased from 7 to 30 wt% when temperature was changed from 600 to 800 °C. Previous studies [32] on coal chars and activated carbon have demonstrated that potassium carbonate is an effective catalyst for gasification and acts as an oxygen transferring medium, resulting in hydrogen-rich gas. The gasification rate of activated carbon in SCW was investigated and was found to be independent of the total pressure when operating above the critical pressure of water.[33] The study also concluded that methane formation was more likely to be from pyrolysis of the activated carbon rather than resulting from the reaction between carbon and water. They observed an increase in the specific surface area when the activated carbon was subjected to short-term gasification. Lee[34] demonstrated that a binary catalyst consisting of K_2SO_4 and $Ni(NO_3)_2$ exhibited a high catalytic activity on char at 800-850 °C. Others have

demonstrated that calcium hydroxide can also be used as a catalyst and a CO_2 absorbent.[35] Here, temperatures below 650 °C were used to avoid formation of eutectic mixture of calcium compounds to prevent reactor blockage [35c] and to achieve a high carbon conversions (60-80%). Furthermore, Wang[35a] demonstrated that the presence of $Ca(OH)_2$ facilitated the extraction of volatile matter and catalyzed the gasification of char, with increasing yields of H_2 and CH_4. A new process to gasify coal in SCW was developed by Li et al. [36] using a temperature range of 650-800 °C and pressure of 230-270 bar with K_2CO_3 as catalyst and a slurry-like feedstock of 16 wt% coal and 1.5 wt% sodium carboxymethyl cellulose. This process yielded nearly 73% hydrogen with supercritical water playing a role in coal desulphurization.

2.1.4 Objectives of this Study

In this work, the gasification enhancement concept is demonstrated with switchgrass biomass. Alamo variety of switchgrass (*panicum virgatum* species) is used whose characterization has been previously reported (Table 2.1).[37]

Table 2.1 Composition (wt %) of Switchgrass

Glucan	Xylan	Galactan	Arabinan	Klason lignin	Acid soluble lignin	Ash	Acetic Acid
39.5	22.4	1.4	2.9	22.2	1.3	2.2	4.1

C	N	Ca	K
44.61	0.74	0.22	0.57

During hydrothermal treatment, biomass shrinkage occurs but the biochar retains the rudimentary porosity and structure due to its original cellular skeleton. Also, above 120 °C, organic materials in the biomass undergo hydrothermal decomposition with hemicelluloses degrading at 200-260 °C, cellulose at 240-350 °C and lignin at 280-500 °C.[26] The inorganic portion (ash content in switchgrass is 1.3%) also influences the physical structure of the biochar. In this work, biochar is first produced from switchgrass through hydrothermal carbonization. The effect of pretreating or passivating the switchgrass with calcium hydroxide during the production of biochar is also studied. Figure 2.2 depicts the process schematic.

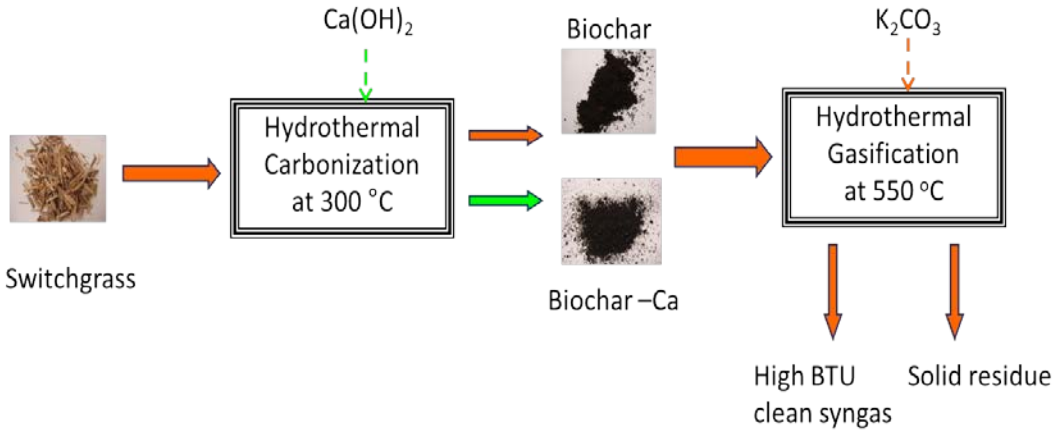

Figure 2.2 Process schematic for biochar production and gasification

$Ca(OH)_2$ was chosen since it had been used before to catalyze coal char gasification.[38] Investigation of both thermal and hydrothermal gasification of switchgrass biochar and the effect of adding K_2CO_3 is also looked into since this catalyst has been proven to be quite effective in biomass gasification.[39] The temperature chosen for hydrothermal gasification is kept below 650 °C to avoid formation of eutectic calcium compounds.[35c]

The key objectives are to understand the thermal and hydrothermal gasification behavior of biochar, the effect of K_2CO_3 catalysis, and whether $Ca(OH)_2$ pretreatment of switchgrass affects the inherent characteristics of the biochar.

2.2 Experimental Section

2.2.1 Biochar Production

2.2.1.1 Biochar

Alamo switchgrass having 7.3 wt% moisture and 5-10 mm length (i.e., chopped) was used as the starting biomass. It was hydrothermally carbonized to produce biochar in a 500 ml hastelloy autoclave high temperature bolted reactor (Figure 2.3).

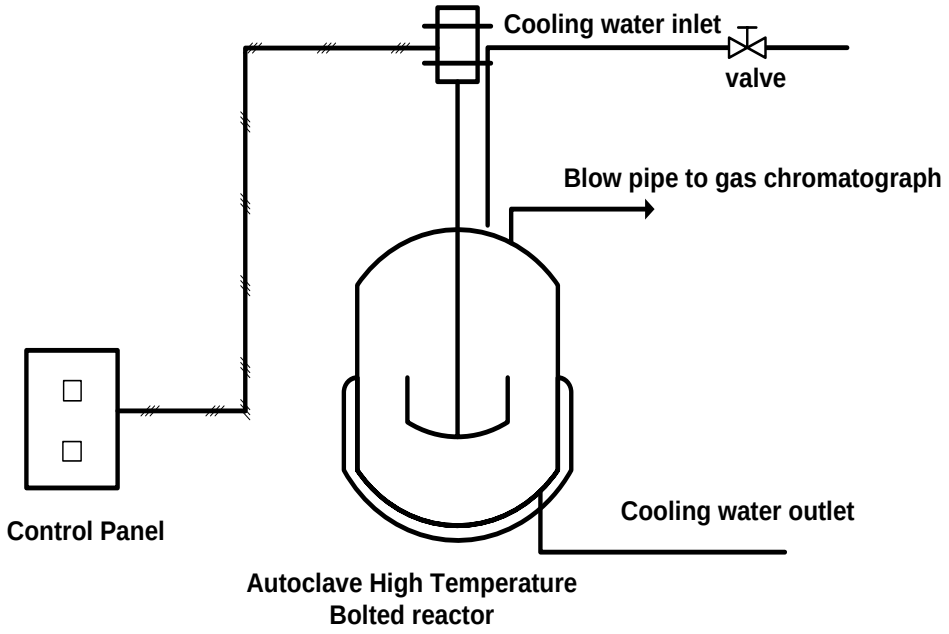

Figure 2.3 Apparatus for biochar production

The water to biomass ratio was kept at 7:1 on mass basis. The reactor was heated at a rate of 7 °C/min from ambient to 300°C where it was maintained for thirty minutes. After

carbonization, the reactor was rapidly cooled by flowing ambient water in the cooling coil, the reactor was opened and the biochar was separated from the liquid product. The biochar was air dried for further analysis and used for the subsequent gasification studies. Table 2.2 summarizes the experiments performed.

Table 2.2 Yields of biochar obtained from different runs

Run No.	Dry Weight of Switchgrass, g	Biochar	
		Dry weight, g	HHV, KJ/g
1	41.7	18.6	28.3
2	41.8	18.3	28.9
3	41.1	17.5	28.7

2.2.1.2 Passivated Biochar (Biochar-Ca)

Passivated biochar was produced at the same conditions as biochar, but 5 wt% calcium hydroxide (obtained from Sigma Aldrich with >95% purity) was also added to the switchgrass. The term 'passivation' is explained in Section 2.4.5 whereby the addition of $Ca(OH)_2$ has been seen to render the ash content inactive (therefore passivating the minerals) by reacting with them and/or by altering their properties. Also, the reaction time was shortened to 5 minutes instead of thirty minutes. The aim was not to let the calcium hydroxide turn to carbonate so that there would be formation of the oxygenated complexes on the carbon surface to enhance gasification (as detailed in Section 2.4.5). Also, the addition of calcium hydroxide catalyzed, to a certain extent, the biochar formation reaction, therefore less residence time was needed.

2.2.2 Biochar Gasification

2.2.2.1 Biochar

Air dried biochar had a moisture content of around 2.5 wt% and an HHV of 28.8 kJ/g while biochar-Ca had a moisture content of 1.5 wt% with an HHV of 26.8 kJ/g. Table 2.3 gives a detailed elemental analysis obtained by inductively coupled plasma ion-spectrometry. As compared to biochar, biochar-Ca has slightly less carbon and much higher calcium content due to the passivation treatment. It is to be noted that the remaining components are hydrogen, nitrogen and sulphur which constitute less than 7 wt% of the dry biomass.

Table 2.3 Compositions of switchgrass, biochar and biochar-Ca

ELEMENTS	C	O	Ash	Ca	K	Mg	P	Fe	Mn	Na	Pb
		wt%		ppm							
Switchgrass	44.6	48.6	1.3	2105	4082	4514	941	115	48	701	1
Biochar	70.5	22.5	3.2	2029	665	2215	481	258	53	395	<0.1
Biochar-Ca	68.28	24.8	5.6	10893	293	2885	1706	3244	126	891	4

2.2.2.2 Gasification Apparatus

Figure 2.4 shows a schematic of the biomass gasification apparatus. It consists of a high-pressure stainless steel reactor tube with 1 in. internal diameter and 80 ml internal volume, which was heated using an electrical furnace. The temperature inside the reactor was measured using a 1/16 in. thermocouple (T1) placed inside the reactor so that the end tip was in the middle of the reactor.

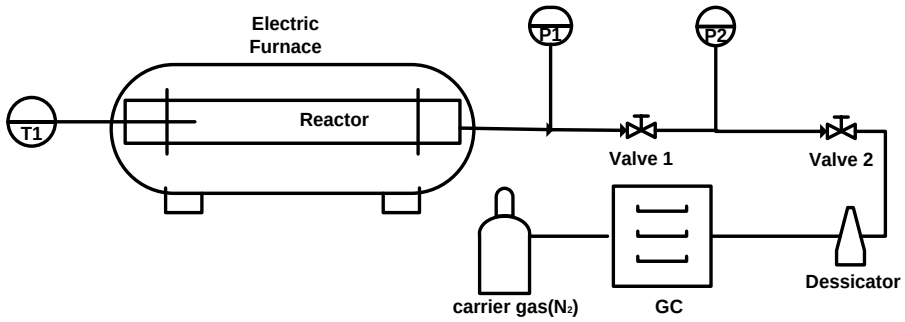

Figure 2.4 Apparatus for biochar gasification

This thermocouple was calibrated before the start of the experiment with an accuracy of ± 0.1 °C. The real-time temperature indicated by this thermocouple was used for all the analyses. At the other end of the reactor, two pressure gauges were connected to record the pressure inside the reactor. P1 recorded the pressure of the gas and had a range of 345 bar while P2 (which is disabled when the system is at > 34 bar) measured the pressure in the range of 0-34 bar. The reason for having a second pressure gage was to be able to get more accurate gas pressure readings below 34 bar. The gas outlet line was connected to a gas chromatograph (GC) to analyze the gaseous products.

2.2.2.3 Experimental Procedure

2.2.2.3.1 Thermal Gasification

In this series of experiments, 1 g (dry weight) of biochar was gasified at temperatures of 550, 650 and 1000 °C. Each time, the reactor was loaded with the biochar and then placed inside the furnace. A stainless steel frit (pore size 2 µm) was placed at the outlet of P2 to prevent entrainment of solids into the GC connecting line.

The temperature of the furnace was set such that the thermocouple T1 would give the desired reaction temperature. Reaction time would start when the desired temperature (indicated by T1) was reached inside the reactor and reaction completion would depend mainly on the set temperature and gas pressure inside the reactor. The reaction was deemed completed when the pressure gage, P1, gave a stable reading for at least 10 minutes. For thermal gasification, reaction completion time had no typical range since the latter varied between 50-275 minutes depending on the temperature chosen. In other words, 50 minutes were needed to complete the reaction at 1000 °C while 275 minutes were required for reaction at 550 °C. After reaction completion, the furnace was switched off and the reactor was allowed to cool. As soon as the pressure reached below 34 bar, valve 1 was opened so that a more accurate reading of the pressure could be obtained from P2. Upon cooling, the temperature and residual pressure due to gas formation were noted before valve 2 was opened so that the gas could be analyzed by the GC. The solid residue was collected from the reactor by washing with deionized water and acetone and then dried for further analysis.

2.2.2.3.2 Hydrothermal Gasification

In a typical experiment, 1g (dry basis) of biochar was added to 10-12 ml of distilled water to form a slurry which was then loaded into the reactor. A desired amount of K_2CO_3 (obtained from Sigma Aldrich with >95% purity) was added to water for catalytic runs. It is to be noted that in this document, 'wt%' refers to the weight of the catalyst divided by the total weight of the dry biomass and catalyst. This does not include the solution weight. The same heating/cooling procedure as in thermal gasification was

performed, and at the end, liquid, solid, gas phases were collected for analysis. For all the hydrothermal experiments, a stainless steel frit of pore size 10 µm was placed at downstream end of the reactor before closing the vessel and connecting to P1. The experiments were carried out at 400, 500, 550, 600, and 650 °C. Typical reaction time for hydrothermal gasification ranged from 25 to 40 minutes and the pressure from 242 – 277 bar. However, pressure for some runs namely 4, 5 & 9 only reached around 201 bar which is near-critical at such temperatures (>400 °C). Table 2.4 gives the detailed experimental conditions for each run.

2.3 Product Characterization

2.3.1 Gas Chromatography (GC) Analysis

The gas composition was determined using a gas chromatograph (SRI 8610C) equipped with a thermal conductivity detector (TCD) and a 60/80 carboxen-1000 carbon molecular sieve column (Supelco 15 ft x 1/8 in.) using nitrogen as the carrier gas. Sample injection to the GC was done online by means of a six-port injection valve having 100 µL sample loop. Carbon gasification efficiency was calculated as follows:

$$\textit{Carbon Gasification Efficiency (\%)} = \frac{\frac{PV}{RT} \times (x_{CO2} + x_{CO} + x_{CH4}) \times 12}{W_C \times m}$$

where P and T are the residual pressure and temperature, respectively, obtained after cooling while V is the effective volume of the reactor. x_{CO2}, x_{CO}, x_{CH4} are the mole percents of CO_2, CO and CH_4 formed, respectively, obtained by the GC analysis while W_C is the carbon fraction in biochar. The carbon fraction, as measured by the proximate analysis (Table 2), was 0.70 in biochar and 0.68 in biochar-Ca. m is the dry weight of

biochar. For biochar-Ca, the amount of calcium hydroxide was subtracted from total dry weight to get *m*. Since the amount of calcium hydroxide was known and using the assumption that all $Ca(OH)_2$ was converted to calcium carbonate during gasification (no peaks of $Ca(OH)_2$ were seen in XRD), the amount of CO_2 absorbed by the $Ca(OH)_2$ was also taken into consideration when calculating carbon gasification efficiency. All measurements were at least taken in triplicate to ensure accuracy and had a standard deviation of around 2 %.

2.3.2 X-Ray Diffractometer (XRD) Analysis

A Rigaku Miniflex powder X-ray diffractometer was used with a Cu $K\alpha_1$ radiation source at 30 kV, 15 mA, a miniflex goniometer and a graphite monochrometer. Diffraction patterns were collected in the 2Θ range of 10-35° at a scan speed of 1^o/min and step size of 0.05°.

2.3.3 Fourier Transform Infrared (FTIR) Analysis

A Nicolet IR100 FTIR spectrometer with infrared spectra of 4000-400 cm^{-1}, was used for the analysis. The equipment used a TGS/PE detector and a silicon beam splitter with 1 cm^{-1} resolution. Samples were oven dried at 105 °C[40] and mixed with KBr to prepare the sample discs. The spectrum of a similar-thickness KBr disc was subtracted from the spectrum of each individual sample.

2.3.4 Scanning Electron Microscope (SEM) Analysis

The biochar and solid residue samples were prepared onto adhesive carbon tape on an aluminum stub, followed by gold sputter coating. An environmental scanning electron microscopy system (Zeiss EVO 50) was used to determine the surface morphology of the samples.

2.3.5 Total Organic Carbon (TOC) Analysis

The liquid products were centrifuged at 3600 rpm, before the TOC was determined by the Shimadzu TOC-V_{CSN} analyzer.

2.4 Results and Discussions

2.4.1 GC Analysis

2.4.1.1 Comparison between Thermal and Hydrothermal Gasification of Biochar

Table 2.4 summarizes the different experimental conditions used to gasify biochar as well as the corresponding carbon gasification efficiency achieved.

Table 2.4 Gasification conditions and results for different runs using biochar*

Gasification type	Set ID	Run no	Temperature °C	K_2CO_3 (wt %)	$Ca(OH)_2$ (wt %)	Carbon Gasification Efficiency, %
Thermal	A	1	550	0	0	5.9
		2	650	0	0	8.5
		3	1000	0	0	41.7

Hydrothermal	B	4	400	0	0	10.3
		5	500	0	0	18.1
		6	550	0	0	23.8
		7	600	0	0	26.7
		8	650	0	0	38.5
Hydrothermal	C	9	500	2.5	0	15.7
		10	550	2.5	0	24.8
		11	600	2.5	0	35.7
	D	12	500	10	0	26.6
		13	550	10	0	28.6
		14	600	10	0	44.8
	E	15	500	25	0	28.7
		16	550	25	0	43.8
		17	600	25	0	38.0
	F	18	500	50	0	35.4
		19	550	50	0	60.6
		20	650	50	0	59.3
Hydrothermal	G	21	500	2.5	2.5	26.6
		22	500	2.5	5	22.5
		23	600	10	10	35.4

**Biochar: obtained by hydrothermally treating switchgrass at 300 °C for 30 minutes*

Figure 2.5 shows how carbon gasification varies with temperature for both thermal and hydrothermal gasification with and without catalyst. The thermal gasification required a much higher temperature to achieve the same gasification efficiency as hydrothermal gasification. For example, at 550 °C, carbon conversion amounted to 5.9% for conventional gasification versus 23.8% with hydrothermal gasification. These results confirm the advantage of using SCW to gasify biochar. The reaction time was also reduced to 30 minutes during hydrothermal gasification. It has also been noticed that for both gasification types, as the temperature was increased, the fraction of hydrogen increased. For thermal gasification, it is the enhancement of the endothermic combustion reactions that contribute to the hydrogen increase since the biochar utilizes the air enclosed in the reactor to combust. In case of SCWG, the formation of hydrogen from the reaction of carbon with SCW is also endothermic (equation 2.1) and therefore providing more heat enhanced hydrogen formation not only through combustion reactions but also through the water-gas shift reaction (equation 2.2).

$$CH_xO_y + (1-y)\,H_2O \longrightarrow CO + (1-y+x/2)\,H_2 \qquad (2.1)$$

$$CO + H_2O \longrightarrow CO_2 + H_2 \qquad (2.2)$$

For example, in hydrothermal gasification, H_2 in the gas increased from 0.3 to 29.8% as the temperature was increased from 400 to 650 °C while an increase from 7.6 to 29% was observed for thermal gasification from 550 to 1000 °C.

The addition of potassium carbonate enhanced the gasification of biochar. At 550 ^oC with 2.5 wt% catalyst, a conversion of 24.8 % was achieved while 28.6 %, 43.8% and 60.6% were obtained at the same temperature with the addition of 10, 25 and 50 wt% K_2CO_3, respectively. It is, however, interesting to note that increasing the temperature

further to 600 ^{o}C, for both 25 and 50% catalyst loadings, slightly decreased the carbon gasification efficiency, indicating that there is an optimum catalyst loading and temperature, beyond which there would be no benefit to gasification.

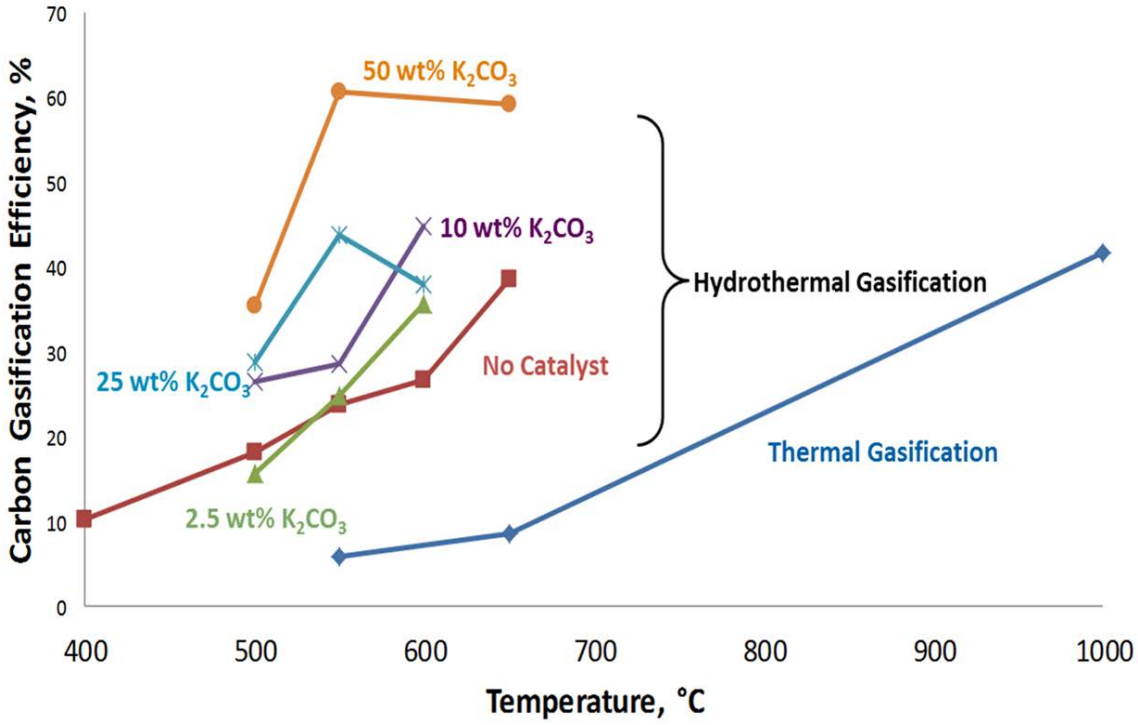

Figure 2.5 Comparison between thermal and hydrothermal gasification of biochar

At 600 °C, there was less methane formation and hence the slight decrease in the carbon gasification efficiency. Methane reforming may have taken place as explained in Section 2.4.1.4. Furthermore, this has been observed only in the case of sample id E (Table 2.4) at 25% catalyst loading. In all the other cases gasification is mostly higher at 600 ^{o}C. The overall effect of temperature and catalyst addition is further discussed in Section 2.4.1.4.

2.4.1.2 Effect of direct addition of Calcium Hydroxide to Biochar for Hydrothermal Gasification

As seen from Table 2.4 (Set ID: G), at 500 °C, as the calcium hydroxide percent increased from 2.5 to 5 wt%, the carbon gasification efficiency decreased from 26.6 to 22.5%, even though both biochar samples also contained 2.5 wt% K_2CO_3, suggesting that increasing calcium hydroxide percent may actually be detrimental to gasification. Comparing the carbon gasification efficiency obtained at the same temperature (500 °C) with only 2.5 wt% K_2CO_3, it was noticed that the gasification increased only slightly since 15.7% carbon gasification efficiency was obtained with 2.5 wt% K_2CO_3 alone. Another experiment was run at 600 °C with 10 wt% of both $Ca(OH)_2$ and K_2CO_3 whereby the carbon gasification efficiency dropped to 35.4% compared to 44.8% obtained with 10 wt% K_2CO_3 alone, implying that the addition of $Ca(OH)_2$ directly to the biochar was not beneficial to the gasification process. This may be due to the inaccessibility of minerals and cellulose in the biochar as detailed in Section 2.4.5.

2.4.1.3 Hydrothermal Gasification of $Ca(OH)_2$-Passivated Biochar (Biochar-Ca)

As described in the experimental procedures in Section 2.2.1.2, calcium hydroxide was added directly to the switchgrass during biochar-Ca production. Here, due to open cellular structure of switchgrass, $Ca(OH)_2$ can penetrate deep in the biomass and react with both organic and inorganic components at the molecular level. Biochar-Ca was hydrothermally gasified at 550 °C with 0, 10, 25, and 50 wt% K_2CO_3, giving gasification efficiencies of 30.9, 48.1, 61.8 and 49.6 %, respectively (Table 2.5).

Table 2.5 Gasification conditions and results for runs using biochar-Ca*

Gasification type	Set ID	Run no	Temperature (°C)	K_2CO_3 (% by weight)	Carbon Gasification Efficiency (%)
Hydrothermal	H	24	550	0	30.9
		25	550	10	48.1
		26	550	25	61.8
		27	550	50	49.6
		28	600	25	74.8

**Biochar-Ca: obtained by hydrothermally treating switchgrass at 300 °C for 5 minutes with 5 wt% $Ca(OH)_2$*

Here the temperature was set at 550 °C since biochar had given the highest carbon gasification efficiency at this temperature. It is noteworthy that 25 wt% catalyst gave a better carbon gasification efficiency than 50 wt%, suggesting that 50 wt% K_2CO_3 is probably in excess and that 25 wt% is sufficient. Also with biochar-Ca, only 25 wt% K_2CO_3 was needed to achieve nearly the same gasification (61.8%) as when using biochar (60.6%) but with 50 wt% catalyst. This further suggests that in the case of biochar, not all the catalyst was used to enhance gasification since a portion may also have reacted with the minerals present.[38] Therefore in biochar-Ca, more of the catalyst was made available since the minerals were passivated by the $Ca(OH)_2$ and could therefore not react with the catalyst. Furthermore, formation of C(O), an adsorbed oxygen/oxygenated species on the carbon surface is favored by addition of $Ca(OH)_2$[38] and this leads to further enhancement of the gasification of biochar. Section 2.4.5 gives

possible explanations of this phenomenon in more details. Moreover, by running an experiment at a higher temperature of 600 °C with 25 wt% catalyst (run 28 in Table 2.5), nearly 75% gasification was obtained. Figure 2.6 compares gasification efficiencies of biochar and biochar-Ca at the same conditions, from which it can be deduced that biochar-Ca gasified much easier than biochar.

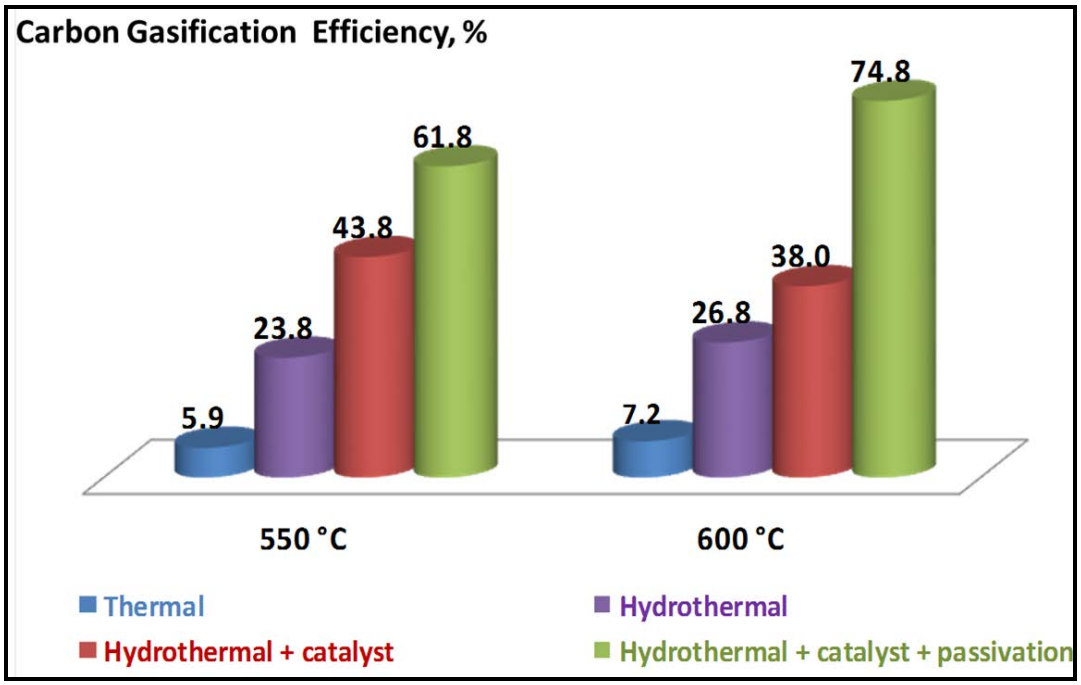

Figure 2.6 Comparison of carbon gasification efficiencies (%) of biochar and biochar-Ca

2.4.1.4 Overall Effect of Reaction Temperature and Catalysis on Gasification Rate

As expected, the carbon gasification efficiency increased with increasing temperature for hydrothermal gasification reactions since hydrogen formation is thermodynamically favored by the water gas shift (WGS) reaction ($CO + H_2O \rightarrow CO_2 + H_2$)[10, 36] due to the high water excess. Carbon gasification efficiency more than doubled

for the SCWG moving from 18.1 to 38.5% as the temperature rose from 500 to 650 °C. However, model compounds like glucose and glycerol exhibit high carbon gasification efficiency (75-90%) for solutions that contain >5 wt% organics, while pinewood, under identical conditions (700 °C in SCW), has a low conversion rate of 45%.[41]

Yamaguchi et al. [31] have also demonstrated that low carbon gasification efficiency (29.9 wt% at 800 °C) was obtained when Victorian brown coal underwent SCW gasification. These results correspond to the biochar gasification data obtained in this study, confirming that substances like lignin are very difficult to gasify. In non-woody biomass, lignin is crossed linked to cellulose and xylans via a range of bonds including covalent, hydrogen, ionic bonds and Van der Waals interactions.[42] This lignin and hemicelluloses complex interference also prevails to some extent in biochar rendering gasification more difficult since access is restricted. Also, glucose and glycerol are easily dissolved in water compared to pinewood, coal and biochar, resulting in the possibility that solubility may also have a role to play in gasification. Compared to a homogeneous gasification due to high solubility, in biochar gasification, there was no complete dissolution and uniform distribution, especially during the fast heating stage. The residue remaining after gasification was due to incomplete gasification of the biochar. Xu et al.,[17] using various charcoals as catalysts for SCWG of organic feedstocks, reported that temperatures above 600 °C and pressures above 250 bar were needed to achieve high gasification efficiencies. It is to be noted that in supercritical medium, temperature has more pronounced effect of reactions than the pressure. Studies by Antal[22] and Byrd[43] have demonstrated that pressure does not really impact on the gas yields.

However, various studies have also demonstrated that the use of appropriate catalysts can enhance gasification rate.[32, 34-35] Hence, in this study, catalysts have been used at various weight percents to determine their effect on the gas yields. Table 2.6 compares the gas fractions obtained when different feedstock to catalyst ratios were used at the same temperature.

Table 2.6 Summary of the gas composition from the different experiments at 550 °C

Run no	Gasification type	Biochar	K_2CO_3 Added (on dry basis) (wt %)	Rx Time (mins)	Composition of gas (mole %)				HHV MJ/Nm^3
					H_2	CO	CH_4	CO_2	
1	Thermal	biochar	0	275	7.6	0	6.7	86	3.4
6	Hydrothermal	biochar	0	30	8	13	21.8	58	10.7
10	Hydrothermal	biochar	2.5	30	25.3	0	20	55	10.6
13	Hydrothermal	biochar	10	35	11.5	9.3	26.5	53	12.5
16	Hydrothermal	biochar	25	35	43.5	1.4	22.7	32	13.9
19	Hydrothermal	biochar	50	90	50	0.6	23.3	29	14.9
26	Hydrothermal	biochar-Ca	25	30	43.7	1.1	23.5	32	14.3
27	Hydrothermal	biochar-Ca	50	30	45.3	6.5	23.9	24	15.3

The gas yields were enhanced as the catalyst weights were increased with the highest yield obtained when the biochar was pretreated first with $Ca(OH)_2$ and then gasified with 25 wt% K_2CO_3 as catalyst. At 550 ^oC and without any catalyst, the fraction of hydrogen

was 8 mol%, which is consistent with the data of Yamaguchi et al. [31] where 7 mol% H_2 was obtained from coal at 600 °C. The fraction of hydrogen increased as the reaction conditions were changed from thermal to hydrothermal medium and as more catalyst was used, reaching a maximum of around 45 mol%. Very likely, it is due to the enhancement of the WGS reaction ($CO + H_2O \rightarrow CO_2 + H_2$) in SCW, and explains the fact that very little CO was detected in most of the gaseous products. A higher yield of hydrogen was also due to gasification of the biochar in SCW, an endothermic reaction.[44] Usually, high temperatures favor free-radical reactions[36] and since hydrogen is a typical product of free-radical reactions, the gasification of char was enhanced. This statement was easily verified by the observation that during most of the experiments where temperatures greater than 500 °C were used, as soon as the temperature would reach around 515 °C, the temperature would decrease for about 10 minutes even though the furnace temperature continued increasing. Therefore, at this stage, the endothermic gasification reaction was dominant. After those 10 minutes, the endothermic reaction would stabilize and WGS reaction would take over, prompting the temperature to increase again. Methane reforming ($CH_4 + H_2O \rightarrow CO + 3H_2$) is often considered as one of the main SCWG pathways but it is known to progress very slowly in low temperature non-catalytic environments.[31, 45] This could explain as to why at 550 ^oC, methane did not undergo reforming and consequently, the gas streams contained about 20% methane in most of the runs where catalyst was used. It is to be noted that for some runs, traces of C_2 hydrocarbons (i.e., C_2H_4 and C_2H_6) were also detected during the gasification, but were not quantified due to their small concentrations.

Potassium carbonate is very soluble in water (1.56 g/cm^3 at 20 °C) and the maximum concentration used in the study was only about 0.05 g/cm^3, suggesting that the salt was mostly solubilized since it was not in excess. Salts are classified as Type 1 or Type 2 depending on their liquid phase solubility which changes with temperature in binary salt-water system saturated with the salt.[25] Potassium carbonate is a Type 1 salt which exhibits high salt solubility in the vicinity of critical point of water compared to Type 2 salts whose solubility in liquid solution decreases with temperature. The temperature and pressure of the hydrothermal environment dictate the solubility of the salts which as a general rule, decrease in supercritical water.[46] $Ca(OH)_2$ has low solubility in water and because its solubility might have decreased further in supercritical medium, solubility was not the driver for the reaction. Rather, as mentioned in section 2.4.5, $Ca(OH)_2$'s ability to form oxygenated complexes on the char surface and to alter the mineral content properties were the main drivers for gasification enhancement.

The HHV of the residual gases were also calculated from molar compositions and the corresponding gross heating value of each component gas. Baratieri et al.[47] pyrolyzed different species of biomass (bagasse, sawdust, grape stalks) at 800 °C and 1 bar to obtain syngas with HHV ranging from 7.3-10.6 MJ Nm^{-3} while Schmieder et al.[39] reported HHV ranging from 3.8-5.3 MJ Nm^{-3} by hydrothermally treating wood and straw at 450 °C. Furthermore, some experiments were carried out whereby switchgrass was hydrothermally gasified at 550 °C, with (10 wt%) and without K_2CO_3 and the HHV of the gases obtained ranged around 3-4 MJ /m^3, indicating the poor quality of the gases obtained from direct gasification of biomass. From Table 2.6, it can be deduced that hydrothermally treating biochar without any catalyst yields an HHV closer to pyrolyzed

biomass. Furthermore, Zheng et al.[48] compared the heating values of clean gas obtained from gasifying coal from 4 different gasifiers. The HHV of the gases ranged from 9-12 MJ/m^3 and are comparable with the HHV values obtained for biochar gasification in this study (Table 2.6). It is evident that the difference in operating procedures, equipment and scale of the gasification apparatus would impact on the HHV value but it can be concluded that the gas obtained from this study is of promising quality. Because of their individual gross calorific value, hydrogen and methane are the main gases contributing to the HHV value of the gas. The fraction of hydrogen in the product gas increased from 8% (run 6) to 25% (run 10) with use of only 2.5 wt% K_2CO_3 whereas CO percentage decreased. A similar trend was observed with further increase of K_2CO_3 percent (runs 16, 19, 26 and 27) due to the enhancement of the water-gas shift reaction as explained earlier.

2.4.2 XRD Analysis

As expected, the crystalline cellulosic peak observed at 22.7^o for switchgrass was not present in the biochar samples due to its degradation. Through the XRD spectra (Figure 2.7), it can be observed that the biochar structure is essentially amorphous in nature but it does contain some local crystallinity, which is in agreement with results of Lehmann et al. [26] The solid residue from runs 1, 6, 19 and 26 have been chosen since they were all obtained after conducting the experiments at 550 °C. It is interesting to note that the biochar samples and the solid residue remaining after thermal gasification at 550 °C have nearly the same intensities while the solid residue from the SCW gasification at 550 °C has lower intensity peaks, illustrating that the amorphous phases (including lignin) have undergone better thermal degradation when exposed to SCW. When catalyst was used to

enhance the reaction, the XRD peaks of the solid residues had even much lower intensities revealing that indeed K_2CO_3 contributed to enhance gasification.

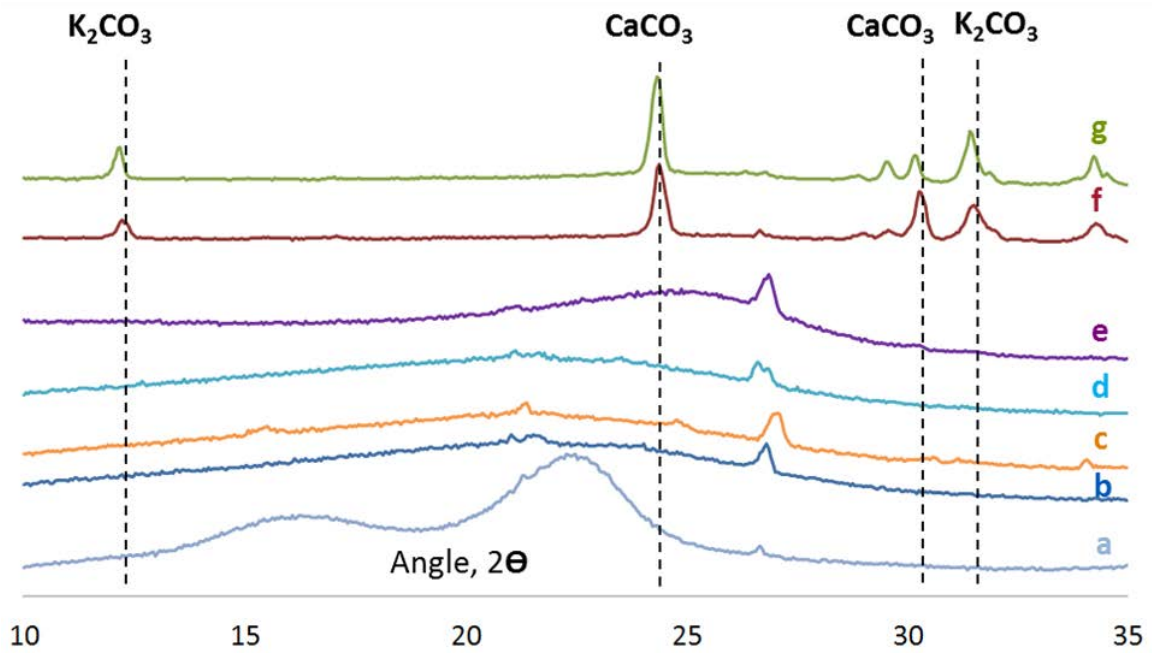

Figure 2.7 XRD plots of different samples (a) switchgrass, (b) biochar, (c) biochar-Ca, solid residues from runs (d) 1, (e) 6, (f) 19, and (g) 26

Runs 19 and 26 show nearly the same XRD profiles confirming that with biochar-Ca, only 25 wt% catalyst is enough to obtain the same carbon gasification efficiency as with biochar but with 50 wt% catalyst. It is to be noted that in the XRD plot of the solid residues with catalysts, the peaks at 12.8° and 30-34.3°, correspond to K_2CO_3 while the peaks at 24.2°and 29.4° [49] relate to the $CaCO_3$ present in the sample.

2.4.3 FTIR Analysis

From Figure 2.8, it can be seen that the peaks at 1060 cm^{-1} (C-O stretching) and 1160 cm^{-1} (C-O-C asymmetry stretching) in the switchgrass spectra were not present in both biochars spectra, revealing that at 300 ^{o}C, cellulose and hemicelluloses were thermally decomposed.

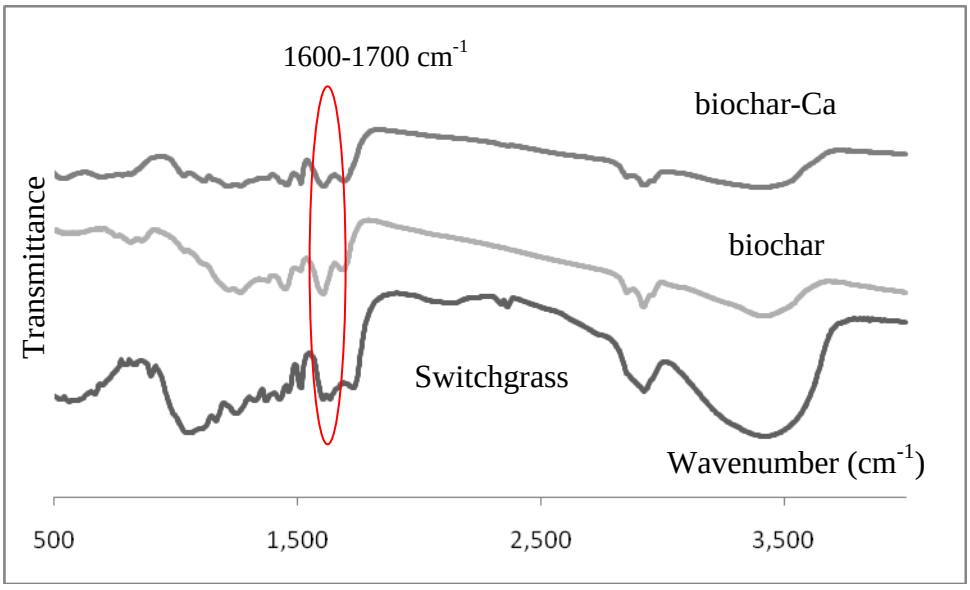

Figure 2.8 FTIR Spectra of switchgrass, biochar and biochar-Ca

Lignin, unlike cellulose, is aromatic and possesses olefinic carbon-carbon double bonds in cyclic structures and in side-chains.[50] Looking at the three spectra, absorption at 1515 cm^{-1} reveals the presence of aromatic skeletal vibrations, confirming the presence of lignin. Peaks at 3400 cm^{-1} indicate the presence of polymeric OH stretch in the switchgrass and the biochar samples but the shift to lower frequency of these bands suggest that the hydroxyl groups are involved in hydrogen bonds and are not "non-bonded" OH groups.[50]

The presence of methylene groups in all the samples was confirmed by absorbance at 2920 cm^{-1} and is related to the C-H asymmetric/symmetric stretch. Carbonyl stretching (C=O) was observed at about 1731 cm^{-1} in the switchgrass sample, indicating the presence of aldehydes while absorptions at 1685 cm^{-1} for both biochars suggest the presence of conjugated ketones. Absorption at 1600 cm^{-1} indicate C=C stretching, especially the olefinic vibrations due to lignin.[37] The band at 1245 cm^{-1} in the switchgrass may be connected to the esters and epoxides band as well as the acyclic C-O-C groups (related to lignin). As compared to biochar-Ca, the biochar has a higher band intensity in the range of 1700-1600 cm^{-1}showing that the corresponding higher reaction time resulted in an increase first in C=O and olefinic C=C and then aromatic C=C bonds. The presence of calcium hydroxide may have also contributed to the fact that the switchgrass did not undergo aromatization during the biochar-Ca production, and hence the lower intensities in the same range. This would explain why biochar-Ca underwent better gasification than biochar.

In Figure 2.9, the top spectrum is for biochar while the rest are for solid residues after gasification at 550 °C but at different conditions as summarized in Tables 2.4 & 2.5. The O-H stretching at 3420 cm^{-1} of the spectra present in the biochar sample has been reduced in intensity as the biochar underwent thermal and hydrothermal treatment. The addition of catalyst has resulted in further hydroxyl absorption and a similar trend was observed for the aliphatic CH, CH_2 stretching at 2918 cm^{-1}. However, the main changes in absorbance were noticed in the range of 600-1800 cm^{-1}. The 1680 cm^{-1} peak in the biochar corresponding to the carbonyl C=O stretching for polyxylose/conjugated ketones, are absent in the solid residue samples. The peaks corresponding to lignin in the biochar

were 1600 cm^{-1} (C=C stretching), 1517 cm^{-1} (benzene ring stretching), 1448 cm^{-1} (CH_2 benching) and 1266 cm^{-1} (C-O-C stretching in alkyl aromatic).[51]

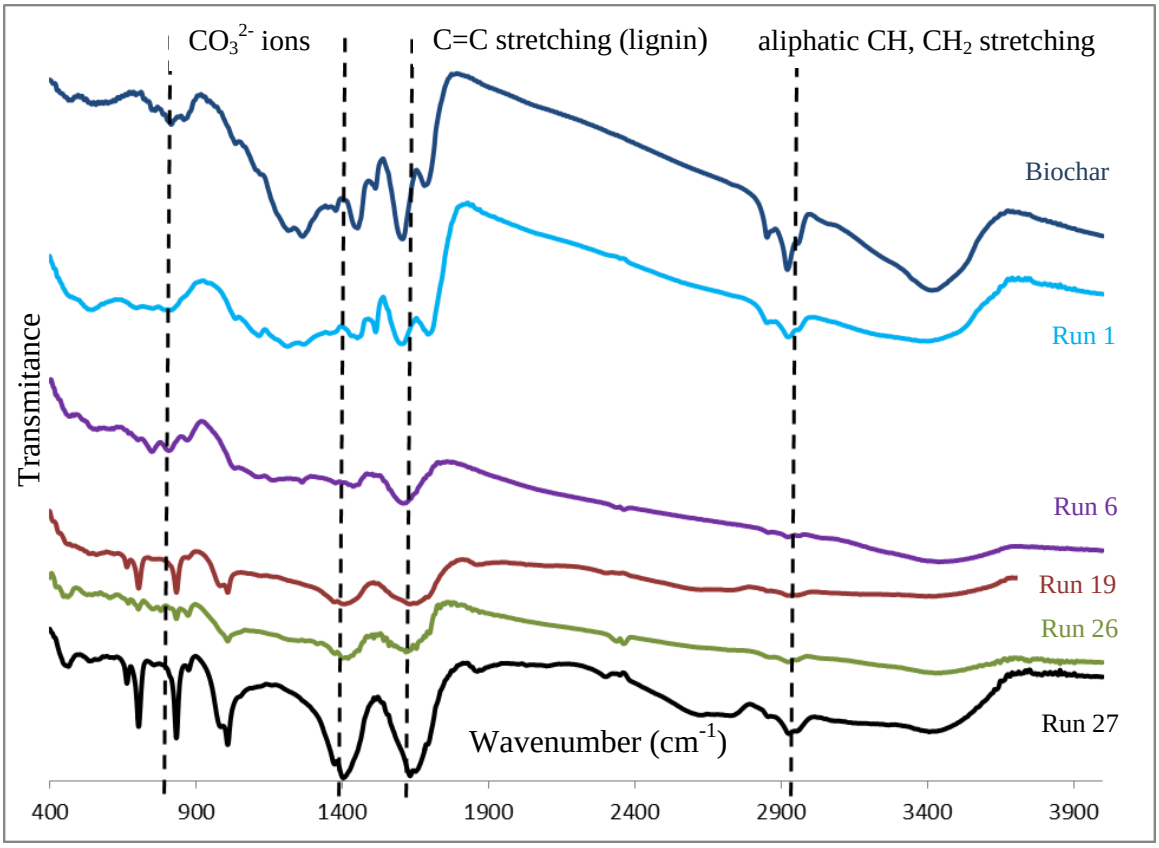

Figure 2.9 FTIR spectra of biochar and solid residues

All the solid residues had the above peaks but the spectra from runs 19 and 26 did not have a high concentration of C=C, especially the spectrum of run 26 confirming that the pretreatment, with $Ca(OH)_2$, may have hindered the aromatization of the biomass. Spectra from runs 19, 24 and 26 have some additional peaks at 830 and 1406 cm^{-1} which correspond to the carbonate ions, with run 27 having a higher absorbance due to the presence of two sources of carbonate ions namely K_2CO_3 and $CaCO_3$.[52]

2.4.4 SEM Analysis

The SEM images in Figure 2.10 show a very clear difference in the biochar types, suggesting that because the switchgrass was allowed to be thermally treated for thirty minutes, biochar (Figure 2.10 a) resulted from the dismantling of the lignocellulosic structure. On the other hand, biochar-Ca has a different structure as seen in the right SEM image (Figure 2.10 b) and deposits of calcium salts can also be observed as flat solid structures in between the lignocellulosic material.

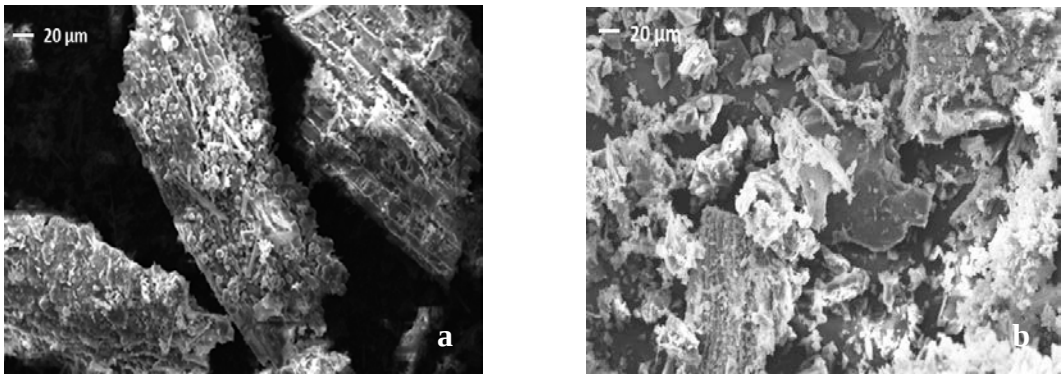

Figure 2.10 SEM images of (a) biochar and (b) biochar-Ca

This is also confirmed by the analysis in Table 2.3 whereby the calcium content in biochar-Ca is more than five times that in biochar. However, biochar-Ca seems less dense than biochar and it may be reasonable to conclude that this difference leads to the observed higher carbon gasification efficiency of biochar-Ca.

Figure 2.11 shows that the solid residues have different macromolecular structure: there are much less lignocellulosic structures present in the biochar-Ca residue (Figure

2.11 b).As seen in the enlarged image of the solid residue of biochar-Ca (Figure 2.11 c), the structure is more “open” and has undergone more degradation.

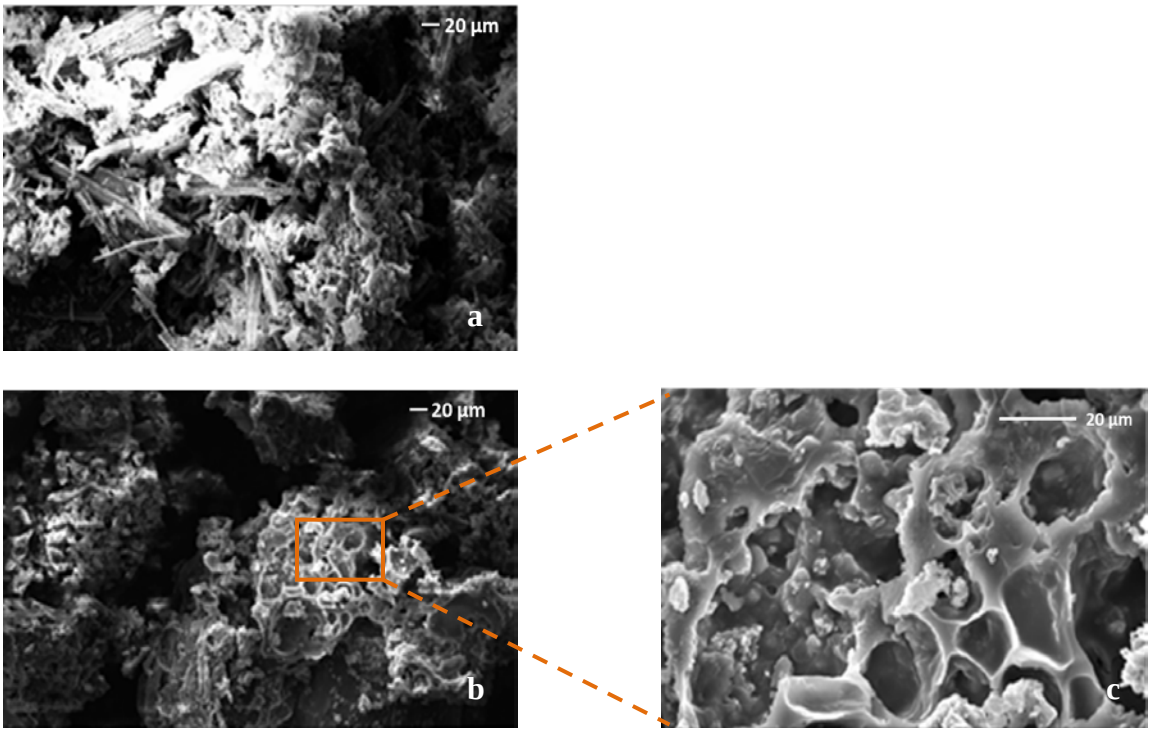

Figure 2.11 SEM images of solid residues after hydrothermal treatment at 550 °C with 25% by weight K_2CO_3 of (a) biochar and (b & c) biochar-Ca

Again, the deposits of calcium carbonate appear in the SEM image of the solid residue (bottom) as in the case of the biochar-Ca (Figure 2.10 b). This was confirmed by the composition analysis which revealed 24386 ppm of calcium, more than twice the concentration in the raw material, biochar-Ca.

2.4.5 Role of Calcium Hydroxide in the Pretreatment of Biochar

In Section 2.4.1.2, it was reported that adding calcium hydroxide directly to the biochar did not enhance gasification. One of the reasons could be that $Ca(OH)_2$ is a weak

catalyst on its own[38] and K_2CO_3 reacted to some extent with the minerals inherently present in the biochar. According to Lemus et al.,[53] the minerals present in Alamo switchgrass are mainly SiO_2, CaO, K_2O, MgO and P_2O_5. Also, according to Kumar et al.,[37] due to the recondensed particles over the biochar fibers, accessibility to minerals and cellulose is made more difficult. Therefore, adding $Ca(OH)_2$ to switchgrass may have provided more accessibility, explaining why biochar-Ca gasified better. This is in agreement with a study by Chang[54] whereby switchgrass was pretreated with lime ($Ca(OH)_2$) so that the ash became less water soluble suggesting that some components in ash must have reacted with the lime to form water-insoluble compounds, therefore passivating the minerals. The same study also concluded that components like lignin, and hemicellulose became more soluble with 9 wt% $Ca(OH)_2$ pretreatment of 2 hours at 120 °C. Since biochar-Ca production used higher temperature, less reaction time and less lime, there is the possibility that the lignin, cellulose and hemicelluloses intertwining structure may have been weakened rather than digested.

Furthermore, according to the oxygen transfer and intermediate mechanism,[32c] addition of lime is favorable for the formation of C(O), an adsorbed oxygen/oxygenated species on the carbon surface.[38] Also, a reducing form (K_2O-C) and an oxidizing form (K_2O_2-C) of K-C-O intercalates, catalyze carbon gasification by C(O), an intermediate to the gasification pathway. Therefore, the concentration of both K-C-O and C(O) dictate the catalytic gasification which is driven by the competition between two reactions: desorption of C(O) (reaction *a*) and reaction of C(O) with K_2O_2-C (reaction *b*) as illustrated in Figure 2.12. This indicates that if the desorption of the C(O) is favored, there will be more CO formed while if reaction b [K_2O_2-C + C(O) $\rightarrow$ K_2O-C + CO_2] is

favored, more carbon dioxide will be formed. Therefore by analyzing the gas composition, it can be deduced which reaction has been dominant. From the gas analysis reported in Table 2.6, in general more CO_2 was formed than CO. This suggests that in thermal and hydrothermal gasification of biochar, reaction *b* was favored.

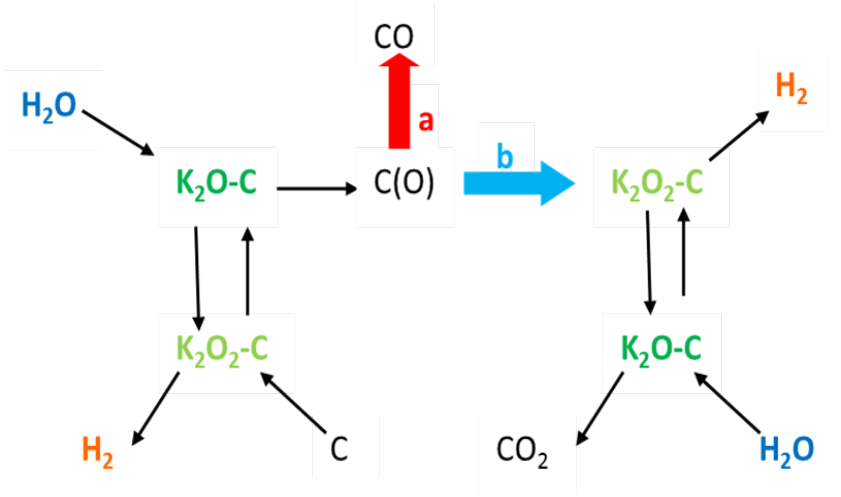

Figure 2.12 Oxygen Transfer and C(O) intermediate hybrid reaction scheme of steam gasification of carbon by potassium[38]

It is also believed that the addition of calcium hydroxide may alter the chemical properties of the minerals (SiO_2, CaO, K_2O, MgO, P_2O_5) present in switchgrass such that there is no interaction between these minerals and the potassium carbonate.[38] Usually, without $Ca(OH)_2$, these minerals would react with the K_2CO_3 to form water-insoluble compounds, thereby deactivating the catalyst to some extent. Adding $Ca(OH)_2$ to switchgrass significantly avoided the reactions between the catalyst and the minerals and hence carbon gasification efficiency was increased since more K-C-O intercalates were available for gasification. It is suggested that $Ca(OH)_2$, may have reacted to some extent with the minerals present but it is believed that $Ca(OH)_2$ may have actually altered

the chemical properties of the mineral particle surface hindering the latter's reaction with the catalyst.[38] According to the same study, it is suggested that at temperatures less than 700 °C, char is more inclined to the formation of C(O) on its surface during gasification, resulting in higher reactivity for reactions *a* and *b*. Furthermore, the enhancement effect of calcium on CO_2 evolution has been postulated by another study [55] which stipulated that calcium oxide facilitated the formation of oxygen complexes on carbon. This leads to the conclusion that because there was more C(O) formation on the char, due to the presence of $Ca(OH)_2$, K_2CO_3-catalysed gasification was enhanced.

2.5 Conclusions

Biochar can be effectively gasified using supercritical water. The carbon gasification efficiency was much greater than the thermal gasification under similar reaction conditions: at 550 °C, 5.9 % gasification was observed for conventional gasification versus 23.8 % with SCW. Addition of potassium carbonate enhanced the rate of gasification and also the yield of hydrogen indicating its effect on influencing the water-gas shift reaction. The approach of pre-treating switchgrass with calcium hydroxide, before subjecting it to SCWG, further aided the gasification process with nearly 75% carbon gasification efficiency at 600 °C. A possible explanation could be that $Ca(OH)_2$ mitigated the catalyst deactivation by preventing the reaction between K_2CO_3 and the minerals present in switchgrass. $Ca(OH)_2$ was believed to alter the chemical properties of the inherent minerals present in switchgrass and also enhance the oxygen complex formation on carbon, hence promoting carbon gasification reaction.

Lime also decreased the water-solubility of ash such that the inorganic components form insoluble compounds and were hence passivated.

2.6 Acknowledgments

This work was funded by grants from the National Science Foundation (NSF-CBET-0828269), Alabama Center for Paper and Bioresource Engineering, and the U.S. Department of Energy (DE-FC26-05NT42456). Authors are thankful to Dr. Lingzhao Kong for his advice and experimental assistance

2.7 References

1. Abuadala, A.; Dincer, I.; Naterer, G. F., Exergy analysis of hydrogen production from biomass gasification. *International Journal of Hydrogen Energy* **2010,** *35* (10), 4981-4990.

2. Savage, P. E., Organic Chemical Reactions in Supercritical Water. *Chemical Reviews* **1999,** *99* (2), 603-622.

3. Kumar, S.; Gupta, R. B., Hydrolysis of Microcrystalline Cellulose in Subcritical and Supercritical Water in a Continuous Flow Reactor. *Industrial and Engineering Chemistry Research* **2008,** *47* (23), 9321-9329.

4. Hui, J.; Youjun, L.; Bo, L.; Liejin, G.; Ximin, Z., Hydrogen production by coal gasification in supercritical water with a fluidised bed reactor. *International Journal of Hydrogen Energy* **2010,** *35*, 7151-7160.

5. Dermibas, A., Current activities and future developments. . *Energy Conversion and Management* **2009,** *50*, 2782-2801.

6. Calzavara, Y.; Joussot-Dubien, C.; Boissonnet, G.; Sarrade, S., Evaluation of biomass gasification in supercritical water process for hydrogen production. *Energy Conversion and Management* **2005,** *46*, 615-631.

7. Matsumara, Y.; Minowa, T.; Potic, B.; Kersten, S. R. A.; Prins, W.; Van Swaaij, P. M.; Van De Beld, B.; Elliott, D. C.; Neuenschwander, G. G.; Kruse, A.; Antal, M. J., Review- Biomass gasification in near- and super-critical water: Status and prospects. . *Biomass and Bioenergy* **2005,** *29*, 269-2925.

8. Watanabe, M.; Inomata, H.; Arai, K., Catalytic Hydrogen Generation from biomass (glucose and cellulose) with ZrO2 in supercritical water. . *Biomass and Bioenergy* **2002,** *22*, 405-410.

9. Elliott, D. C.; Sealock, L. J.; Baker, E. G., Chemical processing in high-pressure aqueous environments. 2. Development of catalysts for gasification. *Industrial & Engineering Chemistry Research* **1993,** *32* (8), 1542-1548.

10. Byrd, A. J.; Pant, K. K.; Gupta, R. B., Hydrogen Production from Glucose Using Ru/Al_2O_3 Catalyst in Supercritical Water. *Industrial & Engineering Chemistry Research* **2007,** *46* (11), 3574-3579.

11. Calzavara, Y.; Joussot-Dubien, C.; Boissonnet, G.; Sarrade, S., Evaluation of biomass gasification in supercritical water process for hydrogen production. *Energy Conversion and Management* **2005,** *46* (4), 615-631.

12. (a) Antal Jr, M. J., Tower Power: Producing Fuels from Solar Energy. *Bulletin of the Atomic Scientists* **1976,** *32* (5), 58-62; (b) Antal, M., Synthesis gas production from organic wastes by pyrolysis/steam reforming. *Energy from Biomass and Wastes* **1978**, 14-18.

13. (a) Antal Jr, M. J.; Friedman, H.; Rogers, F., Kinetics of cellulose pyrolysis in nitrogen and steam. *Combustion Science and Technology* **1980,** *21* (3-4), 141-152; (b) Mok, W. S.-L.; Antal, M. J., Effects of pressure on biomass pyrolysis. II. Heats of reaction of cellulose pyrolysis. *Thermochimica acta* **1983,** *68* (2), 165-186.

14. Modell, M., Gasification and liquefaction of forest products in supercritical water. *Fundamentals of thermochemical biomass conversion* **1985**, 95-119.

15. Antal Jr, M. J.; Varhegyi, G.; Jakab, E., Cellulose pyrolysis kinetics: revisited. *Industrial & Engineering Chemistry Research* **1998,** *37* (4), 1267-1275.

16. (a) Kabyemela, B.; Takigawa, M.; Adschiri, T.; Malaluan, R.; Arai, K., Mechanism and kinetics of cellobiose decomposition in sub-and supercritical water. *Industrial & Engineering Chemistry Research* **1998,** *37* (2), 357-361; (b) Kabyemela, B. M.; Adschiri, T.; Malaluan, R.; Arai, K., Degradation kinetics of dihydroxyacetone and glyceraldehyde in subcritical and supercritical water. *Industrial & Engineering Chemistry Research* **1997,** *36* (6), 2025-2030; (c) Kabyemela, B. M.; Adschiri, T.; Malaluan, R. M.; Arai, K., Kinetics of glucose epimerization and decomposition in subcritical and supercritical water. *Industrial & Engineering Chemistry Research* **1997,** *36* (5), 1552-1558; (d) Kabyemela, B. M.; Adschiri, T.; Malaluan, R. M.; Arai, K., Glucose and fructose decomposition in subcritical and supercritical water: detailed reaction pathway, mechanisms, and kinetics. *Industrial & Engineering Chemistry Research* **1999,** *38* (8), 2888-2895.

17. Xu, X.; Matsumura, Y.; Stenberg, J.; Antal, M. J., Carbon-Catalyzed Gasification of Organic Feedstocks in Supercritical Water *Industrial & Engineering Chemistry Research* **1996,** *35* (8), 2522-2530.

18. (a) Sealock Jr, L. J.; Elliott, D. C., Method for the catalytic conversion of lignocellulosic materials. Google Patents: 1991; (b) Sealock Jr, L. J.; Elliott, D. C.; Baker, E. G.; Butner, R. S., Chemical processing in high-pressure aqueous environments. 1. Historical perspective and continuing developments. *Industrial & Engineering Chemistry Research* **1993,** *32* (8), 1535-1541.

19. (a) Minowa, T.; Fang, Z., Hydrogen Production from Cellulose in Hot Compressed Water Using Reduced Nickel Catalyst: Product Distribution at Different Reaction Temperatures. *Journal of chemical engineering of Japan* **1998,** *31* (3), 488-491; (b) Minowa, T.; Inoue, S., Hydrogen production from biomass by catalytic gasification in hot compressed water. *Renewable Energy* **1999,** *16* (1), 1114-1117; (c) Minowa, T.; Ogi, T., Hydrogen production from cellulose using a reduced nickel catalyst. *Catalysis Today* **1998,** *45* (1), 411-416.

20. (a) Elliott, D. C.; Phelps, M.; Sealock Jr, L. J.; Baker, E. G., Chemical processing in high-pressure aqueous environments. 4. Continuous-flow reactor process development experiments for organics destruction. *Industrial & Engineering Chemistry Research* **1994,** *33* (3), 566-574; (b) Elliott, D. C.; Sealock, L. J. J.; Baker, E. G., Chemical processing in high-pressure aqueous environments. 3. Batch reactor process development experiments for organics destruction. *Industrial & Engineering Chemistry Research* **1994,** *33* (3), 558-565.

21. (a) Delgado, J.; Aznar, M. P.; Corella, J., Calcined dolomite, magnesite, and calcite for cleaning hot gas from a fluidized bed biomass gasifier with steam: Life and usefulness. *Industrial & Engineering Chemistry Research* **1996,** *35* (10), 3637-3643; (b) Delgado, J.; Aznar, M. P.; Corella, J., Biomass gasification with steam in fluidized bed:

Effectiveness of CaO, MgO, and CaO-MgO for hot raw gas cleaning. *Industrial & Engineering Chemistry Research* **1997,** *36* (5), 1535-1543; (c) Aznar, M. P.; Corella, J.; Delgado, J.; Lahoz, J., Improved steam gasification of lignocellulosic residues in a fluidized bed with commercial steam reforming catalysts. *Industrial & Engineering Chemistry Research* **1993,** *32* (1), 1-10.

22. Antal, M. J.; Allen, S. G.; Schulman, D.; Xu, X.; Divilio, R. J., Biomass Gasification in Supercritical Water. *Industrial & Engineering Chemistry Research* **2000,** *39* (11), 4040-4053.

23. Yip, K.; Tian, F.; Hayashi, J.-i.; Wu, H., Effect of Alkali and Alkaline Earth Metallic Species on Biochar Reactivity and Syngas Compositions during Steam Gasification *Energy & Fuels* **2009,** *24* (1), 173-181.

24. Abdullah, H.; Wu, H., Biochar as a Fuel: 1. Properties and Grindability of Biochars Produced from the Pyrolysis of Mallee Wood under Slow-Heating Conditions. *Energy & Fuels* **2009,** *23* (8), 4174-4181.

25. Kumar, S. Hydrothermal Treatment for Biofuels: Lignocellulosic Biomass to Bioethanol, Biocrude, and Biochar. AUburn University, Auburn, 2010.

26. Lehmann, J.; Joseph, S., *Biochar for Environmental Management, Science and technology*. Earthscan: London, UK, 2009.

27. Uchimiya, M.; Lima, I. M.; Klasson, K. T.; Wartelle, L. H., Contaminant immobilization and nutrient release by biochar soil amendment: Roles of natural organic matter. *Chemosphere* **2010,** *80* (8), 935-940.

28. Abdullah, H.; Mediaswanti, K. A.; Wu, H., Biochar as a Fuel: 2. Significant Differences in Fuel Quality and Ash Properties of Biochars from Various Biomass Components of Mallee Trees. *Energy & Fuels* **2010,** *24* (3), 1972-1979.

29. Salleh, M.; Kisiki, N. H.; Yusuf, H.; Ab Karim Ghani, W., Gasification of biochar from empty fruit bunch in a fluidized bed reactor. *Energies* **2010,** *3* (7), 1344-1352.

30. Matsumura, Y.; Nonaka, H.; Yokura, H.; Tsutsumi, A.; Yoshida, K., Co-liquefaction of coal and cellulose in supercritical water. *Fuel* **1999,** *78* (9), 1049-1056.

31. Yamaguchi, D.; Sanderson, P. J.; Lim, S.; Aye, L., Supercritical water gasification of Victorian brown coal: Experimental characterisation. *International Journal of Hydrogen Energy* **2009,** *34* (8), 3342-3350.

32. (a) Wigmans, T.; Hoogland, A.; Tromp, P.; Moulin, J. A., The influence of potassium carbonate on surface area development and reactivity during gasification of activated carbon by carbon dioxide. *Carbon* **1983,** *21* (1), 1-12; (b) Miura, K.; Hashimoto, K.; Silveston, P. L., Factors affecting the reactivity of coal chars during gasification, and indices representing reactivity. *FUEL* **1989,** *68*, 1461-1475; (c) Wang, J.; Jiang, M.; Yao, Y.; Zhang, Y.; Cao, J., Steam gasification of coal char catalyzed by K2CO3 for enhanced production of hydrogen without formation of methane. *Fuel* **2009,** *88* (9), 1572-1579.

33. Matsumura, Y.; Xu, X.; Antal jr, M. J., Gasification characteristics of an activated carbon in supercritical water. *Carbon* **1997,** *35* (6), 819-824.

34. Lee, W. J.; Kim, S. D., Catalytic activity of alkali and transition metal salt mixtures for steam-char gasification. *Fuel* **1995,** *74* (9), 1387-1393.

35. (a) Wang, J.; Takarada, T., Role of Calcium Hydroxide in Supercritical Water Gasification of Low-Rank Coal. *Energy & Fuels* **2001,** *15* (2), 356-362; (b) Lin, S.; Harada, M.; Suzuki, Y.; Hatano, H., Continuous experiment regarding hydrogen production by coal/CaO reaction with steam (I) gas products. *Fuel* **2004,** *83* (7-8), 869-874; (c) Lin, S.; Harada, M.; Suzuki, Y.; Hatano, H., Continuous experiment regarding hydrogen production by Coal/CaO reaction with steam (II) solid formation. *Fuel* **2006,** *85* (7-8), 1143-1150.

36. Li, Y.; Guo, L.; Zhang, X.; Jin, H.; Lu, Y., Hydrogen production from coal gasification in supercritical water with a continuous flowing system. *International Journal of Hydrogen Energy* **2010,** *35* (7), 3036-3045.

37. Kumar, S.; Gupta, R. B., Biocrude Production from Switchgrass Using Subcritical Water. *Energy & Fuels* **2009,** *23* (10), 5151-5159.

38. Wang, J.; Yao, Y.; Cao, J.; Jiang, M., Enhanced catalysis of K_2CO_3 for steam gasification of coal char by using $Ca(OH)_2$ in char preparation. *Fuel* **2010,** *89* (2), 310-317.

39. Schmieder, H.; Abeln, J.; Boukis, N.; Dinjus, E.; Kruse, A.; Kluth, M.; Petrich, G.; Sadri, E.; Schacht, M., Hydrothermal gasification of biomass and organic wastes. *The Journal of Supercritical Fluids* **2000,** *17* (2), 145-153.

40. Sluiter, A. H., B. ; Ruiz, R. ; Scarlata, C.; Sluiter, J.; Templeton, D., Crocker,D. *Determination of Structural Carbohydrates and Lignin in Biomass*; National Renewable Energy Laboratory: 2008.

41. Kersten, S. R. A.; Potic, B.; Prins, W.; Van Swaaij, W. P. M., Gasification of Model Compounds and Wood in Hot Compressed Water. *Industrial & Engineering Chemistry Research* **2006,** *45* (12), 4169-4177.

42. Laureano-Perez, L.; Teymouri, F.; Alizadeh, H.; Dale, B., Understanding factors that limit enzymatic hydrolysis of biomass. *Applied Biochemistry and Biotechnology* **2005,** *124* (1), 1081-1099.

43. Byrd, A. J.; Pant, K. K.; Gupta, R. B., Hydrogen Production from Ethanol by Reforming in Supercritical Water Using Ru/Al_2O_3 Catalyst. *Energy & Fuels* **2007,** *21* (6), 3541-3547.

44. Basu, P.; Mettanant, V., BIomass Gasification in Supercritical Water- A Review. *International Journal of Chemical Reactor Engineering* **2009,** *7*.

45. Kruse, A.; Dinjus, E., Hydrogen from Methane and supercritical water. *Angewandte Chemie, International Edition* **2003,** *42* (8), 909-911.

46. Wofford, W. T.; Gloyna, E. F., Solubility of Potassium Hydroxide and Potassium Phosphate in Supercritical Water. *Journal of Chemical & Engineering Data* **1995,** *40* (4), 968-973.

47. Baratieri, M.; Baggio, P.; Fiori, L.; Grigiante, M., Biomass as an energy source: Thermodynamic constraints on the performance of the conversion process. *Bioresource Technology* **2008,** *99* (15), 7063-7073.

48. Zheng, L.; Furinsky, E., Comparison of Shell, Texaco, BGL and KRW gasifiers as part of IGCC plant computer simulations. *Energy Conversion and Management* **2005,** *46* (11-12), 1767-1779.

49. Pastor-Villegas, J.; Gómez-Serrano, V.; Durán-Valle, C. J.; Higes-Rolando, F. J., Chemical study of extracted rockrose and of chars and activated carbons prepared at different temperatures. *Journal of Analytical and Applied Pyrolysis* **1999,** *50* (1), 1-16.

50. Gomez-Serrano, V.; Pastor-Villegas, J.; Perez-Florindo, A.; Duran-Valle, C.; Valenzuela-Calahorro, C., FT-IR study of rockrose and of char and activated carbon. *Journal of Analytical and Applied Pyrolysis* **1996,** *36* (1), 71-80.

51. Guido, G. C.; George, B. J., FT-IR Characterization of different lignin preparations from agricultural by-products. *Chimica Acta Turcica* **1991,** *19* (3), 251-256.

52. Coates, J., Interpretation of Infrared Spectra, A Practical Approach. In *Encyclopedia of Analytical Chemistry*, Meyers, R. A., Ed. John Wiley & Sons, Ltd: Chichester, 2000; pp 10815-10837.

53. Lemus, R.; Brummer, E. C.; Moore, K. J.; Molstad, N. E.; Burras, C. L.; Barker, M. F., Biomass yield and quality of 20 switchgrass populations in southern Iowa, USA. *Biomass and Bioenergy* **2002,** *23* (6), 433-442.

54. Chang, V.; Burr, B.; Holtzapple, M. T., Lime pretreatment of switchgrass. *Applied Biochemistry and Biotechnology* **1997,** *63-65* (1), 3-19.

55. Zhang, Z. G.; Kyotani, T.; Tomita, A., Dynamic behavior of surface oxygen complexes during oxygen-chemisorption and subsequent temperature-programmed desorption of calcium-loaded coal chars. *Energy & Fuels* **1989,** *3* (5), 566-571.

Chapter 3

Production of Biocrude from Biomass by Acidic Subcritical-Water followed by Alkaline Supercritical-Water Two-Step Liquefaction

3.1 Introduction

Biomass to biofuel conversion by thermochemical routes can be achieved via direct liquefaction to fuel substitutes or by gasification to synthesis gas (Chapter 2) for FT fuels production[1]. As mentioned earlier in Chapter 1, biomass typically contains 20-30 wt% hemicelluloses, 40-50 wt% cellulose, and 20-30 wt% lignin[2] along with a number of inorganic compounds in small amounts. So far, numerous studies have been conducted to convert biomass into energy-dense biocrude via liquefaction with the main aim to depolymerize biomass into monomer fragments which further convert into oily compounds[3] (Figure 3.1). Usually, the high-pressure direct liquefaction processes operate at around 280-380 °C and 70-300 bar with 10-60 minutes reaction time in hot compressed water or solvents such as alcohols and acetone[4] with or without catalysts and sometimes in the presence of reducing gases such as hydrogen and carbon monoxide.

Hydrothermal treatment of biomass has a number of advantages[5] including high throughputs, high energy and separation efficiencies, feedstock flexiblity, and the production of drop-in biofuels without needing biological enzymes or catalysts which otherwise require careful control.[6] Section 1.4 details the unique properties of subcritical

and supercritical water. By varying temperature and pressure, these properties can be tuned to control the reaction rates.[7] In addition, during the hydrothermal liquefaction of biomass, water acts as both the reaction medium and the reactant and therefore the feedstock does not have to be dried. In most studies, subcritical water has been used as opposed to supercritical water (above 374 °C and 220 bar) to avoid gasification of the products.[8]

3.1.1 Sub- and Supercritical Water (SCW) Liquefaction of Biomass and its Components

The degradation products of biomass components (carbohydrates, lignin, proteins and lipids) in sub- and SCW are different but the basic reaction mechanisms are biomass depolymerization, biomass decomposition into monomers (through cleavage, dehydration, decarboxylization, deamination)[9] and recombination of the reactive fragments (to form bio-oil and biochar), as illustrated in Figure 3.1. Cellulose, hemicellulose and starch are the most abundant carbohydrates in biomass and they undergo hydrolysis, during hydrothermal treatment, to form glucose and other saccharides, which are then further decomposed. Several authors[9-10] have reviewed the sub- and SCW liquefaction of carbohydrates. Cellulose, being crystalline therefore insoluble in water and resistant to attack by enzymes, hydrolyses slower than hemicelluloses and starch. But in subcritical environment, cellulose readily solubilizes and hydrolyses. Sasaki et al.[11] has proposed a reaction mechanism for microcrystalline cellulose conversion in sub- and SCW water. They proposed that in subcritical water, the crystallite is hydrolyzed at the surface only giving low conversion rates while in SCW,

the crystallite swells or dissolves around the surface region to form inactive amorphous-like cellulose molecules. These can be easily hydrolyzed to lower degree of polymerization celluloses and cellooligosaccharides.

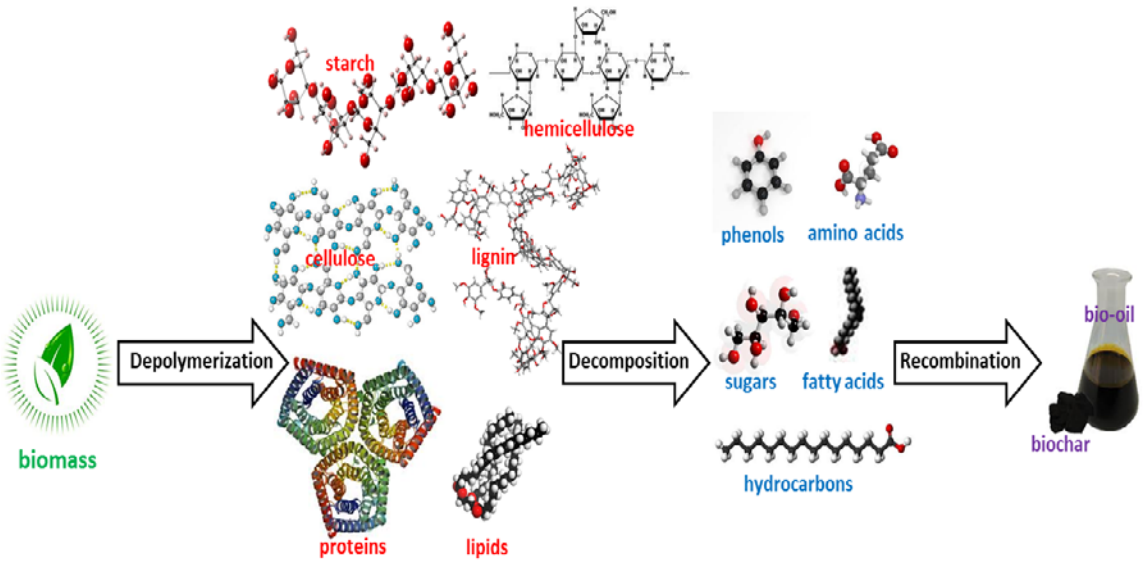

Figure 3.1 Basic reactions in hydrothermal liquefaction

A kinetic study[12] on the hydrolysis of cellulose, starch and protein was carried out and it was found that the rates were significantly different. Rapid heating was deemed important to avoid depolymerization of some biopolymer. At 25 MPa and between 240-310 °C, the cellulose hydrolysis rate in water increased tenfold and at 280 °C, 100% cellulose conversion was achieved within 2 min. In general, cellulose hydrolysis is considerably slower than starch hydrolysis and glucose decomposition rate increases with temperature. Another kinetic study looked into the dissolution and hydrolysis of cellulose in subcritical and SCW (320–400 °C, 25 MPa, and 0.05–10.0 s). Hydrolysis products were obtained at 400 °C but at 320–350 °C, aqueous decomposition products of glucose,

such C3–C6 sugars, aldehydes and furans, were the main products. It was therefore postulated that below 350 °C, the cellulose hydrolysis rate is slower than the glucose decomposition rates.

Above 180 °C, hemicelluloses are easily solubilized and hydrolyzed in water and the hydrolysis can be both acid- and base-catalyzed.[10b] The released saccharides will also be degraded in the same manner as those released from cellulose. Well-controlled decomposition experiments of D-xylose in subcritical and supercritical water at 360–420 °C and 25–40 MPa with residence times of 0.02–1 s were carried out.[13] The dominant reaction was the retro-aldol condensation of d-xylose with glycolaldehyde, glyceraldehyde and dihydroxyacetone as the main products. Garrote et al.[14] reviewed reaction kinetics for hemicellulose degradation into sugars and subsequently into furfurals and other degradation compounds. They found that most studies reported hemicellulose extraction and recovery as sugars or oligomers at yields of 65 to 82%.

Starch, another biomass polysaccharide, has also been decomposed using hydrothermal conditions.[15] Sweet potato starch was completely solubilized at 180 °C after 10 minutes reaction time but low yields of glucose were observed. The glucose yield increased to a maximum of 60% at both 200 °C and 30 mins residence time and 220 °C and 10 min residence time. At 240 °C, glucose yield dropped since it degraded to 5-hydroxymethylfurfural (HMF). The conclusion of this study was that at lower temperatures, dehydration was favored while defragmentation to short-chained acids and aldehydes was dominant at higher temperatures. Hydrolysis of starch by Miyazawa et al.[16] have also shown the same results. In brief, all the carbohydrates hydrolyze to

monosaccharides, mostly glucose which further degrades according to the mechanism in Figure 3.2.

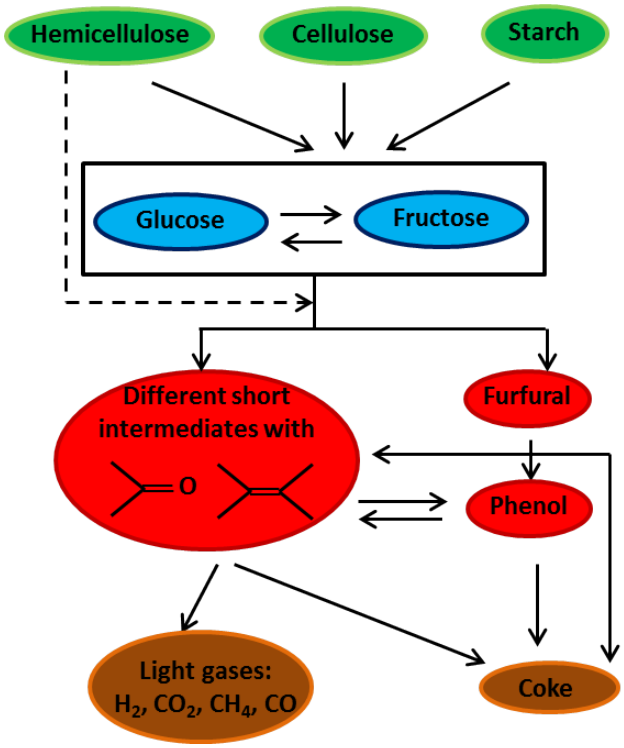

Figure 3.2 Reaction mechanism for carbohydrate degradation at sub- and supercritical conditions (*Adapted from* Kruze et al., 2006.[17])

Green wood (hardwood) lignin was used to produce aldehydes from alkaline (13.5 wt% NaOH) steam-explosion in the presence of pure oxygen and Cu^{2+} and Fe^{3+} as catalysts at 170 °C. The combined aldehydes (vanillin, syringaldehyde and hydroxybenzaldehyde) yield reached 14.6 wt% of the lignin, which represented 2.5 wt % of the dry wood.[18] A number of other studies have liquefied lignin to extract potentially valuable chemicals.[19] One study[20] investigated the decomposition of lignin in supercritical water with and without phenol at 400 °C. Without phenol, the yield of tetrahydrofuran (THF)-insoluble (TIS) products decreased while the molecular weight

distribution of THF-soluble (TS) products shifted toward lower molecular weights as the water density increased since lignin conversion was enhanced. With phenol, there was a decrease in the yield of TIS products while the molecular weight distribution of TS products shifted towards even lower molecular weights. Because phenol reacted with some decomposition products, some alkylphenols were also detected. They concluded that the reaction of phenol with reactive sites occurred in supercritical water and suppressed cross-linking reactions among reactive sites of large fragments. This promoted the decomposition of lignin to lower-molecular-weight compounds.

Recently, hydrothermal conversion of lignin was conducted in subcritical temperatures of 300–370 °C and residence times of 0.5–10 s at a pressure of 25 MPa to compare with another study that used supercritical conditions at 390–450 °C.[21] Under subcritical regime, lignin conversion occurred rapidly while a higher degree of depolymerization was achieved under supercritical temperatures (Figure 3.3). Also, there was enhanced char formation in supercritical conditions. Therefore free radical reactions played a vital role in char formation mechanism and the studies found that the rate constant of the overall lignin decomposition under both sub- and supercritical conditions obeyed Arrhenius behavior.

An alternative oil extraction method from high lipid feedstock such as microalgae is hydrothermal treatment, especially because the high moisture feedstocks do not require drying during this treatment.[22] One group[23] processed a range of microalgae and lipids extracted from terrestrial oil seed at 350 °C and 150–200 bar in water. The triglycerides were converted to fatty acids and alkanes in the presence of certain heterogeneous catalysts which increased de-oxygenation of the biocrude. The $Co/Mo/Al_2O_3$ and

Pt/Al_2O_3 appear to selectively deoxygenate carbohydrate and protein fractions, whereas Ni/Al_2O_3 deoxygenated the lipid fraction. The biocrude yields from the microalgae were increased slightly with the use of catalysts but the higher heating value (HHV) and de-oxygenation increased, by up to 10%.

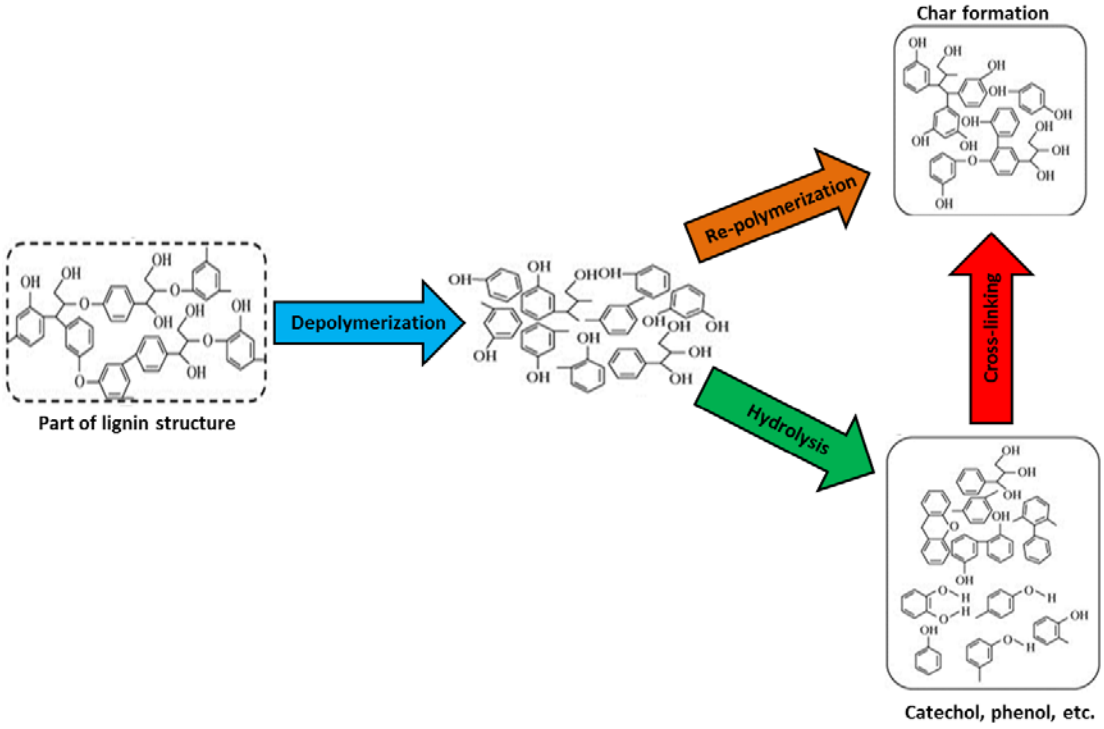

Figure 3.3 Scheme for lignin degradation under near and supercritical water conditions (*Adpated from* Wahyudiono et al., 2008.[24])

Savage's research group has also worked on producing biodiesel from algae using hydrothermal treatment.[25] They developed a 2-step, catalyst-free process with intracellular hydrolysis followed by supercritical in situ transesterification (SC-IST/E).[26] At subcritical conditons, the wet algal biomass (80% moisture) underwent intracellular lipids hydrolysis. The cells conglomerated into an easily filterable solid that retained the lipids. This wet fatty acid (FA) rich solids were subjected to SC-IST/E with ethanol to

produce biodiesel in the form of fatty acid ethyl esters (FAEEs). Some protein-rich biomass, like marine waste and algae, have been investigated as a potential source of amino acids which have high commercial value (for use in feed, food, pharmaceuticals and cosmetics). A number of studies[27] have investigated hydrothermal extraction of amino acids from various protein -rich feedstocks. The peptide (C–N) bond linking the amino acids together into proteins will rapidly hydrolyze in hydrothermal systems.

Apart from the considerable work done with model compounds, lignocellulosic biomass liquefaction has also been investigated by a number of research groups. In their pioneering work, Appell et al.[28] converted a variety of lignocellulosic feedstock to oily products in a continuous process with a temperature range of 330-370 °C in the presence of 5% Na_2CO_3 as catalyst, CO or H_2 as reducing gas and water (2.8 kg/kg wood) with a residence time of 10-30 minutes. However, this process took place in an oil-rich phase which required a recycled oil ratio of 19:1 and the yields were 45-55 wt%. This technology was further investigated and advanced by Elliot[29] and coworkers with an oil yield of about 48-58 wt% with a heating value of 37 MJ/kg. Shell developed a liquefaction process in the 1980's termed as "Hydrothermal Upgrading" or the HTU process which was abandoned later due to low oil prices. However, this research was resumed by Goudriaan et al.[30] in 1997, in which biomass was heated to 330-350 °C, 100-180 bar with residence time of 5-20 minutes to obtain a water-insoluble oil of 30-35 MJ/kg heating value and 10 wt% oxygen content.[4b] He et al.[31] converted swine manure into oils at 285-335 °C and 69-103 bar using a batch reactor with 2 hours of residence time, resulting in a 35 MJ/kg heating value oil. The oil yield increased from 8 to 63 wt% by the use of CO as reducing gas. However, in a later study by the same group[32], the

same oil yields were obtained by using inert gases like CO_2 and N_2 but no clarification was given about this phenomenon and the role, if any, of the reducing gases in the liquefaction.

Bobleter et al.[10b, 33] utilized subcritical water for pretreatment of biomass by exploiting water's highest ionic product at around 250 °C, before enzymatic hydrolysis. Mok and Antal[34] solubilized between 40-60 wt% of a suite of biomass with SCW at 200-230 °C and reported that 100% of the hemicelluloses was solubilized in a tubular percolating reactor. Sasaki et al.[35] have also investigated the decomposition behavior of biomass in SCW in a semi-continuous reactor where the temperature was maintained at 180°C for 20 minutes where free sugars, some of the lignin and hemicelluloses solubilized and then ramped up to 285 °C and maintained for another 7 minutes to decompose cellulose. They obtained 95 wt% decomposition for bamboo and chinquapin. In another study by Watanabe et al.,[36] conversion of glucose into oil in SCW at 300 °C was examined and the effects of alkali catalyst, cobalt catalyst and a hydrogenating agent (formic acid) were investigated. The study showed that the formic acid inhibited polymerization of produced oil and that catalytic effect of cobalt catalyst was similar to that of alkali but had a low stability at the reaction conditions. Karagoz et al. obtained a yield of 8.5 wt%, which increased to 9.3 wt% upon addition of $Ca(OH)_2$ catalyst at 280 °C for 15 min reaction time.[37] This study also concluded that the addition of 0.94 M K_2CO_3, reduced solid residue from 42 to 4 wt% resulting in an oil consisting mainly of phenolic compounds[38] with carbon number between 9 and 11.[38a, 39] Minowa et al.[40] liquefied a variety of feedstocks including bagasse, coconut shell, model garbage and

cellulose to heavy oil (33-37 MJ/kg and 21-60 wt% yield) using SCW at 300-340 °C and up to 240 bar with Na_2CO_3 as catalyst.

3.1.2 Rationale for using a Two-Step Liquefaction Process instead of a Conventional Single-Step Treatment

In summary, the above studies show that the most important factors influencing the liquefaction yield are: lignin content, solvent used, type and amount of catalyst, temperature and pressure, mass ratio of solvent to biomass and residence time.[10a] Therefore, in an endeavor to enhance the yield, these factors need to be studied and optimized. In addition, the different liquefaction chemistries of the three major biomass components - cellulose, hemicelluloses, and lignin - need to be considered. In order to accommodate these differences and to utilize the tunable properties of SCW, this work examines the effect of using hydrothermal process with a two-step treatment: acidic subcritical followed by alkaline supercritical water liquefaction. The rationale of using two steps is that the organic materials in the biomass undergo thermal decomposition at different temperatures with hemicelluloses degrading at 180-290°C, cellulose at 240-350 °C and lignin at 280-500 °C.[4b] Therefore, using a temperature of around 200 °C at first would solubilize and mainly degrade the hemicelluloses resulting into xylose sugars[4b, 29d] and the subsequent degradation of these sugars into furfurals and other compounds, as illustrated[41] in Figure 3.4. Therefore, first at a low temperature, hemicelluloses would be solubilized to form biocrude (oily phase) which would be extracted in the first step. Then lignin and cellulose are liquefied at a higher temperature and pressure (supercritical state) with the use of calcium hydroxide as catalyst since alkaline medium favors lignin

extraction.[42] Furthermore, $Ca(OH)_2$ is inexpensive, safe and can be easily recycled.[43] For example, existing pulp mills already have lime recycle systems in place whereby the calcium carbonate formed is calcined to produce quicklime, CaO ($CaCO_3 \rightarrow CaO + CO_2$) and the lime can then be reacted with water to regenerate the calcium hydroxide used, as per the following reaction: $CaO + H_2O \rightarrow Ca(OH)_2$.

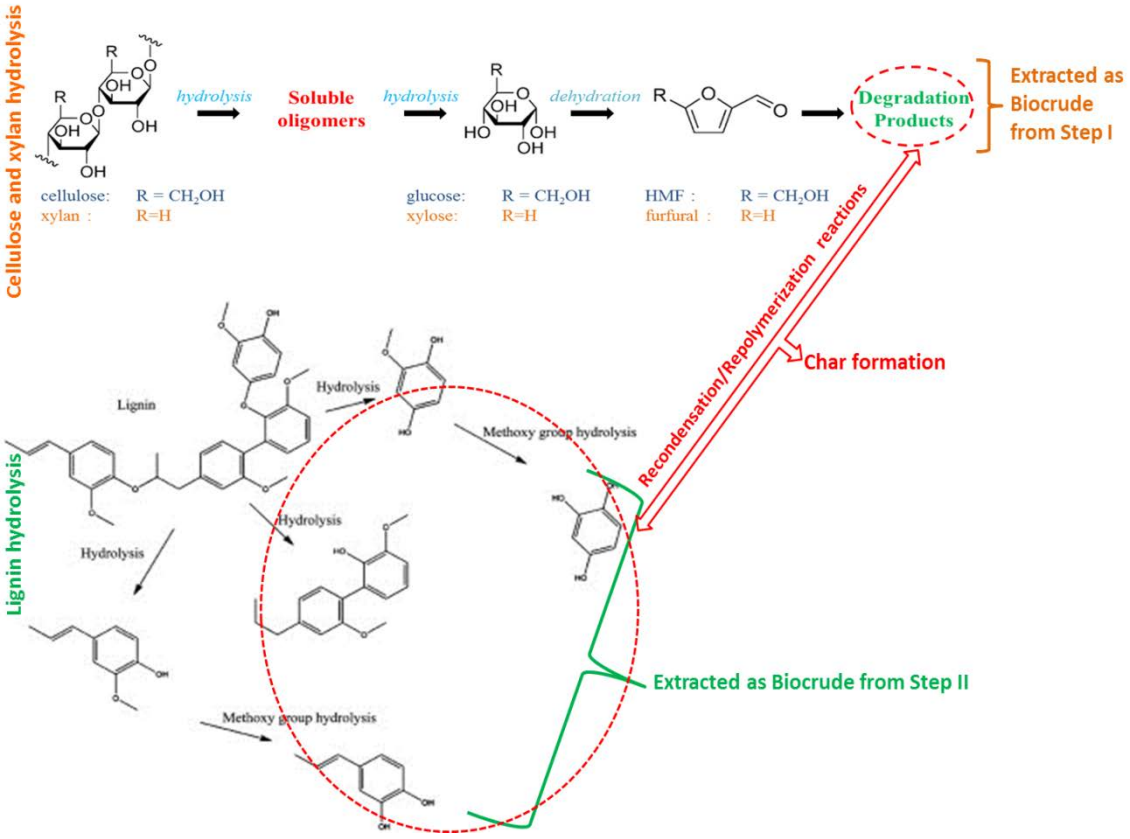

Figure 3.4 Hydrolysis reactions cellulose, xylan (hemicellulose) and lignin

3.1.3 Objectives of this Study

The objectives of this study is to study the difference in yield between the proposed two-step process versus a single step hydrothermal liquefaction. The effect of recycling the water-soluble portion of biocrude (biocrude-W) from the first step to make the reaction medium acidic as well as the addition of $Ca(OH)_2$ in the second step are also

examined. A schematic of the proposed two-step liquefaction process is shown in Figure 3.5.

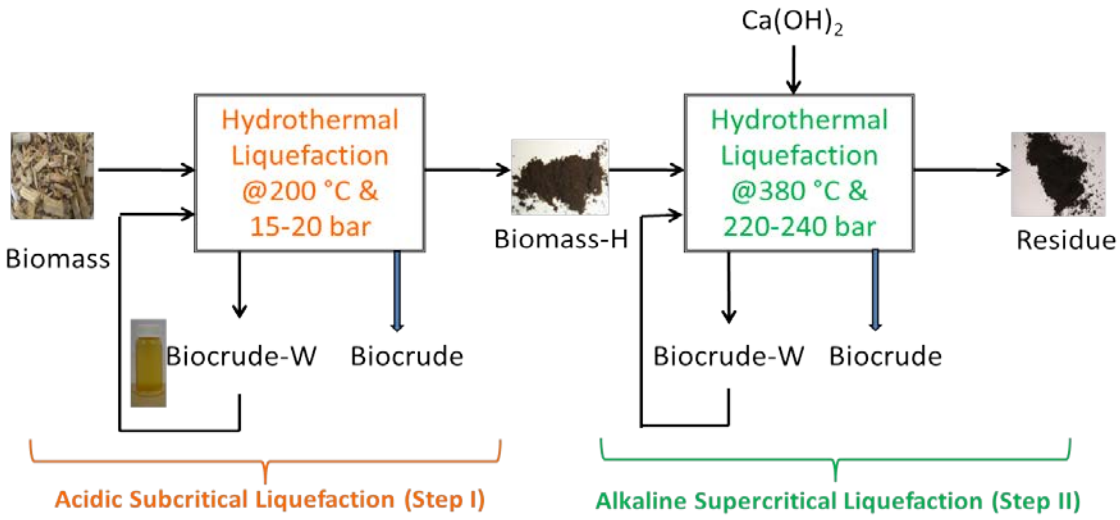

Figure 3.5 Schematic of proposed two-step liquefaction process

3.2. Experimental Section

3.2.1 Materials and Apparatus

Alamo switchgrass having 7.3 wt% moisture and 5-10 mm length (i.e., chopped) was used as the feedstock biomass, for which the compositional analysis is presented elsewhere.[44] The same set-up used for gasification was used for switchgrass liquefaction. Section 2.2.2.2 details the reactor and fittings used.

3.2.2 Experimental Procedure

3.2.2.1 Acidic Subcritical-Water Liquefaction (Step I)

3.2.2.1.1 Water as Reaction Medium

In this step, 5 g (dry basis) of switchgrass and 30 ml of deionized water were fed to the reactor, which was then heated to 200 °C by an electric furnace for 30 minutes. A

stainless steel frit (pore size 2 µm), placed at the outlet of the reactor, prevented entrainment of solids in the exiting stream. The temperature of the furnace was set such that the thermocouple T1 would give the desired reaction temperature. Reaction time started when the desired temperature (indicated by T1) was reached inside the reactor. Typically, a pressure of 15-20 bar is generated upon heating. After completion of the reaction, the furnace was switched off and the reactor was allowed to cool. As soon as the pressure reached below 34 bar, valve 1 was opened so that an accurate reading of the pressure could be obtained from P2. Upon cooling, the temperature and residual pressure due to formed gas were noted before valve 2 was opened for GC analysis. After depressurization, the reactor was opened to collect biocrude and the un-liquefied biomass termed biomass-H. Throughout this paper, the collected aqueous phase will be termed as biocrude-W while the "oily" phase will be referred to as biocrude. Biocrude-W was obtained by simply collecting the liquid from the reactor. Biocrude was extracted by washing the biomass-H and reactor walls with acetone and subsequently evaporating off acetone using a rotary evaporator. The un-liquefied biomass, biomass-H, left was then dried for further analysis and liquefaction in the second step (see Section 3.2.2.2). The collected components were analyzed using the analytical procedures shown in Figure 3.6.

3.2.2.1.2 Recycle of Biocrude-W

The collected biocrude-W was recycled and utilized in the subsequent step I experiments. This recycling was done in two ways. In a first instance of half recycle, makeup water was added to biocrude-W so that each time the 1:6 biomass to water ratio was maintained. In a second instance, only biocrude-W was used as the liquefying liquid instead of water or a water/biocrude mixture as in previous half recycles. It is to be noted

that biocrude-W had a pH of around 3 due to the decomposition of hemicellulose to form carboxylic acids. Therefore when biocrude-W was recycled in the process, the liquefaction medium automatically became acidic as reported in Table 3.1.

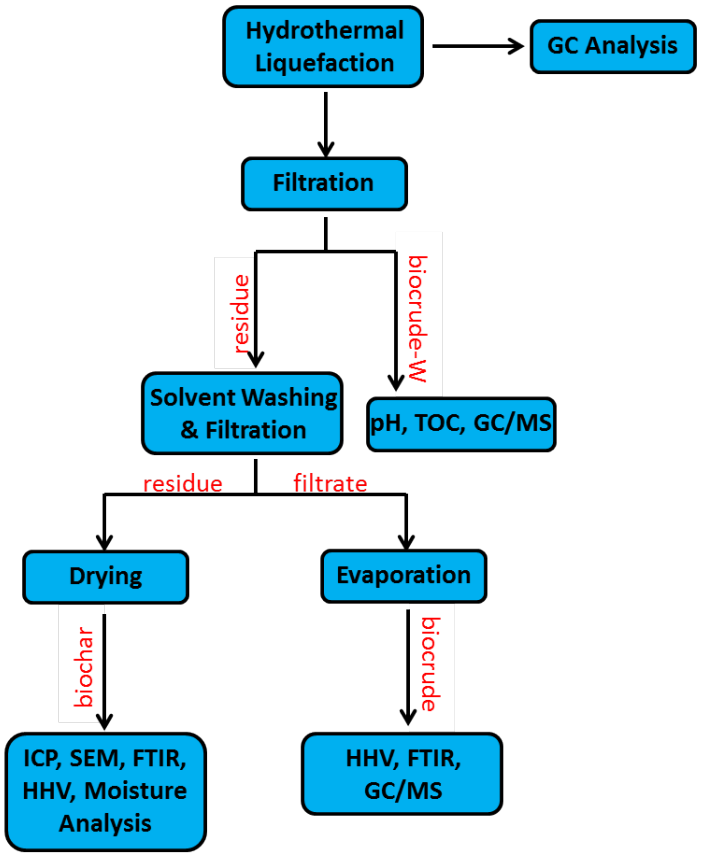

Figure 3.6 Analytical procedure after hydrothermal liquefaction

3.2.2.2 Alkaline Supercritical-Water Liquefaction (Step II)

The biomass-H collected from acidic subcritical water treatment was then subjected to supercritical water treatment at 380 °C and 220-240 bar for about 30 minutes but with 2.5 g (dry basis) of biomass-H and 25-35 g of water. Compared to switchgrass which had 44.6 wt% C and 48.6 wt% O, biomass-H contained 47.5 wt% C and 43.5 wt%

O, from inductively coupled plasma ion spectrometry analyses. The experimental and analytical procedures were similar to tep I as described earlier. Calcium hydroxide (obtained from Sigma Aldrich with >95% purity) of different weight percent was used as catalyst in the second step; here, 'wt%' refers to the weight of the catalyst divided by the total weight of the dry biomass and catalyst, i.e. the calculation does not use the solution weight.

3.3 Product Characterization

3.3.1 Gas Chromatography (GC), Fourier Transform Infrared (FTIR), Total Organic Carbon (TOC) & Scanning Electron Microscope (SEM) Analysis

The gas composition was determined using the same gas chromatograph (SRI 8610C) described in Chapter 2 (Section 2.3.1). The same equipment, as detailed by Section 2.3.3, was also used to determine the FTIR spectra while Sections 2.3.4 and 2.3.5 respectively describe the microscope (SEM) used to determine the surface morphology and total organic carbon equipment used.

3.3.2 Gas Chromatograph Mass Spectrometer (GC-MS) Analysis

The biocrude samples were analyzed using an Agilent 7890 GC/5975MS equipped with DB-1701 column 30 m in length, 0.25 mm i.d. and 0.25 mm film thickness. Five data points were generated for calibration in such a way that the concentration of biocrude compounds fell within the range. A known amount of biocrude (~40-60 mg) was dissolved in 1-2 ml of methanol and then made to 10 ml by adding dichloromethane. Aliquots of solution were diluted with dichloromethane to different

concentrations so that the biocrude compounds concentration fell within the range. The injector and GC-MS interface were kept at constant temperatures of 280 and 250 °C, respectively. The column was kept at an initial temperature of 40 °C for 2 minutes before ramping up to 250 °C at a rate of 5 °C/min and the column was then left at 250 °C for a total of 8 minutes. Ultra-pure helium was used as carrier gas at 1.2 mL/min flowrate. Compounds were ionized at 69.9 eV electron impact conditions and analyzed over a mass per charge (*m*/*z*) range of 50–550. The compounds were identified by comparing the mass spectra with the NIST library.

3.3.3 Biocrude Yield (wt%) Calculation

Total biocrude yield, based on weight, has been calculated using the following:

$$Yield\ (wt\%) = \frac{Weight\ of\ biocrude\ from\ (step\ I + step\ II)}{Dry\ weight\ of\ switchgrass\ used} \times 100$$

3.4 Results and Discussions

3.4.1 Acidic Subcritical-Water Liquefaction (Step I)

For comparison, a single step hydrothermal liquefaction (run 1) of 5 g dry switchgrass was performed at 380 °C with 30 ml water for 30 minutes as the reaction time, to obtain a biocrude yield of 0.38 g (HHV= 28.9 KJ/g). Then, as part of the two-step process, the same amount of switchgrass was hydrothermally treated at only 200 °C for 30 minutes. From the results (Table 3.1) and comparing with the yield obtained at 380 °C, it can clearly be seen that the yield of biocrude is about doubled when a lower temperature of 200 °C is used where hemicelluloses partially solubilizes and degrades while the lignin and cellulose remain mainly unsolubilized. Such treatment reduces the

probability of re-condensation and re-polymerisation which occurs at the higher temperature of 380 °C of the traditional single-step process. Water-soluble products found in biocrude-W were also formed by the decomposition of hemicelluloses.[38a] In general, it can be seen that the TOC of biocrude-W is higher when half or full recycle is used instead of using only pure water.

Table 3.1 Acidic subcritical-water switchgrass liquefaction (Step I)

Recycle type	Run no	Liquefaction medium				Product				
		Water ml	Biocrude-W ml	pH	TOC ppm	Biomass-H[a] g (dry)	Biocrude-W[b] ml	pH	TOC*	Biocrude[c] g
None	2	30	0	5.57	125	2.6	15	3.2	16020	0.7
Half	3 (1st)	17	13	3.57	10060	2.4	13	3.2	25620	1.5
	4 (2nd)	20	10	3.32	7785	2.7	13	3.3	19470	1.3
	5 (3rd)	18	12	3.18	6500	2.4	14	2.9	21130	1.3
Full	6	0	30	3.37	14780	2.5	13	3.1	24671	1.1
	7	0	30	3.06	15190	2.5	15	3.4	23800	1.1

[a]*Biomass-H is the un-liquefied biomass obtained after hydrothermal treatment at 200°C*

[b]*Biocrude-W is the aqueous phase biocrude obtained after hydrothermal treatment*

[c]*Biocrude is the extracted oily phase obtained after hydrothermal treatment*

**TOC is measured in ppm*

This can be explained by the fact that more hemicelluloses decompose in the acidic medium, not only to form the heavier compounds but also to form some water solubles compounds such as carboxylic acids and furanics.

The biocrude yield is strongly dependent on temperature as it significantly decreased as temperature increased from 200 to 380 °C (run 1). This reduction in yield can be attributed to the cracking of the liquid products in supercritical water (380 °C) to gases and formation of char by isomerization, dehydration, fragmentation and condensation reactions.[8] A much higher gas yield is obtained at 380 °C as compared to that at 200 °C. Furthermore, it has been reported that sugar or its degradation products like furfural can react with lignin to form insoluble-lignin,[14] which also explains the low yield of biocrude at 380 °C. Therefore, by first extracting the furfurals (in biocrude) from hemicelluloses, this condensation reaction and "loss" of furfural can be avoided, so that lignin can be hydrothermally liquefied in step II. The other observation is that the full recycles of biocrude-W does not increase the biocrude yield further as compared to half recycles. The pH of the recycle stream, for both the half and full recycles, is around 3 which facilitates the hemicelluloses decomposition.[45]

3.4.2 Alkaline Supercritical-Water Liquefaction (Step II)

Table 3.2 describes the process conditions and results obtained when biomass-H was subjected to alkaline hydrothermal treatment. Cellulose is a linear polymer chain formed by joining the anhydroglucose units into glucan chains by β-(1,4)-glycosidic linkages.[4b] During liquefaction, the chains are first cleaved to glucose, which converts to glucosan through the removal of a water molecule.[46] However, for cellulose degradation to have good kinetics, the supercritical-water regime[4b] is preferred and hence the choice of using 380 °C and 220 bar for the second step. It has also been postulated that high

pressure blocks depolymerization of cellulose but allows competing dehydration and crosslinking reactions.[46]

Table 3.2 Alkaline supercritical-water switchgrass liquefaction (Step II) at 380 °C

Run no.	Feedstock			Product				
	Biomass-H, g(dry basis)	Water, ml	$Ca(OH)_2$, g (wt%)	Biocrude-W ml	TOC,ppm	Biocrude g	HHV, KJ/g	Residue* g
8	2.5	25	0 (0)	10	16760	0.1	28.5	1.1
9	2.5	25	0.1 (5)	22	8027	0.2	29.9	0.7
10	2.5	25	0.3 (10)	21	8528	0.2	27.5	0.7
11	2.5	30	0.4 (15)	15	9641	0.4	27.7	0.8
12	2.5	30	0.6 (20)	25	8575	0.4	28.8	0.8
13	2.5	35	1.3 (33)	22	8683	0.5	29.5	1.6
14	2.5	35	2.5 (50)	12	20130	0.3	26.5	5.4

**Residue is the carbon-rich solid product obtained after hydrothermal treatment of switchgrass (biochar) and also, depending on the reaction conditions, includes unreacted $Ca(OH)_2$ and $CaCO_3$ formed.*

The second step provides 4.8 wt% biocrude yield for the non-catalytic run, while 8.0 wt% yield was obtained using 5 wt% of catalyst. The mass of the residue − the carbon-rich solid product obtained after hydrothermal treatment of switchgrass (biochar) containing unreacted $Ca(OH)_2$ and $CaCO_3$ formed depending on the reaction conditions − decreased as the yield of the biocrude increased confirming an increased conversion of biomass to

biocrude. Catalytic liquefaction suppressed the conversion of lignin to char by avoiding condensation and repolymerization.[47] Addition of $Ca(OH)_2$ to biomass also removed the acetate groups and uronic acid substitutions from the remaining hemicelluloses[43] and therefore enhancing liquefaction as substantiated by the increase in yield with an increase in $Ca(OH)_2$ amount (Table 3.2).

Lignin is a complex, high molecular-weight compound with more random structure than that of hemicelluloses. Lignin consists of alkylphenols which, especially at 380 °C, partially decompose by hydrolysis to form phenolics, but the low molecular-weight lignin fragments (i.e., free phenoxy redicals) such as formaldehyde, syringols, guaiacols and catehols can undergo cross-linking reactions to form heavy compounds that become solid residues,[48] therefore limiting lignin degradation. A major role of $Ca(OH)_2$ addition is in the removal of lignin from the biomass thus enhancing the reactivity of the remaining polysaccharides.[49] The catalyst therefore reduced the condensation and/or polymerization reactions of the intermediate products formed by lignin decomposition,[50] which resulted in a high biocrude yield as well as a low amount of residue.

The GC-MS analyses (Section 3.4.5) reveal that phenolic compounds increased with increasing amounts of added $Ca(OH)_2$ amount, confirming enhanced lignin decomposition and reduced polymerization reactions. Also, unlike acidic processes, alkaline processes have the advantage of losing less sugars through degradation and the caustic catalysts can either be recovered or regenerated.[51] For example, Zhong et al.[50] liquefied 8 g woody biomass at 300-340 °C with 0.8 g K_2CO_3 in 100 ml water and concluded that the catalyst improved the heavy oil yield and reduced the solid residue yield. A maximum oil yield of 32 wt% was obtained when *cunninghamia lanceolata*

having 32.4 wt% lignin was liquefied at 340 °C compared to 40 wt% yield obtained in this study using switchgrass having 31.7 wt% lignin.[52]

From Table 3.2, it can be observed that increasing the amount of $Ca(OH)_2$ further to 50 wt% did in fact reduce the biocrude yield, indicating that the catalyst was in excess. Hence, there is an optimum amount of catalyst needed for the liquefaction process, beyond which there will be no liquefaction enhancement. Furthermore, it can be postulated that the excess $Ca(OH)_2$ might have reacted with the biocrude formed to give carboxylic salts of calcium and other organic compounds of calcium such as calcium acetate, which might explain the drop in biocrude yield. It is also noteworthy that the high residue yield obtained in run 14 may be due to the formation of a hydrated form of calcium carbonate, monohydrocalcite, $CaCO_3.H_2O$, which is thermally stable up to 171 °C.[53] Since the residue was dried in the moisture analyzer, set at 105 °C, the monohydrocalcite was not dehydrated, hence contributing to a higher than expected weight of the solid residue.

The results in Table 3.2 are in agreement with those obtained by Karagoz et al.[37] where the use of 0.0243 M $Ca(OH)_2$ increased the oil yield from 7.6 to 9.3 wt% and produced about 30 wt% C_6-C_8 oxygenated hydrocarbons compared to only 8 wt% without the catalyst. The presence of $Ca(OH)_2$ therefore increased the phenolics amount due to increased lignin degradation. Caglar and Demirbas (2001) investigated the effect of Na_2CO_3 and K_2CO_3 on the liquefaction of cotton cocoon shell in supercritical water and supercritical acetone.[54] They deduced that the effects of ratio of alkali to biomass on yields was irregular, with no particular trend and observed a maximum yield with 20 wt% alkali. However, in this study, there seems to be an increasing trend in the biocrude yield

as alkali amount is increased. It is believed that the $Ca(OH)_2$ may also weaken the intermolecular interaction of the polymeric chains while catalyzing both intralink dehydration and retroaldol cleavage and condensation of the products.[54-55] The addition of the catalyst therefore weakened the C-C bond and consequently decreased the activation energy for the bond cleavage. Furthermore, the alkali caused swelling of the biomass, leading to an increase in the internal surface area which promoted separation of the structural linkages between hemicellulose, cellulose and lignin.[56] The values obtained from the experiments are also consistent with literature data. For example, Mazaheri et al.[57] used subcritical water to liquefy fibers from oil palm fruit press to produce 15.7-27.6 wt% bio-oil at 210-330 °C with a maximum yield of 43.3% with 10% Na_2CO_3 at 290 °C. Hydrothermal liquefaction of algae at 300 °C and 5 wt% Na_2CO_3 led to a bio-oil yield of 23 wt% with an HHV of 29.9 kJ/g[58] as compared to 28.5 kJ/g obtained for the non-catalytic biocrude while the HHV of the catalytic biocrude was 29.5 kJ/g when 33 wt% $Ca(OH)_2$ was used to yield 40 wt% biocrude.

3.4.3 Energy Conversion

Since the primary use of the liquid product from biomass is intended for fuel purposes, the energy content is more indicative than the mass of the product when designing the process. Table 3.3 shows the amount of energy present initially in the switchgrass as well as that in the produced biocrude. The 'energy in' is calculated by multiplying the amount (dry weight) of biomass used with its higher heating value (HHV) while the 'energy out' is calculated by multiplying the amount of biocrude/bio-oil weight with its HHV.

Table 3.3 Energy conversion comparison using different biomass and technologies

Biomass	Energy in kJ[a]	Energy out kJ[b]	Energy conversion, %[c]	Note/Reference
Switchgrass	85.0	56.6	66.6	This study
Macroalgae	57.0	34.4	60.2	Hydrothermal liquefaction at 300 °C with 5 wt% Na_2CO_3[58]
Microalgae Spirulina Chlorella Nannochloropsis sp.	 63.6 69.6 17.6	 20.88 30.4 15.1	 32.8 43.7 85.8	Hydrothermal liquefaction (a) 350 °C with 1 M Na_2CO_3 for 1 hour[59] (b) 350 °C, 350 bar[25a]
Switchgrass	94.1	42.1	44.8	Fluidized-bed fast pyrolysis[60]
Legume straw Corn stalk Cotton stalk Wheat straw	71.8 71.8 70.6 63.4	21.7 17.6 14.4 16.6	30.2 24.6 20.4 26.2	Samples and water heated to 350 °C and 10-13 MPa and maintained for 2-3 hours[61]
Rice husk	78.3	41.2	52.7	Continuous autothermal fast pyrolysis at 475 °C[62]

[a] *HHV of biomass (KJ/g) x initial amount (g)*

[b] *HHV of biocrude/oil (KJ/g) x corresponding yield (g)*

[c] *(Energy out/energy in) x 100*

The conversion is therefore the ratio of energy out to energy in. An energy conversion of 66.6% is achieved in the proposed two-step process which is compared with other technologies and various feedstocks in Table 3.3. Notably most previous efforts had less than 53% energy conversion except that for algae. Both the macroalgae and the microalgae are rich in polysaccharides and proteins with a low content of cellulose, which resulted in a high energy conversion.[58] The particularly high conversion of the *nannochloropsis sp.* microalgae can be explained by the fact that a much higher pressure was used (350 bar) as well as the fact that the feedstock contains only 25.1 wt% oxygen[25a] as compared to switchgrass having 48.6 wt% oxygen.[44] As for the 'herbaceous' non-food biomass like switchgrass, rice husk, corn stalk, etc., they all exhibit a very low energy conversion irrespective of the type of technology used. However, in this study, when the two step hydrothermal approach was used with switchgrass, an energy conversion of 66.6% was obtained which is much better than 45% obtained from pyrolysis of the same feedstock.

A detailed analysis would have to be done in order to assess the total cost associated with this new approach, especially with respect to the potential trade-off of cost versus yield improvement. To further reduce the cost on an industrial scale, the biocrude could be extracted from step I without cooling the biomass-H or biocrude-W. The hot biocrude-W is recycled back in step I so that there are no additional heating costs. The hot biomass-H is further heated up to step II temperature for additional conversion to biocrude. With this proposed system, a single reactor can be used for both the steps, eliminating extra equipment cost and unnecessary cooling and heating. Two low-cost holding talks would be utilized for holding biocrude-W from each steps.

3.4.4 Infrared Spectrometry Analysis

The FTIR spectra of switchgrass and biomass-H are compared in Figure 3.7. The 893 cm^{-1} peak characterizes the β-anomers or β-linked glucose polymers from cellulose; though this peak is still present in biomass-H spectrum, it is absent in both residue spectra as is the case with 1053 cm^{-1} band representing the C-O stretching from cellulose and hemicelluloses. It can be clearly seen that the transmittance peaks at 1100 and 1740 cm^{-1} disappear in the biomass-H spectrum. Both peaks identify hemicellulose components with 1100 cm^{-1} representing the ring asymmetric valence vibration CO deformation (glucose ring stretch) and 1740 cm^{-1}, the unconjugated C=O stretch from xylan.[63]

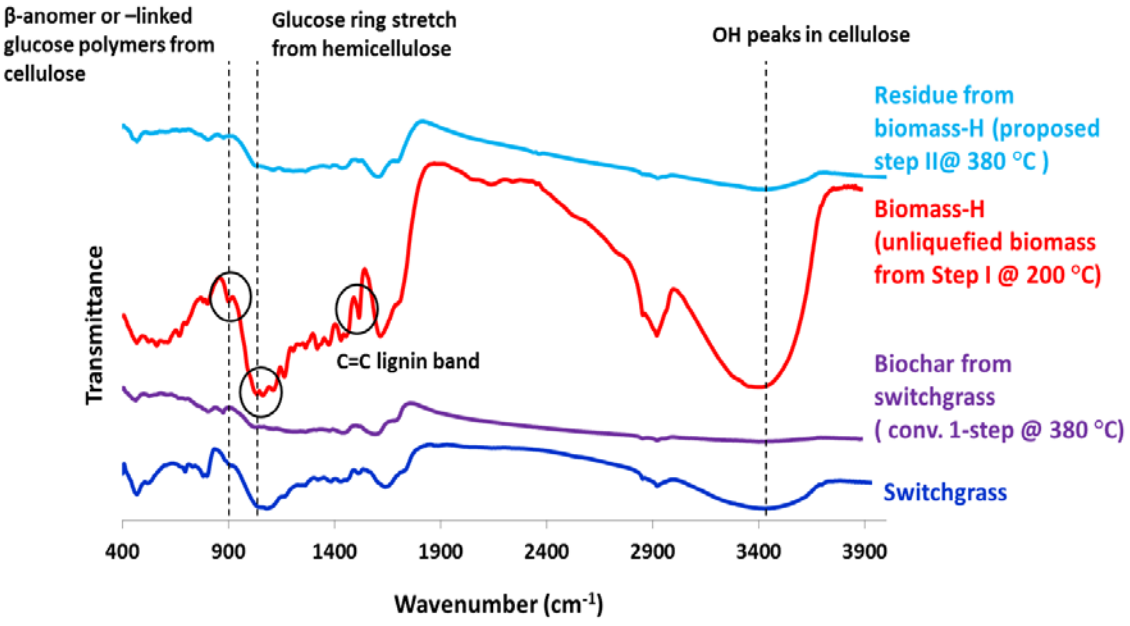

Figure 3.7 FTIR spectra of switchgrass, biomass-H and their respective residues

This is in agreement with the fact that there is removal of a large part of the hemicelluloses at 200 °C to form biocrude. The peak band around 1635-40 cm^{-1},

representing adsorbed water[64], cannot be detected in biomass-H and in the solid residue spectrum. A possible explanation is that the switchgrass structure, where the OH groups always forms hydrogen bonds, is totally broken at higher temperatures.[65] The aromatic C=C stretching lignin band at 1510 cm^{-1} is however significantly enhanced in the biomass-H due to removal of hemicelluloses and also due to the fact that part of lignin might have been released and redeposited on the surface.[65] However, this band disappears completely in the residues formed at 380 °C. The typical lignin peaks at 1425 and 1600 cm^{-1} are still present in the residue spectrum but with a much lower intensity. The 1330 cm^{-1} phenolic OH syringical nuclei peak is absent in the residue spectrum while the 1270 cm^{-1} peak (C-O-C stretching in alkyl aromatic from lignin) becomes less sharp. These observations suggest that aromatic nuclei are quite stable, but get decomposed in supercritical environment. The broad bands at 3340-3570 and 3230-3310 cm^{-1} characterize the hydrogen-bonded OH groups in intramolecular and intermolecular cellulose, respectively. Switchgrass and biomass-H have strong OH peaks but the transmittance is practically none in the residue samples. Between 150-200 °C, the polyglucose from hemicelluloses decomposes to some soluble and insoluble products but above 200 °C, the cellulose crystal structure is transformed through decomposition[63] and hence the cellulosic peak is no longer visible in the spectra.

In Figure 3.8, it can be clearly observed that for low loadings of the catalyst, there is not much calcium carbonate formed. But with 33 wt% of $Ca(OH)_2$, the peaks due to $Ca(OH)_2$ at 875 and 1427 cm^{-1} and due to $CaCO_3$ 711 and 2512 cm^{-1} are all clearly present. The carbon dioxide evolved during switchgrass liquefaction reacted with the calcium hydroxide to form calcium carbonate. This is further substantiated by the GC

analysis whereby CO_2 concentration decreased with the addition of $Ca(OH)_2$: 67.9, 43.5, 27.3 and 24 mol% of CO_2 was detected for 10, 15, 33 and 50 wt% catalyst runs, respectively. The lignin peaks at 1270, 1424 and 1510 cm^{-1} appear to have much lesser intensity when calcium hydroxide was added confirming the delignification of the biomass.

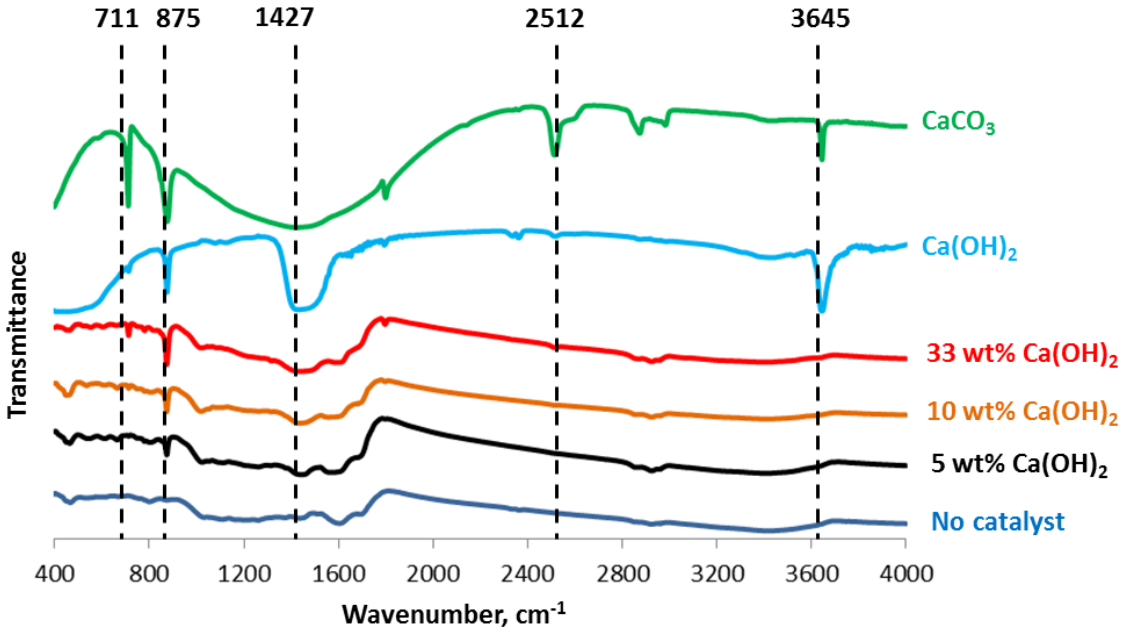

Figure 3.8 Effect of $Ca(OH)_2$ catalyst on the FTIR spectra of residues

From Figure 3.9, it can be observed that the FTIR spectra of the biocrude from the acidic subcritical treatment (run 3) and that from the alkaline supercritical liquefaction (runs 8 and 13) are comparable, meaning that the biocrude samples have similar aliphatic and aromatic functional groups but in different amounts, characterized by the different intensities of the peaks.

Table 3.4 summarizes the functional groups present in the biocrude samples. Biocrude is expected to be a complex mixture of C-H-O compounds in the form of acids, alcohols, aldehydes, esters, ketones, lignin derived phenols, etc. The biocrude obtained from the acidic liquefaction (step I) however has high amounts of alcohol and aromatic compounds apparent from the high intensities of peak numbers 3, 4 and 8.

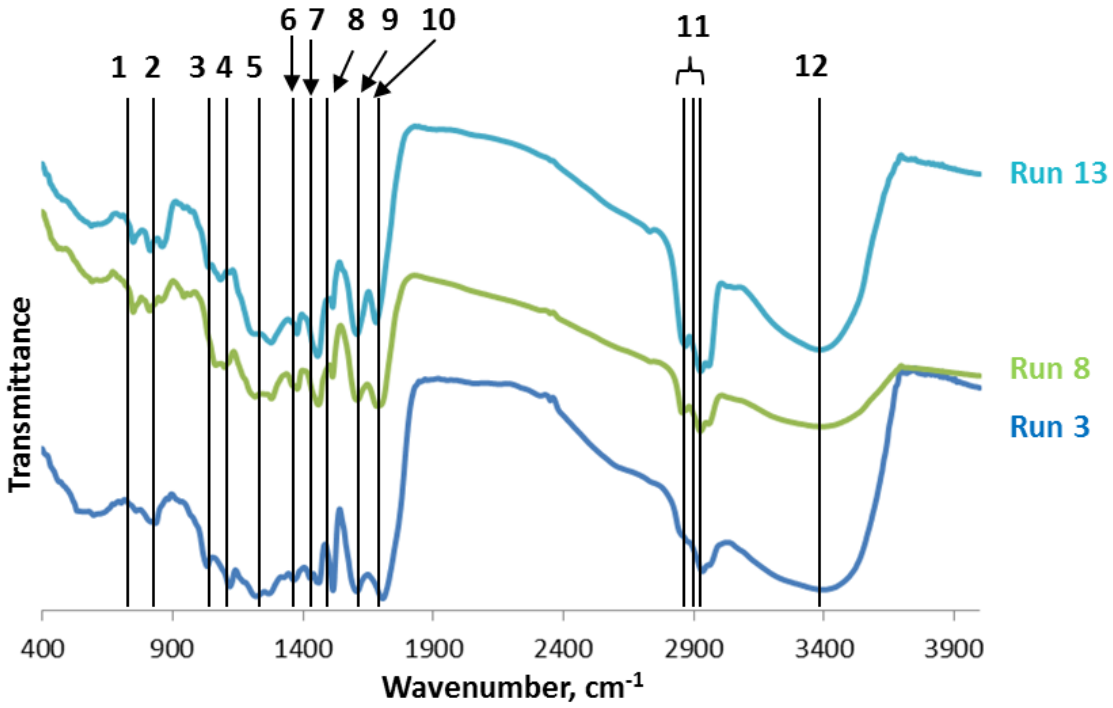

Figure 3.9 FTIR spectra of biocrude

On the other hand, the biocrude alkaline liquefaction (step II) contains high amounts of alcohols, phenols and alkanes apparent from the high intensities of peak numbers 1, 2, 5, 6 and 11. Usually at temperatures higher than 280 °C, cellulose first degrades into 2-furancarboxaldehyde and 5-methyl-2-furancarboxaldehyde which further decompose into acetic acid, which is usually observed as one of the components in the bio-oils.

Table 3.4 Functional groups of biocrude samples determined by FTIR analysis[66]

No.	Wavenumbers (cm^{-1})	Functional groups	Class of compounds
1	806,804,800	O-H bending (lignin)	Aromatic compounds, phenol, esters, ethers
2	1055,1030,1022	C-O stretching (cellulose)	Ethers, alcohols
3	1107,1068,1064	C-O stretching (cellulose)	Primary, secondary or tertiary alcohol
4	1198,1194,1190	C-O-C asymmetry stretching (cellulose)	Aliphatic compounds
5	1234,1245,1246	C-O-C stretching in alkyl aromatic (lignin)	Aromatic compounds
6	1329,1351,1363	C-H bending (cellulose)	Alkanes
7	1458,1377,1375	Aliphatic CH_2 and CH_3 deformation (cellulose, lignin)	Alkanes
8	1556,1516,1457	NO_2 stretching N-H bending Aromatic C=C/benzene ring stretching (lignin)	Nitrogenous compound Aromatic compounds
9	1608,1606,1604	C=C stretching (lignin)	Alkenes
10	1704,1686,1680	Aromatic carbonyl/carboxyl C=O	Ketones, quinones, aldehydes,carboxylic acids

		stretching (polyxylose)	
11	2956,2935, 2867	Aliphatic C-H stretching	Alkanes
12	3367	O-H stretching	Phenols, alcohols

In addition, the decomposition of phenol from lignin may also form acetic acid, especially in an acidic medium. The hydrothermal treatment of lignin usually produces 2-methoxy phenol (guaiacol) and 1,2-benzenediol (catechol) derivatives since phenyl propane, the basic unit of lignin, is a rich source of phenolic compounds[39] and therefore a large number of these phenolic structures are expected to be present in the biocrude. If higher temperatures would have been used, the fragmentation and condensation (instead of hydrolysis) would have taken over to form complex liquid products and char. As for the hemicelluloses, they are mainly present as pentosans and hexosans which undergo thermal decomposition readily to form furan derivatives, which are also expected in the biocrude.

3.4.5 GC-MS Analysis

The chemical compositions of biocrude-W and biocrude from different runs were qualitatively characterized by GC-MS. Table 3.5 compares the identified compounds in biocrude from both the acidic-subcritical and the alkaline-supercritical treatments. Here concentration is taken as the % of total area for each of the identified compounds, with the balance representing the unidentified ones. In biocrude-W, propenoic and butanoic acids were present due to hydrolysis and dehydration reactions from hemicelluloses components, and the use of high temperature and catalyst in step II, almost eliminated

carboxylic acids, probably due to reactions between the acids and the basic catalyst.[8] Though our analytical scheme could not detect aqueous acetic acid but the fact that pH of biocrude-W was usually around 3 (see Table 3.1 and literature[38a, 64]), it can be deduced that biocrude-W must contain a fair amount of acetic acid as well.

Table 3.5 Compounds obtained from switchgrass liquefaction

Compounds	Biocrude-W (%)	Biocrude (%)				
	Run 3	Run 3	Run 8	Run 9	Run 12	Run 13
1,2-Benzenediol *(catechol)*	-	-	2.45	-	-	-
1,2-Benzenediol, 3-methyl-*(3-methylcatechol)*	-	-	1.41	-	-	-
1,2-Cyclopentanedione, 3-methyl-	0.84	-	-	-	-	-
1H-Inden-1-one, 2,3-dihydro-	-	-	-	0.84	0.87	-
1H-Inden-5-ol, 2,3-dihydro-	-	-	1.56	-	-	-
1-Methylindan-2-one	-	-	-	1.6	-	1.32
2,5 -Hexanedione	0.48	-	-	-	-	-
2',6'-Didhydroxyacetophenone	0.23	-	-	-	-	-
2-cyclopenten-1-one, 3-methyl-	-	-	-	-	1.65	-
2-Cyclopentene-1-one, 3-ethyl-2-hydroxy-	0.31	-	-	-	-	-
2-Furancarboxaldehyde, 5-methyl-	1.26	-	-	-	-	-
2-Furancarboxaldehyde,5-(hydroxymethyl)-	0.32	3.83	-	-	-	-
2-Propenoic acid, 3-(4-methoxyphenyl)-	-	-	-	-	-	1.82
Azulene	-	-	0.79	-	-	-
Benzaldehyde,4-hydroxy-3,5-dimethoxy-	-	1.52	-	-	-	-
Benzeneacetic acid, 4-hydroxy-3-methoxy-	0.18	-	-	-	-	-
Butanoic acid, 4-hydroxy	0.31	-	-	-	-	-
Ethanone, 1-(2-furanyl)-	0.93	-	-	-	-	-
Ethanone, 1-(3-hydroxyphenyl)-	-	-	3.13	-	-	-
Furfural	85.66	-	-	-	-	-
Naphthalene	-	2.83	1.07	-	3.12	2.68
Naphthalene, 1,6-dimethyl-	-	1.51	-	-	0.76	1.37
Phenanthrene	-	1.17	-	-	-	-
Phenol	0.44	-	-	2.26	-	-
Phenol, 2,2'-methylenebis[6-(1,1-dimethylethyl)-4-methyl	-	-	-	-	-	2.84
Phenol, 2,4-dimethyl-	-	-	-	2	-	-
Phenol, 2,6-dimethoxy-	0.81	3.24	3.24	6	3.39	-
Phenol, 2-ethyl-	-	2.93	-	-	-	-
Phenol, 2-methoxy- *(o-guaiacol)*	1.46	-	-	2.4	-	-

Phenol, 2-methoxy-4-(-1-propenyl)- *(isoeugenol)*	-	3.73	-	-	-	3.19
Phenol, 2-methoxy-4-methyl- *(p-methylguaiacol)*	0.19	8.62	1.14	5.1	7.58	8.63
Phenol, 2-methoxy-4-propyl- (4-propylguaiacol)	-	-	-	-	-	2
Phenol, 3,4,5-trimethyl-	-	-	-	-	4.59	3.13
Phenol, 3,5-dimethyl-	-	-	-	-	-	1.62
Phenol, 4-ethyl-	0.53	-	3.39	13.6	-	10.4
Phenol, 4-ethyl-2-methoxy-*(4-ethylguaiacol)*	0.59	12.3	3.86	11.7	13.17	14.4
Phenol, 4-ethyl-3-methyl-	-	-	-	1.06	-	-
Phenol, 4-methyl-	-	-	-	1.7	2.86	2.59
Phenol,2-(1-methylethyl)-	-	-	-	2.36	-	-
Tetradecane	-	-	1.17	-	-	-
Vanillin	0.59	4.49	-	-	-	-

Furfural was only found in biocrude-W sample from run 3 and was absent from all the biocrude samples. Furfural is produced during hemicelluloses decomposition and since biocrude-W was produced at low temperature, it did not react with other decomposition compounds from lignin or cellulose. Furfural has a good commercial value due to its use in the petrochemical refining as well as in the manufacture of furan, tetrahydrofuran and furfuran resin.[67] It can also be noticed that furancarboxaldehyde was only found in run 3, in both biocrude-W and biocrude samples, confirming hemicelluloses degradation. Its absence in the other biocrude samples also suggests that these furfural compounds may have converted further at the high temperatures to form phenol.[39]

Compared to biocrude from run 3 (acidic subcritical water treatment), biocrude from run 8 (supercritical water treatment without catalyst) had benzene and C_9-C_{13} compounds while run 9 (supercritical treatment with 5 wt% $Ca(OH)_2$) had more phenolic compounds. In fact, a number of phenolic compounds were identified in all the biocrude samples and their concentrations seem to increase with catalyst presence (runs 12 and 13), similar to the observations of Karagoz et al.[37] Phenolic compounds and their derivatives are primarily formed due to lignin degradation by cleavage of the aryl ether

linkages and by the condensation of carbohydrates originating from cellulose and hemicelluloses degradation.[8] Lignin has guaiacyl and syringyl repeating units and thus the biocrude contains a lot of phenolic compounds including 4-ethylguaiacol, guaiacol, etc., which are typical lignin-derived fragments. Together with the phenolic structures, lignin also has functional groups such as hydroxyl, carbonyl and methoxy groups. The bond between one propyl side chain of a hydroxyphenylpropane with a hydroxyl group attached to another hydroxyphenylpropane unit, is one of the most important ether bonds in lignin. The presence of the phenolic compounds in biocrude indicate that lignin hydrolysis was dominant over lignin fragmentation.[68] The dimethoxy phenols, observed in most of the biocrude samples, originated from the syringyl lignin.[69] The biocrude from step I had about 32% of phenolic compounds as compared to 12, 48, 32 and 49% using 0, 5, 20 and 33 wt% of catalyst in step II. If the phenolic compounds had not been extracted after step I, their yield would have been much less due to subsequent repolymerisation reactions. Phenols are of commercial value due to their wide applications ranging from synthesis of formaldehyde resin, dyes to medicines. Since lignin is the second most abundant polymeric aromatic organic substance in biomass, it can serve as a source for chemical compounds, making lignocellulosic biomass a chemical feedstock for various purposes.[70]

A very low amount of benzene and benzene derivatives is found in the biocrude samples, confirming the difficulty of removing the –OH bond from the phenol ring. In the runs with low amount of catalyst (runs 8 and 9), benzenediol was detected since the methoxy-phenol decomposed further to form the benzenediol. However as the solution became basic with the catalyst addition in step II, there was no decomposition of

methoxy-phenol to form benzenediols. Unlike bio-oil produced by pyrolysis, there was practically no esters detected since the use of sub- and super- critical water drastically reduces the ester yield and increases the proportion of alcohols and phenols, similar to the observations of Chumpoo et al.[3]

3.4.6 SEM Analysis

Figure 3.10 shows the surface morphology of switchgrass and solid residues from different reaction conditions. The original switchgrass structure (3.10 (a)) has a very compact lignocellulosic matrix which decomposed when subjected to low temperature liquefaction to form biomass-H (3.10 (b)) to significantly expose the cellulose fiber.[68] When both switchgrass and biomass-H were subjected to supercritical liquefaction in step II, the structure was significantly broken down further. However at high temperatures, dehydration reactions start competing with cellulose and hemicelluloses hydrolysis reactions to form biochar rather than organic acids, aldehydes, furfurals, phenols and other heavy molecular weight compounds. Figure 3.10 (c), shows precipitation of some globular particles on the fibers[64] due to recondensation and repolymerisation of lignin degradation compounds; here, some fibrous residue can still be seen, confirming that not all the lignocellulosic structure was degraded. On the other hand, the residue obtained from biomass-H hydrothermal treatment (3.10(d)), has a much more 'open', small-pored surface that might be due to the better decomposition of the lignocellulosic structure, enhanced by the high diffusivity of supercritical water. Because the starting material was biomass-H, which had most of the hemicelluloses and some lignin removed, hydrolysis reactions were enhanced and repolymerisation may have been limited.

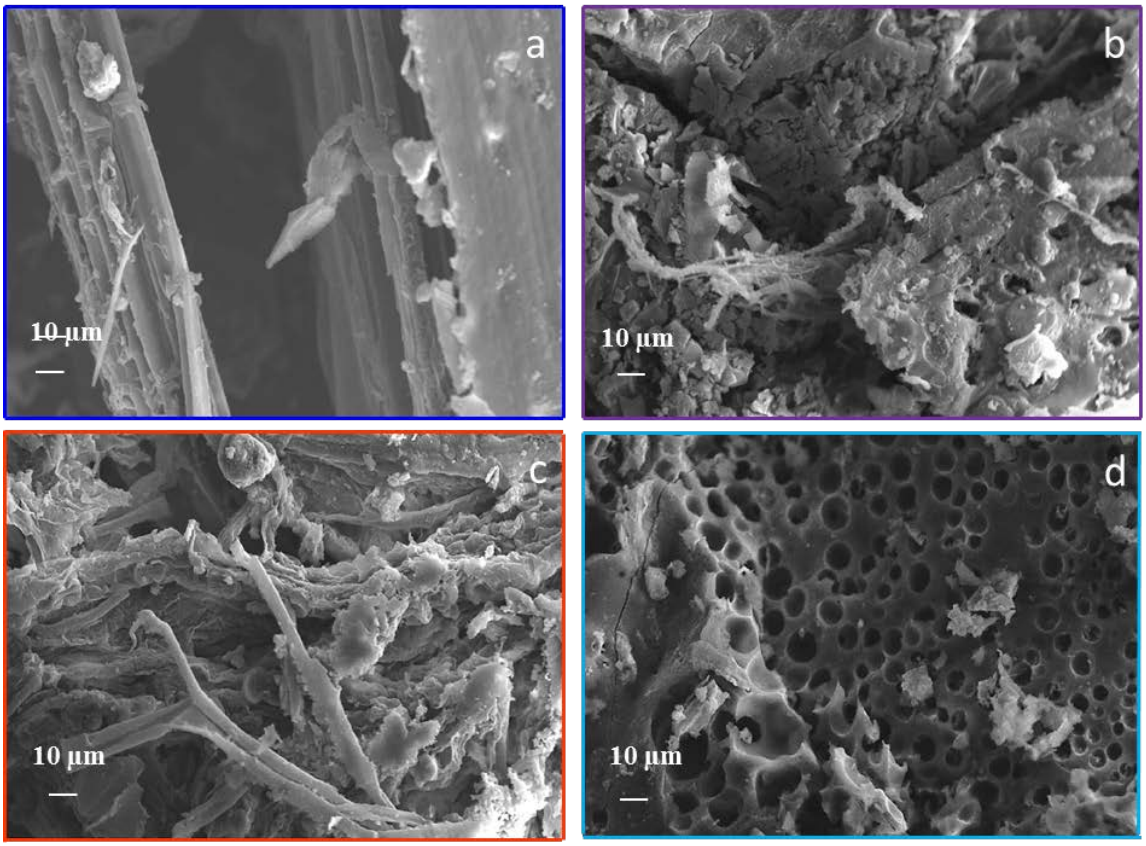

Figure 3.10 SEM photographs (mag:1.5 KX and WD=11.0 mm) of (a) switchgrass, (b) biomass-H, (c) biochar from switchgrass (run 1) and (d) residue from biomass-H (run 8)

3.5 Conclusions

Switchgrass was effectively liquefied using a novel two-step approach: an acidic subcritical, followed by an alkaline supercritical water treatment. The acidic medium (200 °C) favored the hemicelluloses removal and improved the accessibility to lignin and cellulose. Furthermore, by extracting the biocrude so produced, the reactions between the sugar degradation products and lignin to produce char have been avoided. The supercritical alkaline medium (380 °C), due to $Ca(OH)_2$ addition, suppressed char

formation by reducing condensation/polymerization reactions, removed acetate and uronic groups from hemicelluloses, enhanced lignin solubility and therefore increased reactivity of the remaining polysaccharides. $Ca(OH)_2$ also decreased the activation energies for these complex reactions by weakening the C-C bonds. In addition, the alkali promoted biomass swelling, leading to an increase in the internal surface area which separated the structural linkages between hemicellulose, cellulose and lignin. The biocrude had a good amount of phenolic compounds mainly due to lignin hydrolysis and the total biocrude yield accounted for about 40% (on mass basis) and therefore a promising energy conversion of 66.6% was achieved.

3.6 Acknowledgments

This work was funded by grants from the National Science Foundation (NSF-CBET-0828269), Alabama Center for Paper and Bioresource Engineering, and the U.S. Department of Energy (DE-FC26-05NT42456). Authors are thankful to Dr. Sushil Adhikari and Mrs. Suchithra Thangalazhy-Gopakumar for the GC-MS analysis.

3.7 References

1. Vertes, A. A.; Qureshi, N.; Blaschek, H. P.; Yukawa, H., *Biomass to Biofuels: Strategies for Global Industries*. 2010.

2. Cheng, S.; D'cruz, I.; Wang, M.; Leitch, M.; Xu, C., Highly Efficient Liquefaction of Woody Biomass in Hot-Compressed Alcohol-Water Co-solvents. *Energy & Fuels* **2010,** *24* (9), 4659-4667.

3. Chumpoo, J.; Prasassarakich, P., Bio-Oil from Hydro-Liquefaction of Bagasse in Supercritical Ethanol. *Energy & Fuels* **2010,** *24* (3), 2071-2077.

4. (a) Xu, C.; Etcheverry, T., Hydro-liquefaction of woody biomass in sub- and super-critical ethanol with iron-based catalysts. *Fuel* **2008,** *87* (3), 335-345; (b) Peterson, A. A.; Vogel, F.; Lachance, R. P.; Fröling, M.; Antal Jr, M. J.; Tester, J. W., Thermochemical biofuel production in hydrothermal media: a review of sub-and supercritical water technologies. *Energy Environ. Sci.* **2008,** *1* (1), 32-65.

5. Demirbas, A., Competitive liquid biofuels from biomass. *Applied Energy* **2011,** *88* (1), 17-28.

6. Gupta, R. B.; Demirbas, A., *Gasoline, diesel, and ethanol biofuels from grasses and plants*. Cambridge Univ Pr: 2010.

7. Savage, P. E., Organic chemical reactions in supercritical water. *Chemical reviews* **1999,** *99* (2), 603-622.

8. Xu, C.; Lad, N., Production of Heavy Oils with High Caloric Values by Direct Liquefaction of Woody Biomass in Sub/Near-critical Water. *Energy & Fuels* **2007,** *22* (1), 635-642.

9. Toor, S. S.; Rosendahl, L.; Rudolf, A., Hydrothermal liquefaction of biomass: A review of subcritical water technologies. *Energy* **2011,** *36* (5), 2328-2342.

10. (a) Behrendt, F.; Neubauer, Y.; Oevermann, M.; Wilmes, B.; Zobel, N., Direct Liquefaction of Biomass. *Chemical Engineering & Technology* **2008,** *31* (5), 667-677; (b) Bobleter, O., Hydrothermal degradation of polymers derived from plants. *Progress in polymer science* **1994,** *19* (5), 797-841; (c) Yu, Y.; Lou, X.; Wu, H., Some Recent

Advances in Hydrolysis of Biomass in Hot-Compressed Water and Its Comparisons with Other Hydrolysis Methods. *Energy & Fuels* **2007,** *22* (1), 46-60.

11. Sasaki, M.; Adschiri, T.; Arai, K., Kinetics of cellulose conversion at 25 MPa in sub- and supercritical water. *AIChE Journal* **2004,** *50* (1), 192-202.

12. Rogalinski, T.; Liu, K.; Albrecht, T.; Brunner, G., Hydrolysis kinetics of biopolymers in subcritical water. *The Journal of Supercritical Fluids* **2008,** *46* (3), 335-341.

13. Sasaki, M.; Hayakawa, T.; Arai, K.; Adschiri, T., Measurement of the rate of retro-Aldol condensation of D-xylose in subcritical and supercritical water. *Hydrothermal Reactions and Techniques. World Scientific Publishing Co, Singapore* **2003**, 169-176.

14. Garrote, G.; Dominguez, H.; Parajo, J. C., Hydrothermal processing of lignocellulosic materials. *European Journal of Wood and Wood Products* **1999,** *57* (3), 191-202.

15. Nagamori, M.; Funazukuri, T., Glucose production by hydrolysis of starch under hydrothermal conditions. *Journal of Chemical Technology & Biotechnology* **2004,** *79* (3), 229-233.

16. (a) Miyazawa, T.; Funazukuri, T., Polysaccharide hydrolysis accelerated by adding carbon dioxide under hydrothermal conditions. *Biotechnology progress* **2005,** *21* (6), 1782-1785; (b) Miyazawa, T.; Ohtsu, S.; Nakagawa, Y.; Funazukuri, T., Solvothermal treatment of starch for the production of glucose and maltooligosaccharides. *Journal of Materials Science* **2006,** *41* (5), 1489-1494.

17. (a) Kruse, A.; Gawlik, A., Biomass Conversion in Water at 330-410 °C and 30-50 MPa. Identification of Key Compounds for Indicating Different Chemical Reaction

Pathways. *Industrial & Engineering Chemistry Research* **2002,** *42* (2), 267-279; (b) Kruse, A.; Maniam, P.; Spieler, F., Influence of Proteins on the Hydrothermal Gasification and Liquefaction of Biomass. 2. Model Compounds. *Industrial & Engineering Chemistry Research* **2006,** *46* (1), 87-96.

18. Wu, G.; Heitz, M.; Chornet, E., Improved Alkaline Oxidation Process for the Production of Aldehydes (Vanillin and Syringaldehyde) from Steam-Explosion Hardwood Lignin. *Industrial & Engineering Chemistry Research* **1994,** *33* (3), 718-723.

19. (a) Xiang, Q.; Lee, Y. Y., Production of oxychemicals from precipitated hardwood lignin. *Appl Biochem Biotechnol* **2001,** *91-93* (1-9), 71-80; (b) Quitain, A. T.; Sato, N.; Daimon, H.; Fujie, K., Qualitative Investigation on Hydrothermal Treatment of Hinoki (Chamaecyparis obtusa) Bark for Production of Useful Chemicals. *Journal of Agricultural and Food Chemistry* **2003,** *51* (27), 7926-7929; (c) Okuda, K.; Man, X.; Umetsu, M.; Takami, S.; Adschiri, T., Efficient conversion of lignin into single chemical species by solvothermal reaction in water–p-cresol solvent. *Journal of Physics: Condensed Matter* **2004,** *16* (14), S1325.

20. Saisu, M.; Sato, T.; Watanabe, M.; Adschiri, T.; Arai, K., Conversion of Lignin with Supercritical Water-Phenol Mixtures. *Energy & Fuels* **2003,** *17* (4), 922-928.

21. (a) Yong, T. L.-K.; Matsumura, Y., Reaction Kinetics of the Lignin Conversion in Supercritical Water. *Industrial & Engineering Chemistry Research* **2012,** *51* (37), 11975-11988; (b) Yong, T. L.-K.; Matsumura, Y., Kinetic Analysis of Lignin Hydrothermal Conversion in Sub- and Supercritical Water. *Industrial & Engineering Chemistry Research* **2013,** *52* (16), 5626-5639.

22. Vardon, D. R.; Sharma, B. K.; Blazina, G. V.; Rajagopalan, K.; Strathmann, T. J., Thermochemical conversion of raw and defatted algal biomass via hydrothermal liquefaction and slow pyrolysis. *Bioresource Technology* **2012,** *109* (0), 178-187.

23. Biller, P.; Riley, R.; Ross, A. B., Catalytic hydrothermal processing of microalgae: Decomposition and upgrading of lipids. *Bioresource Technology* **2011,** *102* (7), 4841-4848.

24. Wahyudiono; Sasaki, M.; Goto, M., Recovery of phenolic compounds through the decomposition of lignin in near and supercritical water. *Chemical Engineering and Processing: Process Intensification* **2008,** *47* (9–10), 1609-1619.

25. (a) Brown, T. M.; Duan, P.; Savage, P. E., Hydrothermal Liquefaction and Gasification of Nannochloropsis sp. *Energy & Fuels* **2010,** *24* (6), 3639-3646; (b) Duan, P.; Savage, P. E., Hydrothermal Liquefaction of a Microalga with Heterogeneous Catalysts. *Industrial & Engineering Chemistry Research* **2010,** *50* (1), 52-61; (c) Valdez, P. J.; Dickinson, J. G.; Savage, P. E., Characterization of product fractions from hydrothermal liquefaction of Nannochloropsis sp. and the influence of solvents. *Energy & Fuels* **2011,** *25* (7), 3235-3243.

26. Levine, R. B.; Pinnarat, T.; Savage, P. E., Biodiesel Production from Wet Algal Biomass through in Situ Lipid Hydrolysis and Supercritical Transesterification. *Energy & Fuels* **2010,** *24* (9), 5235-5243.

27. (a) Yoshida, H.; Terashima, M.; Takahashi, Y., Production of Organic Acids and Amino Acids from Fish Meat by Sub-Critical Water Hydrolysis. *Biotechnology progress* **1999,** *15* (6), 1090-1094; (b) Rogalinski, T.; Herrmann, S.; Brunner, G., Production of amino acids from bovine serum albumin by continuous sub-critical water hydrolysis. *The*

Journal of Supercritical Fluids **2005,** *36* (1), 49-58; (c) Quitain, A. T.; Sato, N.; Daimon, H.; Fujie, K., Production of Valuable Materials by Hydrothermal Treatment of Shrimp Shells. *Industrial & Engineering Chemistry Research* **2001,** *40* (25), 5885-5888.

28. Appell, H. R.; Fu, Y. C.; Friedman, S.; Yavorsky, P. M. *Converting organic wastes to oil: A replenishable energy source*; 1971.

29. (a) Elliott, D. C., Bench-scale research in biomass liquefaction by the CO-steam process. *Canadian Journal of Chemical Engineering* **1980,** *58* (6), 730-734; (b) Elliott, D. C.; Sealock, L. J. J.; Baker, E. G., Chemical processing in high-pressure aqueous environments. 3. Batch reactor process development experiments for organics destruction. *Industrial & engineering chemistry research* **1994,** *33* (3), 558-565; (c) Sealock Jr, L. J.; Elliott, D. C.; Baker, E. G.; Butner, R. S., Chemical processing in high-pressure aqueous environments. 1. Historical perspective and continuing developments. *Industrial & engineering chemistry research* **1993,** *32* (8), 1535-1541; (d) Elliott, D. C.; Beckman, D.; Bridgwater, A. V.; Diebold, J. P.; Gevert, S. B.; Solantausta, Y., Developments in direct thermochemical liquefaction of biomass: 1983-1990. *Energy & Fuels* **1991,** *5* (3), 399-410.

30. Goudriaan, F.; van de Beld, B.; Boerefijn, F. R.; Bos, G. M.; Naber, J. E.; van der Wal, S.; Zeevalkink, J. A., *Thermal Efficiency of the HTU® Process for Biomass Liquefaction*. Blackwell Science Ltd: 2008; p 1312-1325.

31. He, B. J.; Zhang, Y.; Yin, Y.; Funk, T. L.; Riskowski, G. L., Operating temperature and retention time effects on the thermochemical conversion process of swine manure. *Transactions of the ASAE* **2000,** *43* (6), 1821-1826.

32. He, B. J.; Zhang, Y.; Yin, Y.; Funk, T. L.; Riskowski, G. L., Preliminary characterization of raw oil products from the thermochemical conversion of swine manure. *Transactions of the ASAE* **2001,** *44* (6), 1865-1872.

33. Bobleter, O.; Niesner, R.; Röhr, M., The hydrothermal degradation of cellulosic matter to sugars and their fermentative conversion to protein. *Journal of Applied Polymer Science* **1976,** *20* (8), 2083-2093.

34. Mok, W. S. L.; Antal, M. J., Uncatalyzed solvolysis of whole biomass hemicellulose by hot compressed liquid water. *Industrial & Engineering Chemistry Research* **1992,** *31* (4), 1157-1161.

35. Sakaki, T.; Shibata, M.; Miki, T.; Hirosue, H.; Hayashi, N., Decomposition of Cellulose in Near-Critical Water and Fermentability of the Products. *Energy & Fuels* **1996,** *10* (3), 684-688.

36. Watanabe, M.; Bayer, F.; Kruse, A., Oil formation from glucose with formic acid and cobalt catalyst in hot-compressed water. *Carbohydrate Research* **2006,** *341* (18), 2891-2900.

37. Karagöz, S.; Bhaskar, T.; Muto, A.; Sakata, Y.; Uddin, M. A., Low-temperature hydrothermal treatment of biomass: effect of reaction parameters on products and boiling point distributions. *Energy & fuels* **2004,** *18* (1), 234-241.

38. (a) Karagöz, S.; Bhaskar, T.; Muto, A.; Sakata, Y.; Oshiki, T.; Kishimoto, T., Low-temperature catalytic hydrothermal treatment of wood biomass: analysis of liquid products. *Chemical Engineering Journal* **2005,** *108* (1-2), 127-137; (b) Karagöz, S.; Bhaskar, T.; Muto, A.; Sakata, Y., Hydrothermal upgrading of biomass: Effect of K_2CO_3

concentration and biomass/water ratio on products distribution. *Bioresource Technology* **2006,** *97* (1), 90-98.

39. Karagöz, S.; Bhaskar, T.; Muto, A.; Sakata, Y., Comparative studies of oil compositions produced from sawdust, rice husk, lignin and cellulose by hydrothermal treatment. *Fuel* **2005,** *84* (7-8), 875-884.

40. (a) Minowa, T.; Murakami, M.; Dote, Y.; Ogi, T.; Yokoyama, S.-y., Oil production from garbage by thermochemical liquefaction. *Biomass and Bioenergy* **1995,** *8* (2), 117-120; (b) Minowa, T.; Zhen, F.; Ogi, T., Cellulose decomposition in hot-compressed water with alkali or nickel catalyst. *The Journal of Supercritical Fluids* **1998,** *13* (1-3), 253-259.

41. Binder, J. B.; Raines, R. T., Fermentable sugars by chemical hydrolysis of biomass. *Proceedings of the National Academy of Sciences* **2010,** *107* (10), 4516.

42. Durot, N.; Gaudard, F.; Kurek, B., The unmasking of lignin structures in wheat straw by alkali. *Phytochemistry* **2003,** *63* (5), 617-623.

43. Chang, V. S.; Burr, B.; Holtzapple, M. T., Lime pretreatment of switchgrass. *Appl Biochem Biotechnol* **1997,** *63* (1), 3-19.

44. Ramsurn, H.; Kumar, S.; Gupta, R. B., Enhancement of Biochar Gasification in Alkali Hydrothermal Medium by Passivation of Inorganic Components Using Ca $(OH)_2$. *Energy & Fuels* **2011**.

45. (a) Hu, Z.; Ragauskas, A. J., Hydrothermal Pretreatment of Switchgrass. *Industrial & Engineering Chemistry Research* **2011,** *50* (8), 4225-4230; (b) Jensen, J.; Morinelly, J.; Aglan, A.; Mix, A.; Shonnard, D. R., Kinetic characterization of biomass

dilute sulfuric acid hydrolysis: Mixtures of hardwoods, softwood, and switchgrass. *AIChE Journal* **2008,** *54* (6), 1637-1645.

46. Demirbas, A., Mechanisms of liquefaction and pyrolysis reactions of biomass. *Energy Conversion and Management* **2000,** *41* (6), 633-646.

47. Demirbas, A., Effect of lignin content on aqueous liquefaction products of biomass. *Energy Conversion and Management* **2000,** *41* (15), 1601-1607.

48. Resende, F. L. P.; Fraley, S. A.; Berger, M. J.; Savage, P. E., Noncatalytic gasification of lignin in supercritical water. *Energy & Fuels* **2008,** *22* (2), 1328-1334.

49. Mosier, N.; Wyman, C.; Dale, B.; Elander, R.; Lee, Y. Y.; Holtzapple, M.; Ladisch, M., Features of promising technologies for pretreatment of lignocellulosic biomass. *Bioresource technology* **2005,** *96* (6), 673-686.

50. Zhong, C.; Wei, X., A comparative experimental study on the liquefaction of wood. *Energy* **2004,** *29* (11), 1731-1741.

51. Kaar, W. E.; Holtzapple, M. T., Using lime pretreatment to facilitate the enzymic hydrolysis of corn stover. *Biomass and Bioenergy* **2000,** *18* (3), 189-199.

52. Kumar, S.; Kothari, U.; Kong, L.; Lee, Y. Y.; Gupta, R. B., Hydrothermal pretreatment of switchgrass and corn stover for production of ethanol and carbon microspheres. *Biomass and Bioenergy* **2011**.

53. (a) Neumann, M.; Epple, M., Monohydrocalcite and Its Relationship to Hydrated Amorphous Calcium Carbonate in Biominerals. *European Journal of Inorganic Chemistry* **2007,** *2007* (14), 1953-1957; (b) Kimura, T.; Koga, N., Thermal Dehydration of Monohydrocalcite: Overall Kinetics and Physico-geometrical Mechanisms. *The Journal of Physical Chemistry A* **2011,** *115* (38), 10491-10501; (c) Kimura, T.; Koga, N.,

Monohydrocalcite in Comparison with Hydrated Amorphous Calcium Carbonate: Precipitation Condition and Thermal Behavior. *Crystal Growth & Design* **2011,** *11* (9), 3877-3884.

54. Çaglar, A.; Demirbas, A., Conversion of cotton cocoon shell to liquid products by supercritical fluid extraction and low pressure pyrolysis in the presence of alkalis. *Energy Conversion and Management* **2001,** *42* (9), 1095-1104.

55. Rustamov, V. R.; Abdullayev, K. M.; Samedov, E. A., Biomass conversion to liquid fuel by two-stage thermochemical cycle. *Energy Conversion and Management* **1998,** *39* (9), 869-875.

56. Sun, P.; Heng, M.; Sun, S.; Chen, J., Direct liquefaction of paulownia in hot compressed water: Influence of catalysts. *Energy* **2010,** *35* (12), 5421-5429.

57. Mazaheri, H.; Lee, K. T.; Bhatia, S.; Mohamed, A. R., Sub/supercritical liquefaction of oil palm fruit press fiber for the production of bio-oil: Effect of solvents. *Bioresource technology* **2010,** *101* (19), 7641-7647.

58. Zhou, D.; Zhang, L.; Zhang, S.; Fu, H.; Chen, J., Hydrothermal liquefaction of macroalgae Enteromorpha prolifera to bio-oil. *Energy & Fuels* **2010,** *24* (7), 4054-4061.

59. Ross, A. B.; Biller, P.; Kubacki, M. L.; Li, H.; Lea-Langton, A.; Jones, J. M., Hydrothermal processing of microalgae using alkali and organic acids. *Fuel* **2010,** *89* (9), 2234-2243.

60. He, R.; Ye, X. P.; English, B. C.; Satrio, J. A., Influence of pyrolysis condition on switchgrass bio-oil yield and physicochemical properties. *Bioresource technology* **2009,** *100* (21), 5305-5311.

61. Wang, C.; Pan, J.; Li, J.; Yang, Z., Comparative studies of products produced from four different biomass samples via deoxy-liquefaction. *Bioresource Technology* **2008,** *99* (8), 2778-2786.

62. Lu, Q.; Yang, X.; Zhu, X., Analysis on chemical and physical properties of bio-oil pyrolyzed from rice husk. *Journal of Analytical and Applied Pyrolysis* **2008,** *82* (2), 191-198.

63. Kobayashi, N.; Okada, N.; Hirakawa, A.; Sato, T.; Kobayashi, J.; Hatano, S.; Itaya, Y.; Mori, S., Characteristics of Solid Residues Obtained from Hot-Compressed-Water Treatment of Woody Biomass. *Industrial & Engineering Chemistry Research* **2008,** *48* (1), 373-379.

64. Kumar, S.; Gupta, R. B., Biocrude production from switchgrass using subcritical water. *Energy & Fuels* **2009,** *23* (10), 5151-5159.

65. Xiao, L.-P.; Sun, Z.-J.; Shi, Z.-J.; Xu, F.; Sun, R.-C., Impact of hot compressed water pretreatment on the structural changes of woody biomass for bioethanol production. *Bioresources* **2011,** *6* (2), 1576-1598.

66. (a) Ozcimen, D.; Ersoy-Mericboyu, A., Characterization of biochar and bio-oil samples obtained from carbonization of various biomass materials. *Renewable Energy* **2010,** *35* (6), 1319-1324; (b) Sensoz, S.; Angin, D.; Yorgun, S., Influence of particle size on the pyrolysis of rapeseed (Brassica napus L.): fuel properties of bio-oil. *Biomass and Bioenergy* **2000,** *19* (4), 271-279; (c) Lu, Q.; Yang, X.-l.; Zhu, X.-f., Analysis on chemical and physical properties of bio-oil pyrolyzed from rice husk. *Journal of Analytical and Applied Pyrolysis* **2008,** *82* (2), 191-198; (d) Qian, Y.; Zuo, C.; Tan, J.;

He, J., Structural analysis of bio-oils from sub-and supercritical water liquefaction of woody biomass. *Energy* **2007,** *32* (3), 196-202.

67. Yu, F.; Ruan, R.; Chen, P.; Deng, S.; Liu, Y.; Lin, X., Liquefaction of corn cobs with supercritical water treatment. *Trans. ASABE* **2007,** *50* (1), 175-180.

68. Cheng, L.; Ye, X. P.; He, R.; Liu, S., Investigation of rapid conversion of switchgrass in subcritical water. *Fuel Processing Technology* **2009,** *90* (2), 301-311.

69. Ingram, L.; Mohan, D.; Bricka, M.; Steele, P.; Strobel, D.; Crocker, D.; Mitchell, B.; Mohammad, J.; Cantrell, K.; Pittman, C. U., Pyrolysis of Wood and Bark in an Auger Reactor: Physical Properties and Chemical Analysis of the Produced Bio-oils. *Energy & Fuels* **2007,** *22* (1), 614-625.

70. Mahinpey, N.; Murugan, P.; Mani, T.; Raina, R., Analysis of Bio-Oil, Biogas, and Biochar from Pressurized Pyrolysis of Wheat Straw Using a Tubular Reactor. *Energy & Fuels* **2009,** *23* (5), 2736-2742.

Chapter 4

Deoxy-Liquefaction of Switchgrass in Supercritical Water with Calcium Formate as an *in-situ* Hydrogen Donor

4.1 Introduction

As mentioned earlier in Chapter 1, upgrading biomass to liquid fuel is usually a two-step process: depolymerizing biomass to a liquid product (bio-oil or biocrude) mainly through pyrolysis or hydrothermal liquefaction and then upgrading the bio-oil/biocrude usually via catalytic cracking or catalytic hydrotreatment.[1] Biomass liquefaction usually occurs at 50-200 atm and 250-450 °C to produce a water-insoluble biocrude. The reactor feed consists of a slurry of biomass and solvent, reducing gases and catalyst (including alkali, metals and Ni/Ru heterogeneous catalysts), if required.[2] Chapter 1 gives the advantages of hydrothermal liquefaction while Chapter 3 (Section 3.1.1) details biomass liquefaction in sub- and supercritical water. In this study, supercritical water has been used to liquefy biomass because of its unique properties: both density and dielectric constant decrease with temperature while the ionic product increases first and then decreases, as supercritical state is reached. Therefore, these properties can be tuned to control the reaction rates by varying the temperature and pressure.[3] Supercritical water (SCW) has high reactivity, and hydrolysis reactions in SCW are determined by the pressure dependence of the solvent (water) properties

including density, dielectric constant and solubility parameter.[4] According to Klein et al.,[5] the mechanism in SCW is as follows: molecules containing a saturated carbon attached to a heteroatom (any atom that is not carbon or hydrogen)-containing leaving group are transformed through simultaneous pyrolysis and hydrolysis reactions.

After the depolymerization and fragmentation of the lignocellulosic biomass, the biocrude formed is an oxygenated multi-component mixture of different size molecules.[1] Since the direct use of biocrude is not feasible, chemical transformation is required to increase its volatility, thermal stability, heating value and to reduce its viscosity through oxygen removal and molecular weight reduction.[6] One of the main upgrading routes is hydrodeoxygenation (HDO) which entails the removal of oxygen in the form of H_2O, the reduction in molecular weight and the formation of saturated C-C bonds. Usually, HDO involves treatment of bio-oils at 300-600 °C with high pressure H_2 (10-20 MPa) in the presence of heterogeneous catalysts.[2] In most studies, hydrodeoxygenation has been conventionally carried out on sulfided alumina-supported CoMo and NiMo catalysts. Their surfaces are extremely dynamic and flexible, keeping their ability to facilitate several reactions through different mechanisms.[7] Chapter 1 (Section 1.3.3.1) gives an overview on the HDO process.

4.1.1 Upgrading of Biocrude using Hydrogen Donors

On the other hand, a number of studies have been conducted whereby hydrogenation of oxygenated hydrocarbons have been performed using a hydrogen donor, instead of hydrogen gas and sulfide catalysts. Boudjouk and Hann[8] found formic acid (FA) and Pd/C to be effective in olefin hydrogenation at room temperature and

pressure with sonication. Sasson et al.[9] also used aqueous FA salt solutions and heterogeneous Pd/C to investigate soybean oil methyl ester hydrogenation. Complete hydrogenation was achieved with 10 M potassium formate at 80 °C, 0.2-0.4% Pd for 16 hours. Kleinert and Barth[10] used formic acid/alcohol mixtures as reaction medium to convert lignin to oil in a pyrolysis/solvolysis process. The reactions were carried out at 380 °C and were run overnight (14-17 hours) to give liquid yields of about 90%. The liquid oil had a heating value of 35.6-44 MJ/kg. They postulated that since formic acid acted as a hydrogen donor and the alcohol as a co-solvent, the yield and H/C ratio were improved to obtain a hydrogen-rich, oxygen-depleted product. Heeres et al.[11] hydrogenated C6 sugars to ɤ-valerolactone (GVL) in the presence of FA and Ru/C hydrogenation catalyst. The highest yield of GVL was 52 mol% obtained at 180 °C, 16 h reaction time and fructose as the C6 sugar. A similar conversion was reported by Kopetzki and Antonietti[12] whereby transfer hydrogenation from FA to levulinic acid was achieved under hydrothermal conditions and sulfate catalyst.

The use of FA as a hydrogen donor, an acid catalyst and a deoxygenating agent was exploited by another study[13] to convert 5-(Hydroxymethyl)furfural (HMF) to 2,5-dimethylfuran (DMF) and fructose to DMF, in one-pot and in the presence of Pd/C, THF and H_2SO_4. A yield of >95% was obtained when a solution of HMF was heated in refluxing THF with formic acid, H_2SO_4, and Pd/C for 15 hours. Dehydration of fructose with formic acid at 100 °C in 10 mol% H_2SO_4 for 5 hours gave an HMF selectivity of 93%. Bulushev and Ross[14] have effectively hydrogenated ethylene and propylene by using FA over a Pd/C catalyst. They found that 95% of H_2 formed by FA decomposition was consumed for ethane formation with a conversion of > 90%. Wheeler and his

group[15] have also worked on stabilizing formic acid as a calcium salt which would decompose at relevant pyrolitic temperatures to give hydrogen. Both formic and levulinic acids, obtained from biomass hydrolysis, were mixed with $Ca(OH)_2$ to form the respective calcium salts before thermal deoxygenation at 450 °C. The oil yield and deoxygenation of levulinic acid improved with formate salt addition, as evidenced by the detection of more aromatics and alkenes via NMR. They also proposed a new method for the preparation of lignin by first pretreating it with $Ca(OH)_2$, then FA was added before the mixture was dried and ground.[16] Here, the so-formed calcium formate was the source of hydrogen during pyrolysis at 500 °C with a maximum liquid yield of 32.5% and an HHV of 41.7 MJ/kg.

4.1.2 Rationale for using Calcium Formate as a Hydrogen Donor

In this study, instead of using formic acid, calcium formate has been examined as a more environmental-friendly hydrogen donor since it has been used as road de-icer, concrete cure accelerator and in the animal feed industry.[17] Furthermore, it is safer and easier to handle and use in the laboratory setting when compared with formic acid whose use could be associated with additional costs for corrosion-resistant materials. $Ca(HCOO)_2$ was intended to be directly used as a source of hydrogen during hydrothermal liquefaction of biomass. The biomass used here was switchgrass instead of pure model compounds like lignin or cellulose, so the results obtained from HDO could be used to postulate some mechanism. Furthermore, it was hypothesized that the simultaneous H_2 formation from the decomposition of the formate salt and oxygenated

hydrocarbon compounds production from biomass liquefaction would result in HDO, and hence result in a biocrude of a higher energy density.

4.1.3 Objectives of this Study

This investigation aimed at first studying the decomposition behavior of calcium formate in supercritical water as a potential hydrogen donor. The main objective was to see how the presence of calcium formate during biomass liquefaction would affect the biocrude quality so that a biocrude upgrading mechanism could be proposed.

4.2. Experimental Section

4.2.1 Materials and Apparatus

Alamo switchgrass, having 7.3 wt% moisture, was ground to pass through a 1-mm screen and used as the feedstock biomass, with the compositional analysis presented elsewhere.[18] The same set-up used for gasification and liquefaction has been used. Section 2.2.2.2 details the reactor and fittings used.

4.2.2 Experimental Procedure

4.2.2.1 Thermogravimetric Analysis of Calcium Formate

In order to determine the decomposition temperature of calcium formate, thermogravimetric analysis (TGA) was performed with a Thermal Analysis Instruments (New Castle, DE) TGA Q50. A 10 mg sample of calcium formate (obtained from Alfa Aesar, 98%) was placed in a platinum pan in argon atmosphere. The samples were heated from room temperature to 900 °C at a heating rate of 10 °C/min. The TGA

results, as shown in Figure 1, revealed the thermal decomposition behavior of the formate salt. The salt decomposed within 315-423 °C range but maximum weight loss was obtained at ~ 400.75 °C.

The decomposition reaction is as follows:

$$Ca(HCOO)_2 \longrightarrow CaCO_3 + CO + H_2 \quad (1)$$

The second peak at ~ 599 °C represents the decomposition of the carbonate to calcium oxide. This data therefore indicates that below 300 °C, the salt does not decompose or act as the hydrogen donor. The hydrothermal liquefaction experiments were therefore carried in the range of 350-450 °C.

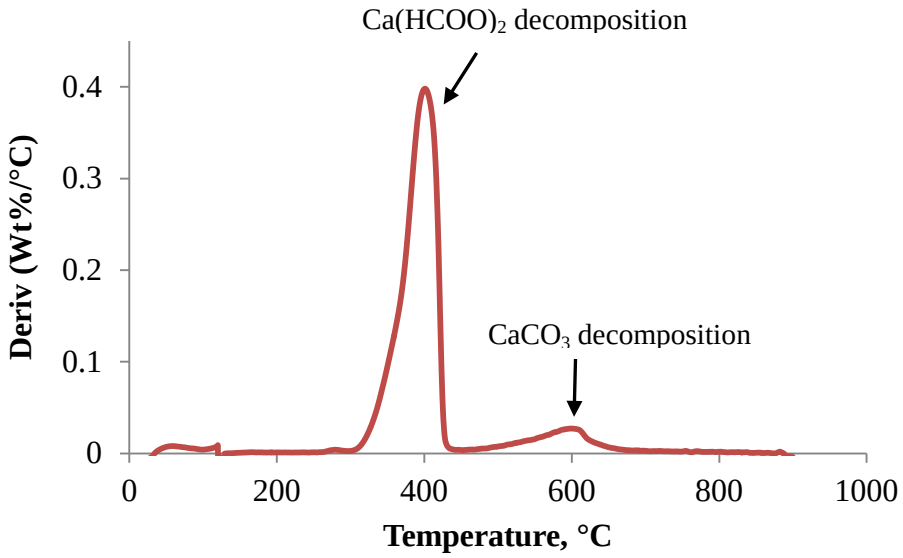

Figure 4.1 Thermogravimetric analysis (TGA) of calcium formate

4.2.2.2 Hydrothermal Decomposition of Formate Salt

2 g (dry basis) of calcium formate (obtained from Alfa Aesar, 98%) and 20 ml of deionized water were fed to the reactor, which was then heated to 350, 400 and 450 °C by

an electric furnace for 30 minutes. As per the TGA results, the temperature dictates the decomposition of the salt and partial decomposition would result in less hydrogen available for deoxy-liquefaction. Hence, the behavior of the formate salt in hydrothermal media at these three different temperatures was investigated. It is to be noted that in our lab, previous work done on switchgrass [19,20] had determined that 20-30 minutes was the optimum reaction time to depolymerize the biomass to obtain maximum biocrude yield. Also, through observation, it takes about 30 mins for the reaction to stabilize. This is usually indicated by no pressure fluctuations/change on the gages. Therefore, using less than 30 minutes will be detrimental to the biocrude yield and more time might shift the reaction in the gasification mode. A stainless steel frit (pore size 2 μm), placed at the outlet of the reactor, prevented entrainment of solids in the exiting stream. The temperature of the furnace was set such that the thermocouple T1 would give the desired reaction temperature. Reaction time started when the desired temperature (indicated by T1) was reached inside the reactor. Typically, a pressure of 160-270 bar was generated upon heating, depending on the operating temperature. The effect of pressure was not investigated since in supercritical medium, pressure has a minor effect on yield.[21] After completion of the reaction, the furnace was switched off and the reactor was air-cooled. As soon as the pressure reached below 41 bar, a valve was opened so that an accurate reading of the pressure could be obtained from P2. Upon cooling, the temperature and residual pressure due to formed gas were noted before GC analysis was performed. After depressurization, the reactor was opened to collect the water and solid residue. The water was analysed for pH and then evaporated to recuperate any dissolved solids. All residues were collected for further analysis.

4.2.2.3 Hydrothermal Liquefaction of Switchgrass

1 g (dry basis) of switchgrass and 20 ml of deionized water were fed to the reactor. The same procedure as described in Section 4.2.2.1 was used. Upon depressurization, the reactor was opened to collect biocrude and the remaining biomass. Biocrude-W (aqueous phase) was obtained by simply collecting the liquid from the reactor. Biocrude (oily/non-polar phase) was extracted by washing the unliquefied biomass and reactor walls with acetone and subsequently evaporating off the acetone using a rotary evaporator. The biochar and salt residues left were then dried for further analysis. The yield of biocrude was calculated using:

$$Yield\ (\%) = \frac{weight\ of\ biocrude\ obtained, g}{dry\ weight\ of\ switchgrass\ used, g} x\ 100$$

4.2.2.4 Hydrothermal Liquefaction of Switchgrass in the presence of Calcium Formate

Here, 1 g (dry basis) of switchgrass, 2-4g of calcium formate and 20 ml of deionized water were fed to the reactor. Through some basic calculations, it was found that theoretically at least 2 g of calcium formate were required to remove all the oxygen present in 1 g of switchgrass in the form of CO_2 and H_2O. This is why 2 g was used as the starting weight of the hydrogen donor. The same procedures as described in sections 4.2.2.2 and 4.2.2.3 were used. All experiments throughout this paper were at least run twice to ensure repeatability and the standard deviations for the yields were found to be around 1.2-2.3%, 1.5-6.6%, and 4.3-5.3% for Tables 4.1, 4.2 and 4.3 respectively. It is to be noted that the same formula for the yield (Section 4.2.2.3) was used since any

undissolved calcium formate would remain in the aqueous phase (biocrude-W) while the calcium carbonate formed will remain in the residues.

4.3 Product Characterization

4.3.1 Gas Chromatography (GC), Fourier Transform Infrared (FTIR) & Total Organic Carbon (TOC) Analysis

The gas composition was determined using the same gas chromatograph (SRI 8610C) described in Chapter 2 (Section 2.3.1). Section 2.3.3 describes the apparatus used to determine the FTIR spectra while Section 2.3.5 details the total organic carbon analyzer used.

4.3.2 Gas Chromatograph Mass Spectrometer (GC-MS) Analysis

The biocrude samples were analyzed using an Agilent 7890 GC/5975MS equipped with DB-1701 column 30 m in length, 0.25 mm i.d. and 0.25 mm film thickness. Section 3.3.2 gives the operating conditions and the procedures used to dilute the biocrude samples. The same procedure was also used for biocrude-W except that 250 mg of the sample was dissolved in 1-2 ml of methanol only.

4.3.3 High-Pressure Liquid Chromatography (HPLC) Analysis

Biocrude-W (aqueous phase) samples were analyzed using HPLC having a Bio-Rad Aminex HPX-87H column, refractive index detector, 0.01 N sulfuric acid mobile phase, and column temperature of 60 °C.

4.4 Results and Discussion

4.4.1 Hydrothermal Decomposition of Calcium Formate

Table 4.1 shows the results obtained when 2 g of calcium formate was subjected to hydrothermal treatment with 20 ml of water. It can be seen that the residual pressure increases with temperature due to the decomposition of the additional formate. At 350 °C, there is partial decomposition of calcium formate while at 400 °C, most of the salt decomposes, in accordance with the TGA results (Figure 4.1). This shows that even in supercritical conditions, the decomposition temperature of the formate salt is similar to that under inert atmosphere and therefore it can be used as an in-situ hydrogen donor within 350-450 °C range. There is not much difference in the results obtained at 400 and 450 °C since most of the calcium formate decomposes at around 400 °C.

Table 4.1 Results of calcium formate decomposition in hydrothermal media, without biomass

Run No.	Temperature, °C	Residual pressure, bar	Residue, g	Gas Composition (mole %)			
				H_2	CO	CH_4	CO_2
1.	350	6.9	1.1	65.3	29.3	0	5.5
2.	400	11.0	1.4	58.2	17.3	0.7	23.9
3.	450	12.1	1.4	59.2	12.4	1.3	27.1

Theoretically, 2 g of $Ca(HCOO)_2$ should yield 1.54 g of $CaCO_3$. Both at 400 and 450 °C, about 1.4 g of residue was collected confirming nearly complete decomposition (91%) of

the formate salt to carbonate while only 1.1 g (71%) of calcium carbonate was obtained at 350°C due to partial formate decomposition.

From Figure 4.2, it can be observed that as temperature was increased, the yield of hydrogen and carbon dioxide increased too. The analysis of the residual gas showed quite clearly that the major products were H_2 and CO_2 for the higher temperatures while at 350°C, the main products were H_2 and CO.

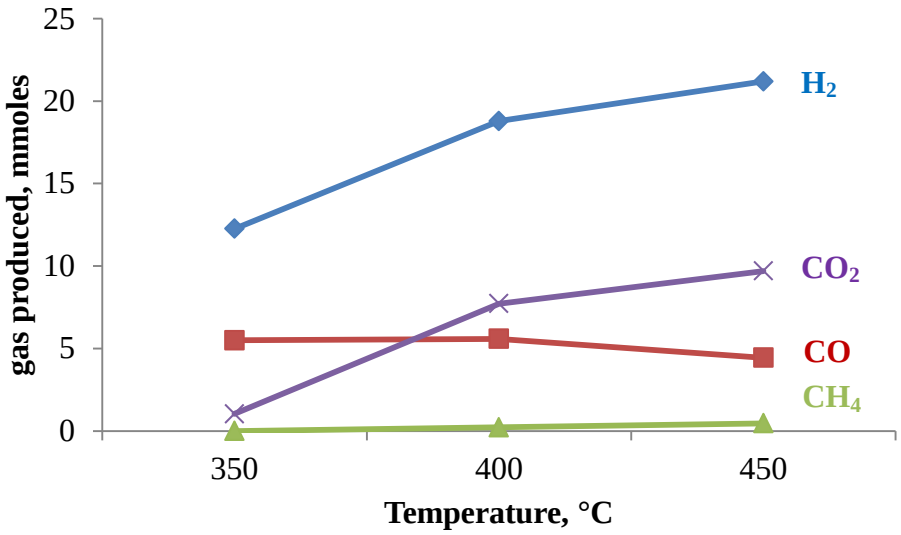

Figure 4.2 Gas composition after hydrothermal decomposition of 2 g (15.4 mMoles) of $Ca(HCOO)_2$

This means that at lower temperatures, the decomposition of formate salt is mainly due to reaction 1 whereby the products are $CaCO_3$, CO and H_2 while a hydrolysis reaction (reaction 2) was favored at higher temperatures:

$$Ca(HCOO)_2 + H_2O \longrightarrow CaCO_3 + CO_2 + 2H_2 \qquad (2)$$

In fact, reaction 1 should yield 15 mmoles of H_2 if all 2 g of $Ca(HCOO)_2$ decomposed while 31 mmoles would be obtained if the formate salt was hydrolyzed completely as in

reaction 2. From Figure 4.2, the number of mmoles of H_2 obtained was 12, 19 and 21 at 350, 400 and 450 °C respectively. This confirms the hypothesis that at 350 °C, reaction 1 is dominant while at higher temperatures reaction 2 contributes to the hydrogen production. The CO and CO_2 amounts also indicate the same trend since CO_2 amount is lower than that of CO at 350 °C but is higher than CO at 450 °C. At 350, 400 and 450 °C, CO_2 accounted for 7, 50 and 63 % respectively, of the theoretical amount that should be formed if reaction 2 was considered. A similar trend was observed by Onwudili and Williams[22] who studied the hydrothermal reactions of sodium formate and sodium acetate as model intermediate products of sodium hydroxide-promoted hydrothermal biomass gasification. They postulated that at high temperatures, water acts as a reactant via hydrolysis whereby only the stoichiometric reacting water is required. The rest of the water acts as a reaction medium. In fact, the aqueous phase collected after hydrothermal treatment at high temperatures has been lower than the original amount added, hence confirming that water was indeed participating in the hydrolysis of biomass to produce biocrude and gases. The presence of methane, though very little, is probably due to some methanation reactions:

$$CO + 3H_2 \longleftrightarrow CH_4 + H_2O \quad (3)$$

$$CO_2 + 4H_2 \longleftrightarrow CH_4 + 2\,H_2O \quad (4)$$

Because methanation reactions are exothermic, they were not favored at high temperatures and hence the very low methane yields.

FTIR was performed on the residues from runs 1, 2 and 3 as well as on the dissolved solids in the water obtained from run 1 (solids were obtained by evaporation). Figure 4.3 reveals that the calcium formate decomposed to carbonate even at 350 °C (run

1) but some calcium formate was still found dissolved in the water after the hydrothermal treatment (refer to Figure 4.3, the spectra of the dissolved solids in water from run 1), confirming that not all formate decomposed at 350 °C.

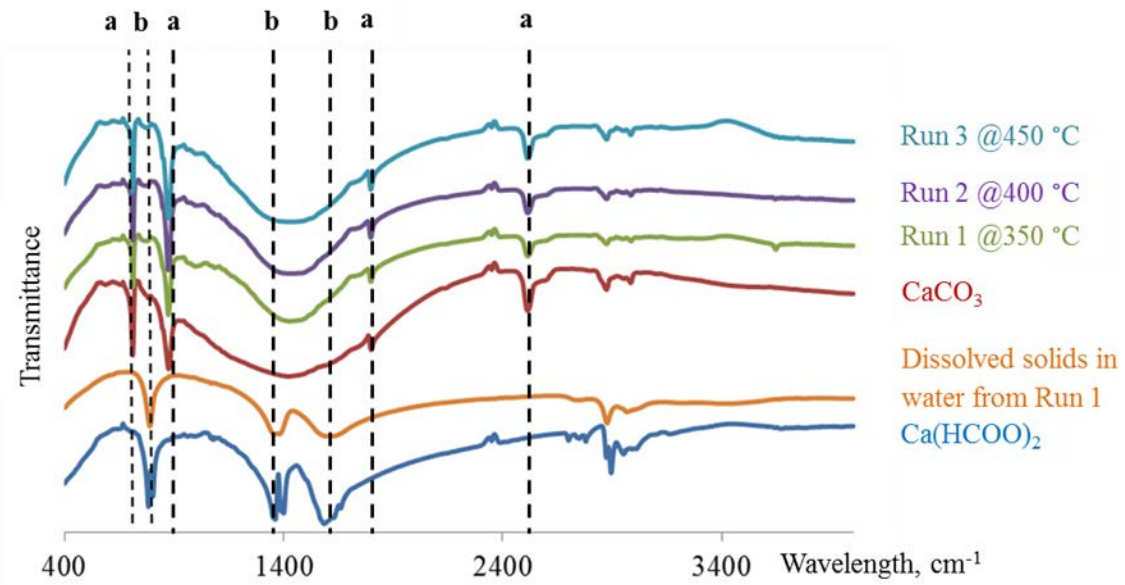

Figure 4.3 FTIR spectra of residues after hydrothermal treatment of calcium formate (Peaks 'a' are due to carbonate and 'b' are due to formate peaks)

Actually about 0.12, 0.08 and 0.06 g of calcium formate were still found dissolved in the water after treatment at 350, 400 and 450 °C respectively, indicating that at 400 °C and above, the salt decomposed almost completely to carbonate. These observations also concord with the residual gas observations discussed earlier.

4.4.2 Hydrothermal Liquefaction of Switchgrass

This series of experiments were carried out to obtain a baseline so that the gas compositions as well as the biocrude yield obtained with and without the formate salt

could be compared. Under hydrothermal conditions, water may catalyze and attenuate reactions like cracking, hydrolysis, decarboxylation, isomerization and cyclization with minimal formation of gases and/or tar.[23]

Table 4.2 Experimental conditions and results for the hydrothermal liquefaction of 1 g of switchgrass

Run No.	Temp, °C	Residual pressure, bar	Biocrude[a] yield,%	Biocrude[a] HHV, kJ/g	Residue, g	Biocrude-W[b] ml	Biocrude-W[b] pH	Biocrude-W[b] TOC, ppm
4.	350	3.1	5.7	27.8	0.2	13	5.3	6294
5.	400	2.8	4.2	28.3	0.2	9	5.9	6780
6.	450	4.5	3.0	28.1	0.1	6	5.8	5716

[a]*Biocrude is the extracted oily phase obtained after hydrothermal treatment*

[b]*Biocrude-W is the aqueous phase biocrude obtained after hydrothermal treatment*

Table 4.2 shows that as temperature was increased, gasification rather than liquefaction was favored since the biocrude yield decreased from nearly 6 to 3 wt%. The heating value of the biocrude was around the same for all three runs, with an average of 28.1 kJ/g compared to switchgrass which has a heating value of 21.3 kJ/g. Run 4 was carried out in subcritical conditions and hence ionic reactions were favored while runs 5 and 6 were performed at supercritical conditions favoring free radical reactions, hence the formation of more gases. At temperatures of 350 and 400 °C, higher methane yields were obtained. Since the conversion of biomass to hydrogen is endothermic while conversion to methane is exothermic[24], the formation of methane was favored at low temperatures according to

Le Chatelier's principle. However, even though the exothermic methanation reactions are suppressed at high temperatures (Figure 4.4), the presence of the calcium carbonate (an alkaline earth salt produced by calcium formate decomposition) catalyzed these reactions to a small extent so that a slight increase in methane was observed with increasing temperature (Figures 4.2 & 4.5).

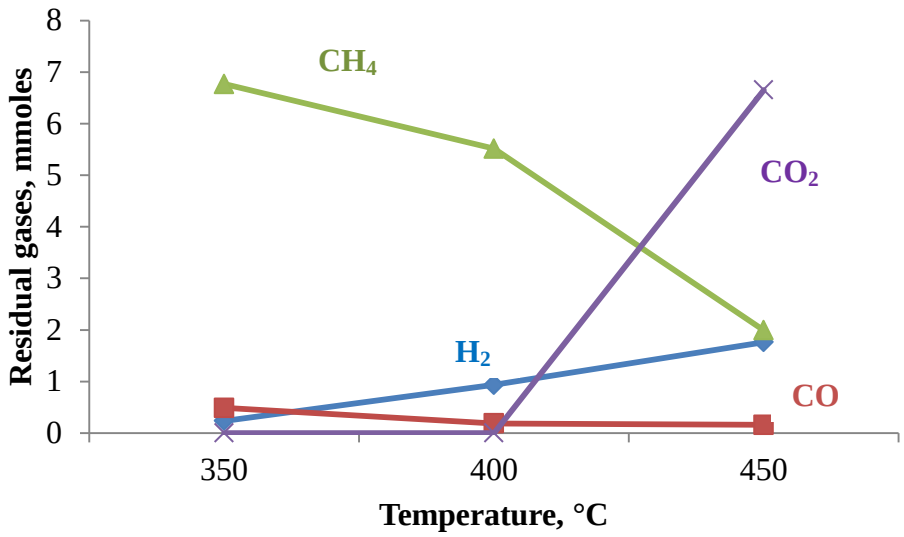

Figure 4.4 Gas compositions after hydrothermal decomposition of 1 g of switchgrass

As the temperature increased, so did the number of moles of hydrogen and carbon dioxide (Figure 4.4), mainly due to steam reforming[25] (reaction 5) of biomass as well as due to the water gas shift (WGS- reaction 6) reactions:

$$CH_xO_y + (1-y)\,H_2O \longrightarrow CO + (1-y+x/2)\,H_2 \qquad (5)$$

$$CO + H_2O \longrightarrow CO_2 + H_2 \qquad (6)$$

Methanation reactions were restrained here since WGS reaction was dominant at high temperatures to form hydrogen. Actually, in supercritical water, ionic dissociation of

water takes place to from OH^- ions which react with CO to form formate anion which in turn decomposes to form CO_2 and the hydride ion, H^-. The latter reacts with water to form hydrogen and OH^- by electron transfer. This explains the low CO amount due to its participation in the WGS reaction.

4.4.3 Hydrothermal Liquefaction of Switchgrass in the presence of Calcium Formate

Table 4.3 shows the experimental conditions and the results obtained for this series of reactions where 2 g of formate was used for 1 g of biomass in 20 ml of water.

Table 4.3 Experimental conditions and results for switchgrass (1 g) hydrothermal liquefaction with calcium formate (2 g)

Run No.	Temp, °C	Residual pressure, bar	Biocrude yield,%	Biocrude HHV, kJ/g	Residue, g	Biocrude-W ml	Biocrude-W pH	Biocrude-W TOC, ppm
7.	350	7.6	9.5	31.2	1.5	11	7.0	8736
8.	400	10.3	9.7	33.9	1.3	7	6.9	10420
9.	450	11.7	13.0	32.2	1.5	12	7.6	8915

The yield of biocrude nearly doubled for all the temperatures used when compared with the yields from Table 4.2 with heating values in the range of 31-34 kJ/g. This increase in the heating value will be discussed in Section 4.4.4. Figure 4.5 reveals that there was excess hydrogen from the calcium formate decomposition during biomass liquefaction

and some of the hydrogen has reacted with the biomass liquefaction products to produce a biocrude of higher quality (less oxygenated).

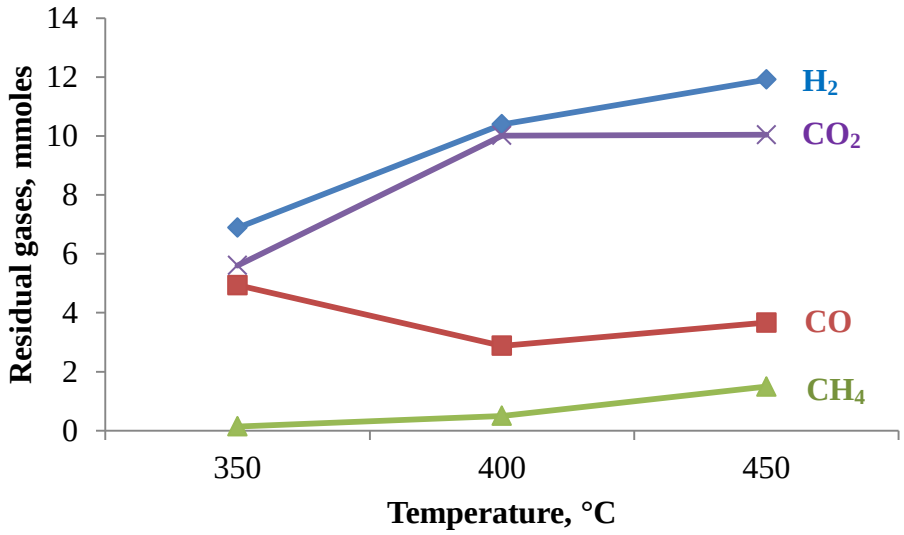

Figure 4.5 Gas compositions after switchgrass (1 g) hydrothermal decomposition with 2 g (15.4 mmoles) calcium formate

This can be better illustrated by using Figure 4.6, which compares the residual moles of hydrogen in the reactor after liquefaction of calcium formate only, switchgrass only and a mixture (2:1 mass basis) of $Ca(HCOO)_2$ and biomass. At all the temperatures, it can be observed that the moles of hydrogen left after biomass and formate salt undergo hydrothermal treatment were less than the amount of hydrogen produced during formate decomposition. This means that some of the hydrogen from the formate salt has been consumed during the liquefaction of biomass to produce hydrogenated biocrude compounds and hence the reason for obtaining a higher heating value of the biocrude. For example at 400 °C, 19 mmoles of hydrogen was generated from 2 g of calcium

formate and 0.9 mmole from biomass but only 10 mmoles was left in the residual gas when 1 g biomass was liquefied with 2 g $Ca(HCOO)_2$.

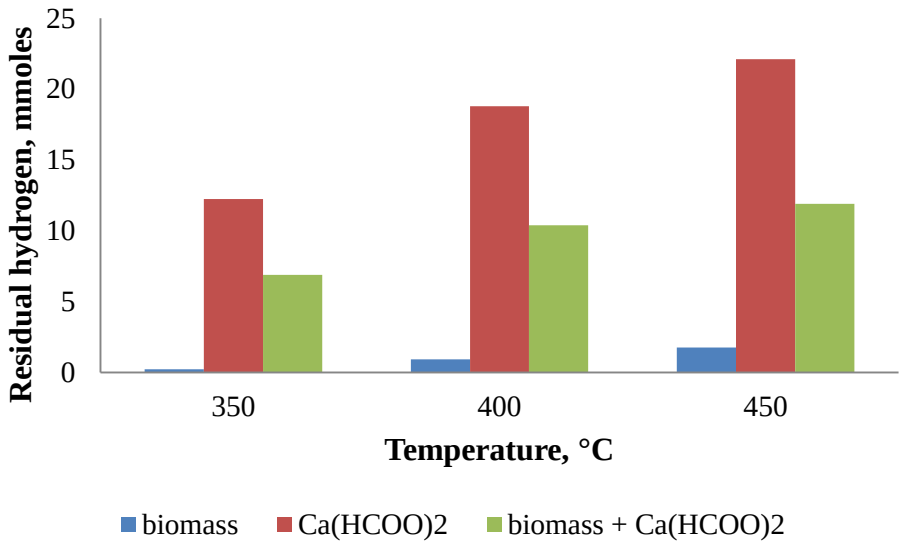

Figure 4.6 Residual moles of hydrogen after hydrothermal treatment

This means that 9.9 mmoles (52%) of hydrogen was consumed for biomass hydrogenation. A similar trend was noted at 350 and 450 °C whereby 46 and 54% H_2 respectively, were used up in the liquefaction of switchgrass.

Some experiments were also carried out using a ratio of 4:1 calcium formate to switchgrass to see the effect, if any, of an even more hydrogen-rich environment on the HDO mechanism and hence on the heating value of the biocrude. However, as seen in Table 4.4, the use of additional calcium formate did not increase the yield or the HHV; however the TOC content of the aqueous phase increased.

Table 4.4 Experimental conditions and results for switchgrass (1 g) hydrothermal liquefaction with calcium formate (4 g)

Run No.	Temp, °C	Residual pressure, bar	Biocrude yield,%	Biocrude HHV, kJ/g	Residue, g	Biocrude-W ml	Biocrude-W pH	Biocrude-W TOC, ppm
10.	350	9.0	9.3	32.1	2.6	8	6.9	18820
11.	400	13.1	12.1	31.2	2.3	5	6.9	15290
12.	450	24.1	11.1	31.8	3.2	5	7.6	12300

In order to understand, the difference in the TOC levels in the biocrude-W of the samples, HPLC analysis was performed on runs 5, 8 and 11. The analysis revealed the presence of carboxylic acids namely formic and acetic acids with very little or none of HMF, sugars, or furfural.

Table 4.5 HPLC analysis of biocrude samples

Compounds	**Run no.5 g/L**	**Run no. 8 g/L**	**Run no. 11 g/L**
Glucose	-	0.3	0.2
Xylose	-	0.3	0.2
Formic Acid	5.4	8.2	35.8
Acetic Acid	2.3	1.4	-
HMF	0.2	0.2	-

The biocrude-W from run no. 5 had more acetic acid but less formic acid than that from runs no. 8 and 11. In the presence of calcium formate, the biocrude-W so produced (runs

no. 8 and 11) had more carboxylic acids with a total of 35.8 g/L (run no.11) and 9.6 g/L (run no. 8) compared to 7.3 g/L from only switchgrass liquefaction (run no. 5). Usually, acetic acid comes from the elimination of acetyl groups originally linked to the xylose unit while formic acid proceeds from carboxylic groups of uronic acid from hemicelluloses.[26] Decomposition of glucose from cellulose and hemicellulose also lead to the formation of formic acid (Figure 4.7).

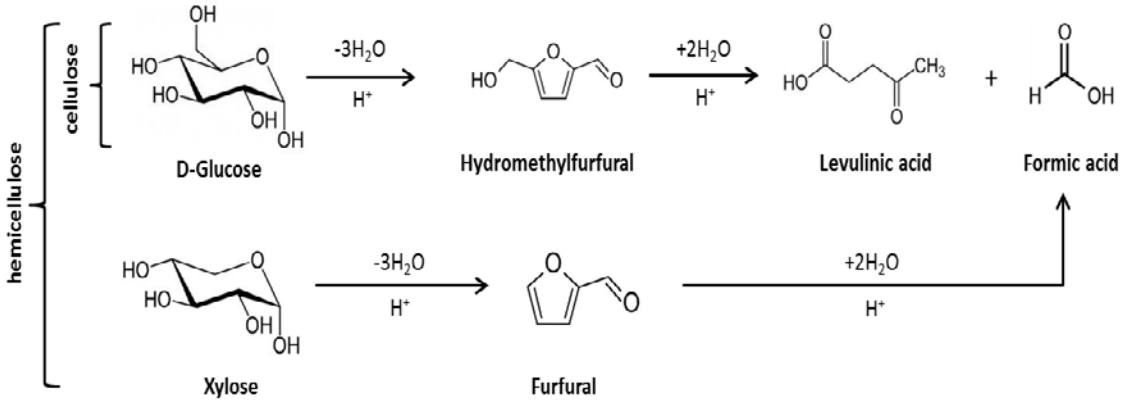

Figure 4.7 Decomposition of hollocellulose components into formic acid

(*Adapted from* Wildschut, J. et al.; 2009 & Palmqvist et al.; 2000)[27]

From the results, it can be deduced that the addition of calcium formate, encouraged the decomposition of glucose and xylose to formic acid, hence the presence of more formic acid in the biocrude-W from runs no. 8 and 11. In fact, in run 11 where 4 g of formate was used, no trace of acetic acid was found in the biocrude but a much higher amount of formic acid was present, hence contributing to the higher TOC value. It is postulated that the hydrogen formed from $Ca(HCOO)_2$ might have acted as a reducing agent and induced the acid-catalyzed decomposition of the hollocellulose. At the same time, the formic acid so-produced could also have further helped to acid-catalyze glucose

and xylose decomposition. But more work has to be done to confirm this postulated mechanism by for example studying the hydrothermal decomposition of glucose and xylose in the presence of calcium formate as the hydrogen donor and catalyst.

Some HMF was still detected in runs 5 and 8 samples but none was found in run no. 11 sample, meaning that all the HMF formed was converted to formic acid due to the hydrogen-rich environment. The formic acid present in the biocrude phase had too low a concentration to be used in turn as a hydrogen donor. Furthermore, the dehydrogenation of formic acid to hydrogen usually requires the presence of some noble metal heterogeneous catalyst like platinum or palladium to facilitate this decomposition and avoid the dehydration route to form water. Usually, at high temperatures (400 °C), repolymerization of the water-soluble liquefaction products occurs[28] to form among others, non-polar higher molecular weight oxygenated hydrocarbons, explaining the low concentration of the acids in the aqueous phase. But the addition of formate and consequently the presence of hydrogen have reduced the re-polymerization reactions which could have led to char formation. According to a proposed mechanism,[29] the presence and availability of hydrogen atoms stabilizes the free radicals formed by cleavage of the bonds in biomass and prevents char formation to a certain extent. This can be substantiated by the presence of the unreacted xylose and glucose in the biocrude-W from runs 8 and 11. Run No. 5, which was devoid of formate salt, did not have any glucose and xylose, leading to the conclusion that these monosaccharides underwent re-polymerization.

4.4.4 GC-MS Analysis

4.4.4.1 Biocrude-W

Samples of biocrude-W (aqueous phase) from runs no. 5 and 8 were analyzed and the results are reported in Table 4.6. It can be clearly observed that the amount of ketones was drastically reduced while that of aldehydes was increased with the addition of the calcium formate. The ketones and aldehydes mainly come from the depolymerization and fragmentation of cellulose and hemicellulose while the phenols originate from lignin decomposition.[30] For instance, cellulose depolymerization produces levoglucosan (1,4-β-D-glucopyranose) which dehydrates to form ketones and aldehydes, according to the mechanism proposed by Pouwels et al.[31]

Table 4.6. GC-MS results of biocrude-W from switchgrass hydrothermal liquefaction with major compound classes relative to the total peak area

Compounds	**Run No. 5** Switchgrass @400°C (Area %)	**Run No. 8** Switchgrass:$Ca(HCOO)_2$ (1:2, mass basis) @400°C (Area %)
Ketones	47.2	3.01
Aldehydes	-	25.5
Phenols	34.16	8.03
Fatty acids & derivatives	1.71	5.02

It is to be noted that most of the aldehydes and ketones are aliphatic with the ketones (cyclopentenone, cyclopentanone) being cyclic and the aldehydes (heptanal, nonanal, decanal) having straight chains.

Cyclic ketones may play an important role in char/coke formation and the addition of formate has reduced its occurrence and produced more linear aldehydes. This means that due to the absence of cyclic ketones, there might be less char formation but poor stability is usually associated with aldehydes because they undergo polymerization reactions. However, the presence of aldehydes, in the aqueous biocrude (biocrude-W) from run 8, means that they did not undergo polymerization /condensation reactions to form tar. This could be explained by the fact that the hydrogen rich environment might have prevented those undesirable reactions to occur. Fewer phenols have been detected when formate salt was added, indicating that the phenols were hydrogenated to other non-polar compounds like benzene (see Section 4.4.4.2 and Figure 4.8), hence upgrading the biocrude. Both the aqueous phase of runs 5 and 8 had trace amounts of 9-octodeceamide. In addition, run no.8 had small amounts of oleic and tridecanoic acids and fatty acid derivatives like 1-octanol. It is to be noted that the apparent increase of the fatty acids and derivatives is mostly due to the presence of water-soluble fatty acid derivatives formed in the presence of the formate salt.

4.4.4.2 Biocrude

Samples of biocrude underwent GC-MS analysis to determine the main compounds present therein and the results are summarized in Table 4.7. The compounds have been grouped into different classes for ease of reference. The major compounds

include highly-oxygenated phenolic compounds, some with methoxy functionalities expected from lignin hydrolysis. The three main structural monomers of lignin namely guaiacylpropane, syringylpropane and *p*-hydroxyphenylpropane are the major contributors for phenolic compounds found in the biocrude.[32]

Table 4.7 Overall GC-MS results of biocrude from switchgrass hydrothermal liquefaction with major compound classes relative to the total peak area

Compounds	**Run No. 5** Switchgrass @400°C (%)	**Run No. 8** Switchgrass: $Ca(HCOO)_2$ (1:2) @400°C (%)	**Run No. 11** Switchgrass: $Ca(HCOO)_2$ (1:4) @400°C (%)	**Run No. 12** Switchgrass: $Ca(HCOO)_2$ (1:4) @450°C (%)
Benzene derivatives	2.8	19.0	9.3	20.2
Phenolic Compounds	8.2	23.8	19.7	13.9
Naphthalene	22.6	15.2	9.7	13.1
Other PAHs	22.7	11.6	12.1	11.7
Piperidinone	-	1.2	-	-
9-Octodeceamide, (Z-)	19.4	-	25.5	21.0

The phenols in the biocrude from run no. 5 (without formate salt) contained methyl- or ethyl-groups as well as alkoxyl groups while the phenols from run no.8, had more methyl/ethyl than alkoxyl groups. This result is in line with the GC-MS analysis done by Mukkamala et al.[16] who performed formate-assisted fast pyrolysis of lignin. The presence of formate salts therefore eliminated significant methoxy functionality from guaiacol-like compounds. This indicated that, in the presence of the formate salt, the aromatic C-O bonds of the alkoxyl groups in lignin were easily fractured to remove the oxygen atoms to enhance deoxy-liquefaction. Indeed, with the addition of calcium formate, the amount of phenolic compounds increased considerably since lignin depolymerisation and hydrodeoxygenation was enhanced. Benzene and related compounds also increased when $Ca(HCOO)_2$ was used. The formate salt reduced the oxygen content in the biocrude through hydrodeoxygenation of phenolic compounds to produce benzene.

Figure 4.8 shows a proposed mechanism by which the phenolic compounds like guaiacol undergo hydrogenation and further recondensation depending on the reaction conditions. Guaiacol is one of the main products obtained during lignin liquefaction due to the cracking of the phenyl-propane units of the macromolecule lattice. Ether and C-C linkages connect the monomeric guaiacylpropane units in lignin with several substructures: the guaiacylglycerol β-aryl ether, the phenyl coumarone, diarylpropane, pinoresinol, biphenyl, diphenyl ether, etc. [33] Ethyl guaiacol has been chosen in the mechanism since it was present in the bio-oil , among other phenolic compounds. The methyl C-O bond is the weakest in the ethyl guaiacol with a bond energy of 245 kJ/mol compared to 356 kJ/mol for the aromatic C-O bond.[33] Therefore, ethyl guaicol will prefer to form ethyl catechol by the cleavage of the aliphatic C-O bond (Figure 4.8,

reaction a). Since there is excess hydrogen present from the formate salt decomposition, the aromatic C-O bond of the hydroxyl group (414 kJ/mol) then cleaves to form ethyl phenol (Figure 4.8, reaction b).

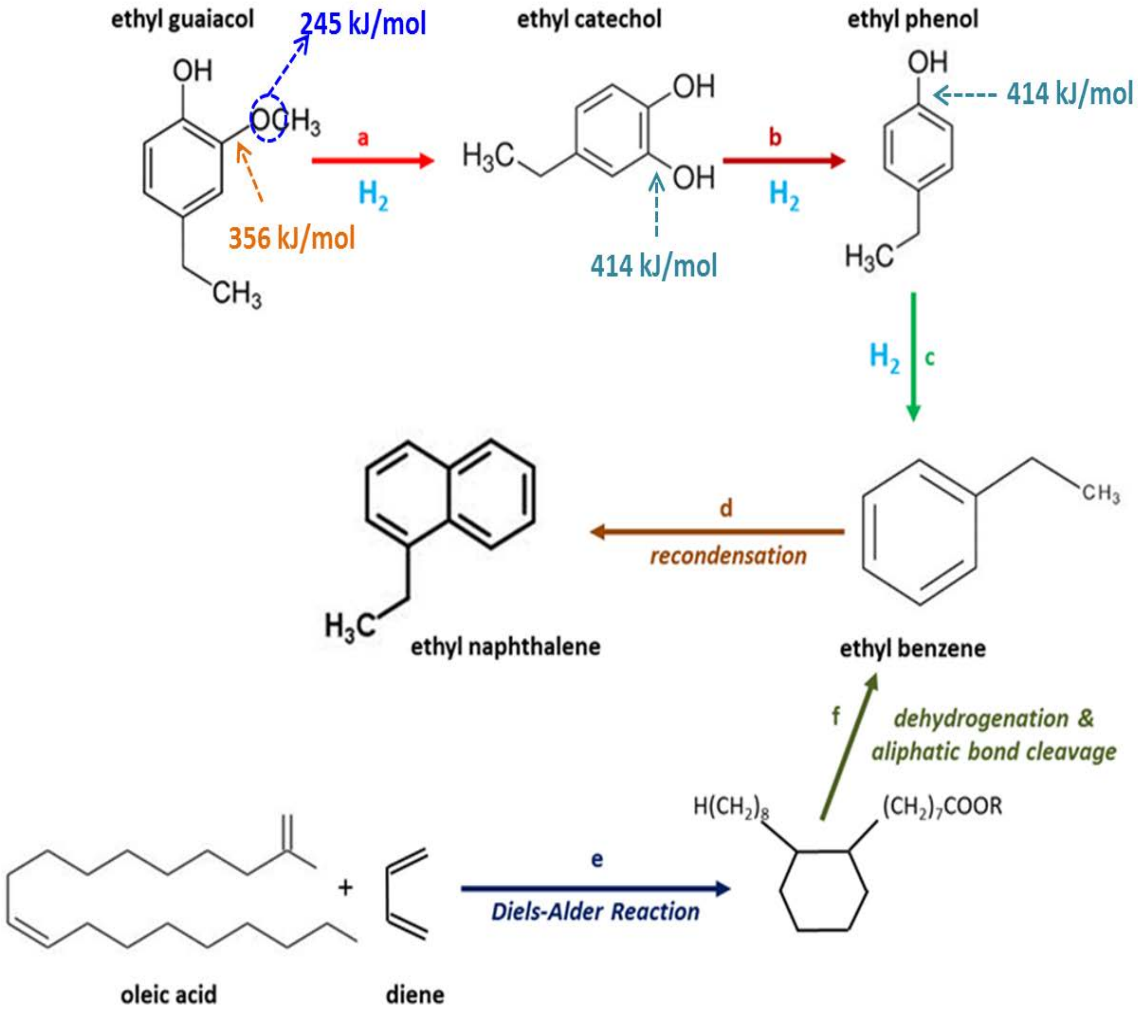

Figure 4.8 Two proposed mechanistic pathways to form benzene: guaiacol hydrodeoxygenation (a,b,c) and subsequent recondensation(d) reaction and Diels-Alder reaction (e) followed by dehydrogenation (f)

The results from Table 4.7 clearly shows an increase in the phenolic compounds as $Ca(HCOO)_2$ was added as a hydrogen source. In the same vein, with an excess of hydrogen, reaction *4.8(c)* takes place whereby the second aromatic C-O bond is cleaved to form a benzene compound. In fact, benzene composition increased from about 3 to 19% with the use of the formate salt.

The presence of the benzene compounds contributed in part towards the increase of the heating value of the biocrude from 28 kJ/kg (run no. 5) to nearly 34 kJ/kg (run no.8). It seems like without $Ca(HCOO)_{2,}$ the benzene compounds undergo recondensation reactions to form polycyclic aromatic hydrocarbons (PAHs) like naphthalene (reaction d). It can be deduced that the formate salts and/or the excess hydrogen limits the formation of PAHs through recondensation. This explains the higher benzene compound percentage in the biocrude in runs 8, 11 and 12 and a reduction of the PAHs amount, therefore lowering health and environmental risks. Furthermore, the reduction of naphthalene and PAHs indicates less probability to form char due to condensation mechanisms.

It is interesting to note that a high molecular weight aliphatic amide, 9-octodeceamide, (Z-) was present in all biocrude except in biocrude from run no. 8 which instead contained 4-piperidinone, another nitrogen compound. 9-Octodeceamide, an amide of the fatty acid oleic acid, is regularly utilized in commercial applications as waterproofing agents, waxes, plastics and lubricants[34] but can also be used as a potential medical treatment for mood and sleep disorders.[35] In one study, it was found that extractives from corn starch was rich in oleic acid while that of wheat straw was rich in 9-octadecadienoic acid (or linoelaidic acid, an omega-6 trans fatty acid and

geometric isomer of linoleic acid).[32] It can therefore be assumed that switchgrass originally contained some unsaturated fatty acid (oleic acid was detected in the aqueous phase using HPLC) which converted into benzene derivatives by Diels-Alder oleic acid addition of a conjugated diene (Figure 4.8, reaction e) followed by dehydrogenation (Figure 4.8, reaction f). The hydrothermal liquefaction of these fatty acids could also result into alkene intermediates which would convert to benzene derivatives by Diels-Alder alkene addition followed by dehydrogenation. The diene compounds for reaction *e* were formed by the dehydrogenation of alkanes (obtained from oleic acid decomposition) to alkenes /dienes. Diels-Alder reaction can also be another route for the formation of the naphthalene and the other PAHs as illustrated in Figure 4.9. Therefore, benzene derivatives could be formed from phenolic compounds, mainly from lignin or from the unsaturated triglycerides in the biomass.

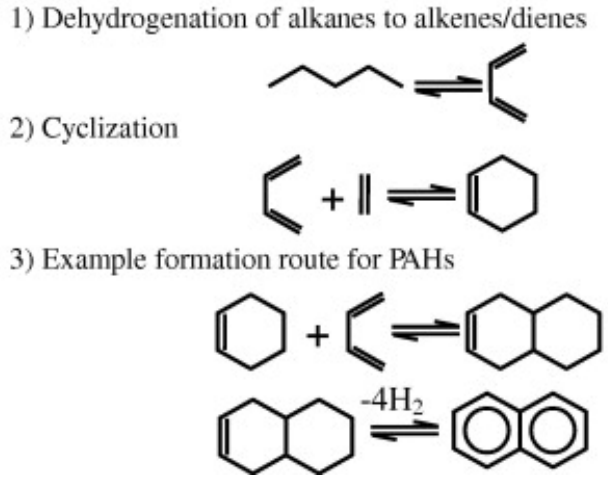

Figure 4.9 Reaction steps for PAHs' formation during hydrothermal liquefaction[36]

(Xu et al., 2013; reproduced with permission of Elsevier Science)

With the doubling of the formate salts but using the same experimental conditions (run no. 11), less benzene was obtained and the amount of octodeceamide was comparable to that of run no. 5 with no formate salt addition. This means that the hydrogen rich environment of run no. 11 was hindering the Diels-Alder mechanism and the dehydrogenation reaction to form benzene. This explains the low benzene amount and the high octodeceamide amount. When the temperature was increased to 450 °C, again there was hindrance in the oleic acid to convert to benzene but the higher temperature promoted more lignin decomposition and hence the so formed phenolic compounds converted into benzene (Figure 4.8, reactions a, b & c). It seems that the mass ratio 1:2 switchgrass: $Ca(HCOO)_2$ gave the better yield of benzene, phenolic compounds and PAHs, explaining the high heating value of the biocrude (34 kJ/kg).

4.5 Conclusions

The use of calcium formate as a hydrogen donor was investigated during the hydrothermal liquefaction of switchgrass. The formate use increases the heating value of biocrude and the amount of benzene, while decreasing the polyaromatic hydrocarbons. This means that there was a reduction in the oxygen content of the biocrude (hence the increase in HHV) through hydrodeoxygenation of mainly phenolic compounds to form benzene rather than to form oxygenated PAHs through recondensation reactions. It is postulated that the benzene formation is due to the hydrogenation of the phenols and through Diels-Alder oleic acid addition of a conjugated diene, followed by dehydrogenation. When the mass ratio of switchgrass to calcium formate was changed from 1:2 to 1:4 at the same temperature of 400 °C, there was no change in the heating

value and in the yield of biocrude. However, by increasing the temperature to 450 °C with 1:4 mass ratio, more benzene compounds were formed due to enhanced hydrogenation of phenols. In summary, by simply using an inexpensive hydrogen donor such as calcium formate, a good quality biocrude can be produced due to hydrodeoxygenation of the depolymerized biomass components.

4.6 Acknowledgments

This work was funded by grants from the National Science Foundation (NSF-CBET-0828269), Alabama Center for Paper and Bioresource Engineering, and the U.S. Department of Energy (DE-FC26-05NT42456). Authors are thankful to Dr. Sushil Adhikari, Ms. Vaishnavi Srinivasan, Dr. Y. Y. Lee, Mr. Tapas Acharjee, Dr. Virginia Davis and Dr Daniel Horn for fruitful discussion and help with chemical analyses.

4.7 References

1. Zhang, S.; Yan, Y.; Li, T.; Ren, Z., Upgrading of liquid fuel from the pyrolysis of biomass. *Bioresource Technology* **2005,** *96* (5), 545-550.

2. Huber, G. W.; Iborra, S.; Corma, A., Synthesis of Transportation Fuels from Biomass: Chemistry, Catalysts, and Engineering. *Chemical Reviews* **2006,** *106* (9), 4044-4098.

3. Savage, P. E., Organic chemical reactions in supercritical water. *Chemical reviews* **1999,** *99* (2), 603-622.

4. Brunner, G., Near critical and supercritical water. Part I. Hydrolytic and hydrothermal processes. *The Journal of Supercritical Fluids* **2009,** *47* (3), 373-381.

5. Klein, M. T.; Torry, L. A.; Wu, B. C.; Townsend, S. H.; Paspek, S. C., Hydrolysis in supercritical water: Solvent effects as a probe of the reaction mechanism. *The Journal of Supercritical Fluids* **1990,** *3* (4), 222-227.

6. Elliott, D. C., Historical Developments in Hydroprocessing Bio-oils. *Energy & Fuels* **2007,** *21* (3), 1792-1815.

7. Ferrari, M.; Bosmans, S.; Maggi, R.; Delmon, B.; Grange, P., CoMo/carbon hydrodeoxygenation catalysts: influence of the hydrogen sulfide partial pressure and of the sulfidation temperature. *Catalysis Today* **2001,** *65* (2-4), 257-264.

8. Boudjouk, P.; Han, B.-H., Palladium-catalyzed and sonically accelerated hydrogenations of olefins using formic acid as a hydrogen transfer agent. *Journal of Catalysis* **1983,** *79* (2), 489-492.

9. Arkad, O.; Wiener, H.; Garti, N.; Sasson, Y., Catalytic transfer hydrogenation of soybean oil methyl ester using inorganic formic acid salts as donors. *Journal of the American Oil Chemists' Society* **1987,** *64* (11), 1529-1532.

10. Kleinert, M.; Barth, T., Towards a Lignincellulosic Biorefinery: Direct One-Step Conversion of Lignin to Hydrogen-Enriched Biofuel. *Energy & Fuels* **2008,** *22* (2), 1371-1379.

11. Heeres, H.; Handana, R.; Chunai, D.; Borromeus Rasrendra, C.; Girisuta, B.; Jan Heeres, H., Combined dehydration/(transfer)-hydrogenation of C6-sugars (D-glucose and D-fructose) to [gamma]-valerolactone using ruthenium catalysts. *Green Chemistry* **2009,** *11* (8), 1247-1255.

12. Kopetzki, D.; Antonietti, M., Transfer hydrogenation of levulinic acid under hydrothermal conditions catalyzed by sulfate as a temperature-switchable base. *Green Chemistry* **2010,** *12* (4), 656-660.

13. Thananatthanachon, T.; Rauchfuss, T. B., Efficient Production of the Liquid Fuel 2,5-Dimethylfuran from Fructose Using Formic Acid as a Reagent. *Angewandte Chemie* **2010,** *122* (37), 6766-6768.

14. Bulushev, D. A.; Ross, J. R. H., Vapour phase hydrogenation of olefins by formic acid over a Pd/C catalyst. *Catalysis Today* **2011,** *163* (1), 42-46.

15. Case, P. A.; van Heiningen, A. R. P.; Wheeler, M. C., Liquid hydrocarbon fuels from cellulosic feedstocks via thermal deoxygenation of levulinic acid and formic acid salt mixtures. *Green Chemistry* **2012,** *14* (1), 85-89.

16. Mukkamala, S.; Wheeler, M. C.; van Heiningen, A. R. P.; DeSisto, W. J., Formate-Assisted Fast Pyrolysis of Lignin. *Energy & Fuels* **2012,** *26* (2), 1380-1384.

17. Jin, F.; Yun, J.; Li, G.; Kishita, A.; Tohji, K.; Enomoto, H., Hydrothermal conversion of carbohydrate biomass into formic acid at mild temperatures. *Green Chem.* **2008,** *10* (6), 612-615.

18. Ramsurn, H.; Kumar, S.; Gupta, R. B., Enhancement of Biochar Gasification in Alkali Hydrothermal Medium by Passivation of Inorganic Components Using Ca (OH) 2. *Energy & Fuels* **2011**.

19. Ramsurn, H.; Gupta, R. B., Production of Biocrude from Biomass by Acidic Subcritical Water Followed by Alkaline Supercritical Water Two-Step Liquefaction. *Energy & Fuels* **2012,** *26* (4), 2365-2375.

20. Kumar, S.; Gupta, R. B., Biocrude production from switchgrass using subcritical water. *Energy & Fuels* **2009,** *23* (10), 5151-5159.

21. Antal, M. J.; Allen, S. G.; Schulman, D.; Xu, X.; Divilio, R. J., Biomass gasification in supercritical water. *Industrial & Engineering Chemistry Research* **2000,** *39* (11), 4040-4053.

22. Onwudili, J. A.; Williams, P. T., Hydrothermal reactions of sodium formate and sodium acetate as model intermediate products of the sodium hydroxide-promoted hydrothermal gasification of biomass. *Green Chemistry* **2010,** *12* (12), 2214-2224.

23. Li, L.; Coppola, E.; Rine, J.; Miller, J. L.; Walker, D., Catalytic Hydrothermal Conversion of Triglycerides to Non-ester Biofuels. *Energy & Fuels* **2010,** *24* (2), 1305-1315.

24. Kruse, A., Hydrothermal biomass gasification. *The Journal of Supercritical Fluids* **2009,** *47* (3), 391-399.

25. Basu, P.; Mettanant, V., Biomass Gasification in Supercritical Water -- A Review. In *International Journal of Chemical Reactor Engineering*, 2009; Vol. 7.

26. Fatih Demirbas, M., Biorefineries for biofuel upgrading: A critical review. *Applied Energy* **2009,** *86, Supplement 1*, S151-S161.

27. (a) Wildschut, J.; Arentz, J.; Rasrendra, C.; Venderbosch, R.; Heeres, H., Catalytic hydrotreatment of fast pyrolysis oil: model studies on reaction pathways for the carbohydrate fraction. *Environmental Progress & Sustainable Energy* **2009,** *28* (3), 450-460; (b) Palmqvist, E.; Hahn-Hägerdal, B., Fermentation of lignocellulosic hydrolysates. II: inhibitors and mechanisms of inhibition. *Bioresource Technology* **2000,** *74* (1), 25-33.

28. Marzialetti, T.; Miller, S. J.; Jones, C. W.; Agrawal, P. K., Switchgrass pretreatment and hydrolysis using low concentrations of formic acid. *Journal of Chemical Technology & Biotechnology* **2011,** *86* (5), 706-713.

29. Vasilakos, N. P.; Austgen, D. M., Hydrogen-donor solvents in biomass liquefaction. *Industrial & Engineering Chemistry Process Design and Development* **1985,** *24* (2), 304-311.

30. Bertero, M.; de la Puente, G.; Sedran, U., Effect of Pyrolysis Temperature and Thermal Conditioning on the Coke-Forming Potential of Bio-oils. *Energy & Fuels* **2011,** *25* (3), 1267-1275.

31. Pouwels, A. D.; Eijkel, G. B.; Boon, J. J., Curie-point pyrolysis-capillary gas chromatography-high-resolution mass spectrometry of microcrystalline cellulose. *Journal of Analytical and Applied Pyrolysis* **1989,** *14* (4), 237-280.

32. Wang, Y.; Wu, L.; Wang, C.; Yu, J.; Yang, Z., Investigating the influence of extractives on the oil yield and alkane production obtained from three kinds of biomass via deoxy-liquefaction. *Bioresource Technology* **2011,** *102* (14), 7190-7195.

33. Demirbas, A., Mechanisms of liquefaction and pyrolysis reactions of biomass. *Energy Conversion and Management* **2000,** *41* (6), 633-646.

34. Grierson, S.; Strezov, V.; Shah, P., Properties of oil and char derived from slow pyrolysis of Tetraselmis chui. *Bioresource Technology* **2011,** *102* (17), 8232-8240.

35. Volli, V.; Singh, R. K., Production of bio-oil from de-oiled cakes by thermal pyrolysis. *Fuel* **2012,** *96* (0), 579-585.

36. Xu, Z. R.; Zhu, W.; Li, M.; Zhang, H. W.; Gong, M., Quantitative analysis of polycyclic aromatic hydrocarbons in solid residues from supercritical water gasification of wet sewage sludge. *Applied Energy* **2013,** *102* (0), 476-483.

Chapter 5

Conclusions

Throughout this work, the unique properties of sub- and supercritical water have been exploited to transform biomass into fuel through gasification, liquefaction and deoxy-liquefaction. In the first part of the dissertation, biomass was hydrothermally converted to syngas. Instead of gasifying biomass (here, switchgrass) directly, it was first hydrothermally carbonized to biochar which is more stable, has less moisture and has a higher energy density. In an industrial setting, biochar can be produced at a remote site where biomass is available, and after pelletizing, the biochar can be transported and used at the centralized facility to produce for e.g., syngas for FT fuels. At 550 °C, the carbon gasification efficiency was 23.9% with SCW as compared to only 5.9% when biochar was gasified thermally. As K_2CO_3 was added as a catalyst, the gasification efficiency increased further with an increase in the hydrogen yield because of the influence on the water-gas shift reaction. At 550°C, the gasification efficiencies were 24.8%, 28.6%, 43.8%, and 60.6% with 2.5, 10, 25 and 50 wt% K_2CO_3, respectively. The novel approach of pre-treating switchgrass with calcium hydroxide, before subjecting it to SCWG, further aids the gasification process with nearly 75% carbon gasification efficiency at 600 °C with 25 wt% K_2CO_3. The addition of $Ca(OH)_2$ decreases the water-solubility of ash (inorganic biomass components) which therefore forms insoluble compounds. $Ca(OH)_2$ passivates the ash and mitigates K_2CO_3 deactivation by preventing the reaction between

K_2CO_3 and the minerals present in switchgrass. In addition, it was also postulated that $Ca(OH)_2$ can alter the chemical properties of the inherent minerals present in switchgrass and also enhance the oxygen complex formation on carbon, hence promoting carbon gasification reaction. The calculated HHV of the syngas obtained was in the range of 14-15 MJ/m^3 and was comparable to the HHV of syngas obtained from low-rank coal gasification. This means that the gas obtained from this study is of promising quality.

High temperature and pressure water was also used as a liquefaction medium using a novel two-step approach: an acidic subcritical at 200 °C, followed by an alkaline supercritical water treatment at 380 °C. The use of 200 °C for the first step targeted the removal of mostly hemicelluloses, enhanced by the acidic medium. The removal of acetate and uronic acid groups from hemicelluloses rendered the aqueous biocrude, from the first step, acidic. It was therefore recycled as the liquefaction medium in that step to increase the yield of biocrude by two-fold (from 14 wt% to 30 wt%). The biocrude from hemicelluloses hydrolysis was extracted before subjecting the un-liquefied biomass to step II. This not only allowed better accessibility to lignin and cellulose (since the tight lignocellulosic biomass structure was broken down) but also avoided the undesired reactions between the sugar degradation products and lignin degradation products to produce char. In the supercritical alkaline medium, 380 °C was chosen so that the reactions would be in the supercritical regime but still in the liquefaction region and also to ensure lignin degradation. The addition of $Ca(OH)_2$ suppressed char formation by reducing condensation/polymerization reactions, removed acetate and uronic groups from remaining hemicelluloses, enhanced lignin solubility and therefore increased reactivity of the remaining polysaccharides. $Ca(OH)_2$ also weakened the C-C bonds and therefore

decreased the activation energies for these complex reactions. It increased the internal surface area due to swelling of the biomass and hence better accessibility to the lignocellulosic biomass. The presence of aldehydes in the biocrude from the first step confirmed hemicelluloses decomposition while a good amount of phenolic compounds in second step biocrude confirmed lignin hydrolysis. Conventional one-step supercritical water liquefaction of switchgrass gave a yield of about 8 wt% at 380 °C while the total biocrude yield accounted for about 40% (on mass basis) for this two-step approach. A promising energy conversion of 66.6% was achieved meaning that nearly 67% of the original amount of energy present in switchgrass could be extracted in the form of biocrude. This conversion was high when compared to other biomass liquefaction methods like pyrolysis.

Biocrude from hydrothermal treatment contains a multitude of oxygenated hydrocarbons and therefore has to be upgraded to remove the oxygen and improve its fuel quality. Therefore, the use of calcium formate as a hydrogen donor was contemplated so that a better quality biocrude could be obtained. This means that while the switchgrass was being liquefied, it was also being deoxygenated due to the decomposition of calcium formate into hydrogen (deoxy-liquefaction). The formate use increased the heating value of the biocrude and the amount of benzene therein, while the amount of polyaromatic hydrocarbons was on the decline. A mechanism was proposed whereby it was postulated that the benzene formation is due to the hydrogenation of the phenols and through Diels-Alder oleic acid addition of a conjugated diene, followed by dehydrogenation. The addition of formate salt has also reduced the occurrence of cyclic ketones (important role in char formation) and phenols but has produced more linear aldehydes in the aqueous

phase of the biocrude. Less phenols in the aqueous phase meant that the phenols were hydrogenated to other non-polar compounds like benzene to upgrade the biocrude. Therefore, by simply using an inexpensive hydrogen donor such as calcium formate, a good quality biocrude can be produced due to hydrodeoxygenation of the depolymerized biomass components.

This dissertation has successfully demonstrated that hydrothermal technology can play an important role in developing future biorefineries. The inherently high moisture content (considered as a major drawback) of biomass can be used advantageously to produce commercially viable biofuels without prior drying. Hydrothermal treatment is attractive from the view point of energy consumption and process integration, making it a promising method for biomass conversion. Despite technical and financial hurdles, significant progress has been made through research and process development. These past years, there has been an increasing focus on modeling and development of catalysts for these technologies. Nanotechnology has already been contemplated in biomass processing. Appendix A gives a review of the use of nanotechnology in biomass conversion and upgrading. Hydrothermal processes hold significant potential for producing biofuels targeted for the heavy transport sector, combustion purposes, and as a raw material for value-added products. Research and development have to progress in order to solve the technological problems and integrate the products into existing markets.

Chapter 6

Future Directions

This dissertation has investigated several ways of using hydrothermal treatment to process biomass and has proposed new approaches to increase the biocrude yield, the gasification efficiency and/or the heating value of the biocrude. Several other related areas of research, as elaborated below, can be investigated to further understand the fundamentals of liquefaction and deoxygenation of biomass.

6.1 Deoxygenation of Bio-oil (Biocrude) to produce Biogasoline using Inexpensive Metals

HDO has been conventionally carried out on sulfided alumina-supported CoMo and NiMo catalysts due to their extremely dynamic and flexible surface and their ability to facilitate several reactions through different mechanisms.[1] Because bio-oil is low in sulfur, sulfiding agents are added to avoid sulphur leaching from the surface in order to maintain the catalytic activity[2] and the level of sulfide structure.[3] Due to stringent environmental requirements, low sulphur emissions are mandatory and therefore the use of H_2S and sulfide catalysts are not recommended. There is also the risk of contamination of the product by sulphur species. Noble metal catalysts have also been tested instead of sulfided catalysts as they are expected to work at lower temperatures and hence partially avoid deactivation of catalysts by coke formation.[2] Besides from being

very expensive, noble metals are also more sensitive towards poisoning and even low concentrations of contaminants could deactivate them. The aqueous acid present (due to biomass depolymerization) could also lead to dissolution of the active metal or catalyst support, hence contaminating the product which would require secondary distillation before use as a fuel.[4]

To therefore address the problems mentioned above, a cheap, expendable catalyst which contains very little toxic heavy metals would be needed. Therefore, metals in either their most stable oxidation state or in the form of their oxides, satisfy these requirements since they would be non-toxic and could be released in the biosphere. The limited list includes Na^+, K^+ and Ca^{2+} (as chlorides, carbonates or hydroxides), TiO_2, SiO_2, Fe_2O_3, Fe_3O_4, Al_2O_3 and $Zn/ZnCO_3$.[4] Iron oxide or iron can be used as a cheap metal for deoxygenating biocrude, together with hydrogen gas. Research can be conducted on the fundamental study of various steps involved so that rational reactor/process design can be done. The mechanism of hydrodeoxygenation and how does the Fe-based catalyst activate the hydrogen for effective HDO also needs to be investigated. The presence of iron catalysts have proven to help in hydrocracking of the C-C bonds under hydrogen pressure[5] and to deoxygenate a number of alcohols and ketones.[6] Based on literature, a proposed hydrodeoxygenation mechanism (Figure 6.1) has been postulated.[7] As example, acetic acid has been used as a model biocrude compound to show how the surface of the iron would help to dissociate the acid molecule to form the acyl surface. A suggested pathway is that the acyl intermediate reacts with hydrogen to form ethanol via formation of the corresponding aldehyde intermediate.

Also, C-C cleavage of the alcohol/aldehyde species may lead to formation of ethane through hydrogenation.

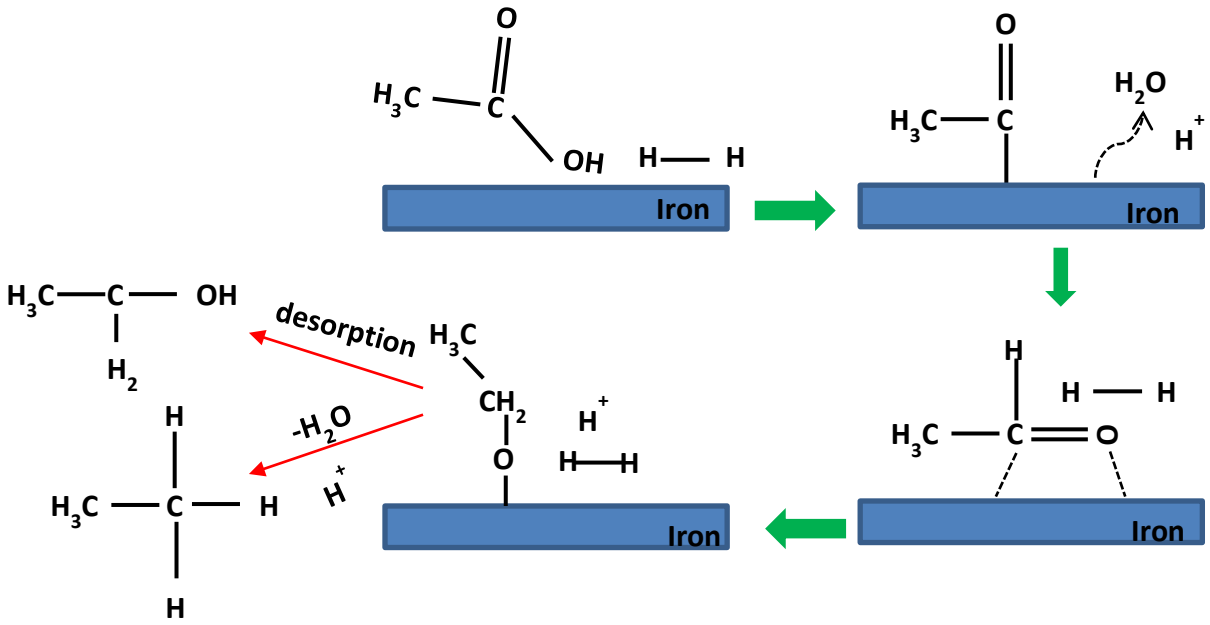

Figure 6.1 Postulated HDO mechanism of model biocrude compound (acetic acid) on iron catalyst surface

Therefore, in this study, some fundamental research on model compounds hydrodeoxygenation mechanism will have to be investigated so that

- a general mechanism can be established as to how the mixture of oxygenated compounds behave under the HDO conditions.
- the effect of catalytic properties (including: pore structure, nature of active sites) on the reaction pathway can be determined.
- activity and selectivity can be maximized for use in next-generation biofuels processes by tailoring catalyst synthesis.

6.2 Production of Activated Biochar as Catalyst Support

After thermally treating biomass, a residue rich in carbon termed as biochar remains. A number of studies have been conducted to use biochar in bioremediation,[8] soil amendment,[9] syngas production,[10] and activated carbon production. However, most of the studies use biochar from pyrolysis as a precursor and chemical activation (e.g. KOH)[11] as their method to prepare activated biochar. In this segment of future directions, activated biochar obtained from hydrothermal carbonization will be activated using phosphoric acid since it has been used to activate a number of lignocellulosic materials.[12] Activated biochar from biomass usually exhibit a marked improvement in their internal surface area (Figure 6.2).[13]

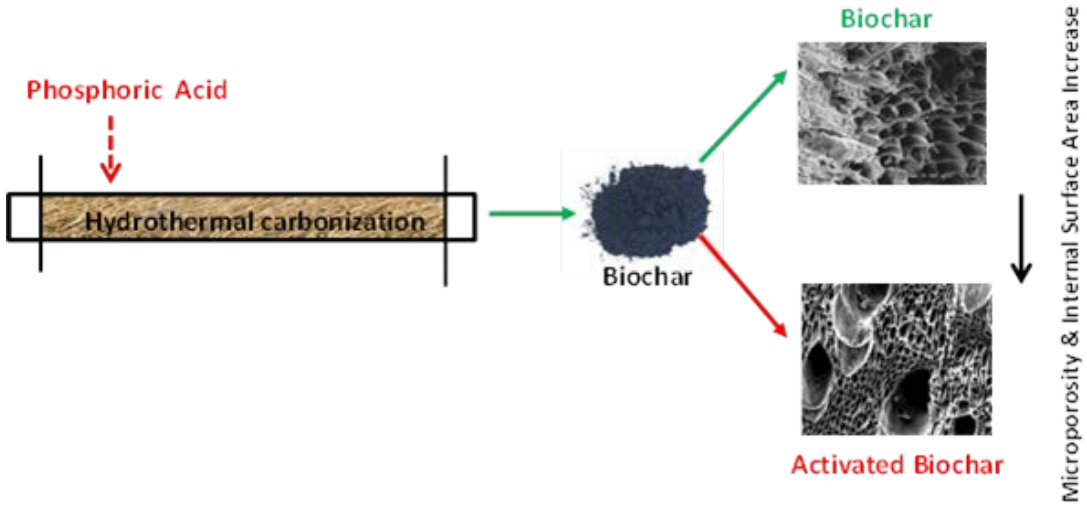

Figure 6.2 Biochar treatment to increase microporosity

Since the activation of biochar from hydrothermal treatment has not been looked into, the following can then be investigated:

- effects of operating conditions of activation process such as temperature and amount of activating agent.

- textural and chemical properties of the activated biochar.
- difference between acid activated and chemical activated biochar.
- measurement of the microporosity of the product using scanning electron microscopy and surface area measurements.
- the structure of the activated carbon by using Fourier-Transform Infrared Spectroscopy and X-ray diffraction.
- impregnation of the activated biochar with metals like Fe in order to study its activity in reactions like deoxygenation for future use in biomass liquefaction to biofuel.

6.3 Transforming Microalgae into Biofuel using Activated Iron Catalyst and Formate Salt as Hydrogen Donor

Because of their high photosynthetic efficiency, faster growth rate, high amount of oil (triglycerides), low land requirements, microalgae is regarded as one of the most promising feedstock for advanced biofuels.[14] Because of algae's high moisture content, hydrothermal liquefaction seems to be an effective way to convert this biomass into biofuel so as to eliminate drying costs as otherwise required by other conventional thermochemical methods. Microalgae are low in cellulose and therefore low in oxygen content and should hence be a suitable candidate for biocrude/bio oil production with high heating values. According to Demirbas,[15] algae can produce 30-100 times more energy per hectar than terrestrial crops which produce second generation biofuels. Liquefaction of algae has been mostly performed unanalyzed with a few using water soluble salts like KOH and Na_2CO_3[16] with 30-40 wt% yields and heating values of

around 36-38 KJ/kg. Duan and Savage[17] have used a suite of heterogeneous catalysts (Pd/C, Pt/C, Ru/C, Ni/SiO_2−Al_2O_3, CoMo/γ-Al_2O_3 (sulfided), and zeolite) under inert (helium) and high-pressure reducing (hydrogen) conditions. They concluded that elemental compositions and heating values of the crude oil (38 KJ/kg) was insensitive to the catalyst used with typical H/C and O/C ratios of 1.7 and 0.09, respectively.

Usually, at higher temperatures (above 300 °C), polycyclic aromatic hydrocarbons (PAHs) and their alkylated derivatives are found in the algal bio-oils and are dominant at 500 °C[14a] (Figure 6.3).

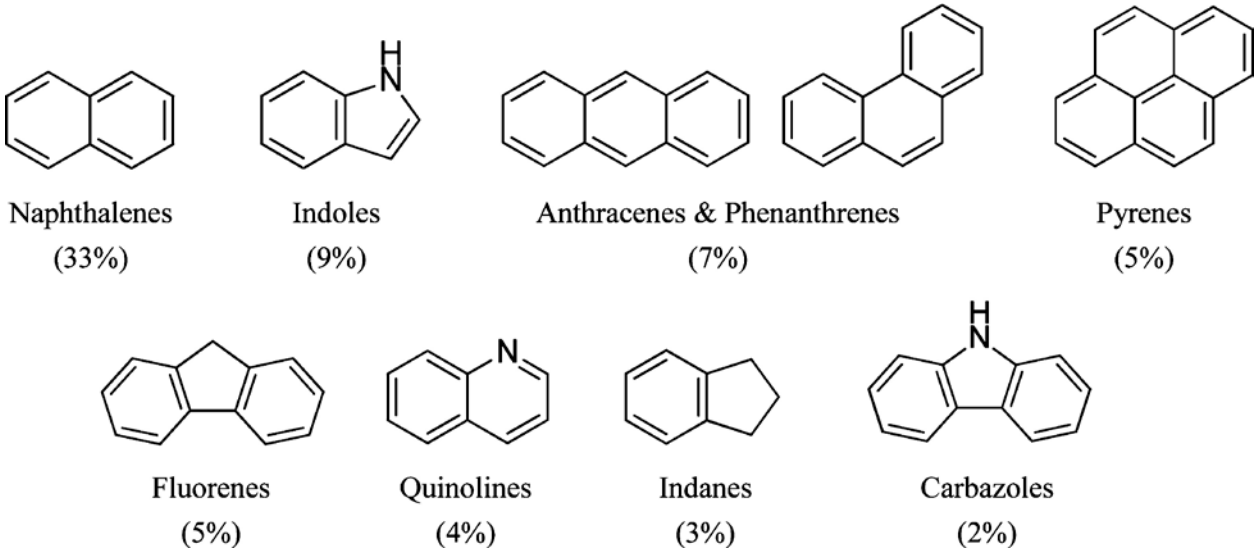

Figure 6.3 PAHs present in algal bio-oil produced at 500 °C[14a]

Naphthalene is the major PAH found in algal bio-oil and hence its hydrogenation would be most desirable due to more stringent environmental regulations and fuel specifications. Also, the cetane number can be improved by reducing the aromatic content of the fuel.[18] The hydrogenation of the aromatic rings would reduce the large bonding energy by reducing C=C bonds to C-C bonds, hence needing a deep aromatic saturation, usually accomplished by the use of noble metal catalysts which are not only expensive but

susceptible to poisoning.[19] It has been reported that hydrogen-reduced iron resulted in a very active catalyst for aromatic ring hydrogenation.[20] In this respect, it is proposed to liquefy algae and hydrogenate the so-produced oil in one step by using a formate salt as the hydrogen donor with an iron catalyst. In Chapter 4, it was demonstrated that calcium formate was a cheap source of in-situ hydrogen donor. The hydrogen so formed will not only provide reactive hydrogen which can directly deoxygenate the bio-oil but also reduce the iron catalyst to its active form. The following reactions are expected to take place:

A. Decomposition of formate salt:

$$Ca(HCOO)_2 \longrightarrow CaCO_3 + CO + H_2$$

$$Ca(HCOO)_2 + H_2O \longrightarrow CaCO_3 + CO_2 + 2H_2$$

B. Hydrothermal liquefaction of algae into bio-oil

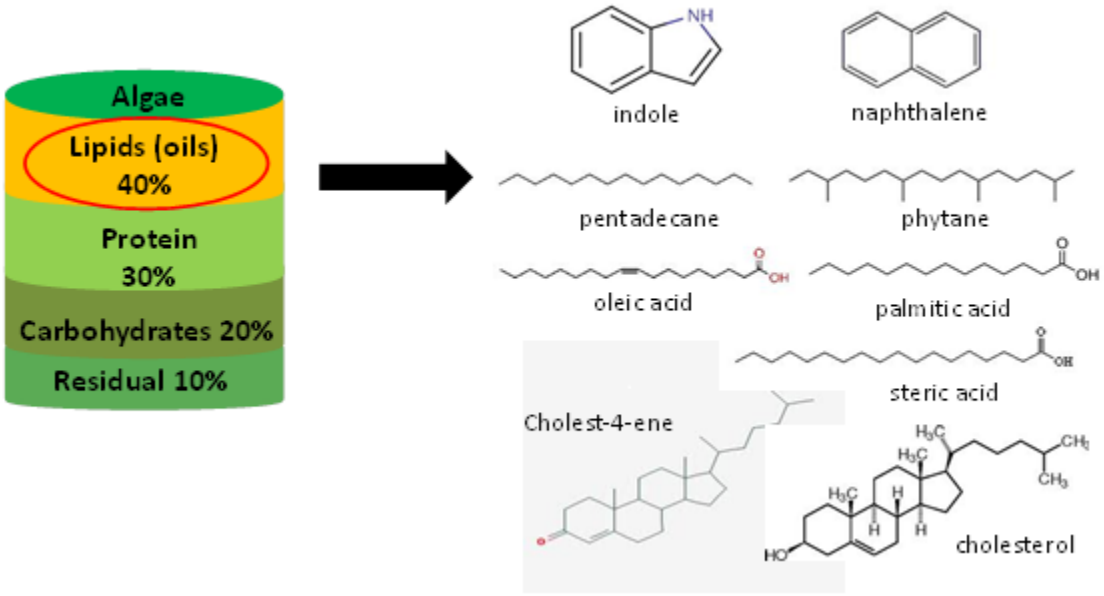

Figure 6.4 Major hydrothermal liquefaction products from algae

C. Water-gas shift (WGS) reaction

$$CO + H_2O \longrightarrow CO_2 + H_2$$

D. Iron catalyst activation

The hydrogen released from the formate salt together with the hydrogen from WGS and biomass decomposition reactions will also reduce the elemental iron to make it more active. One study[21] looked at the effect of pretreating a precipitated iron catalyst (100 Fe/ 3Cu/ 4 K/ 16 SiO_2) with H_2. At 240 °C, the catalyst reduced to magnetite while at 250 and 280 °C, dominant peaks of α-Fe were identified on XRD spectrum.

E. Hydrogenation of bio-oil (naphthalene as model compound)

Simultaneously, as the bio-oil from the algae is being extracted and hydrogen from the formate salt interact, deoxy-liquefaction of the algal bio-oil occurs, resulting in higher heating value bio-oil. As an illustration, the hydrogenation of naphthalene (present in algal bio-oil) is depicted in Figure 6.5.

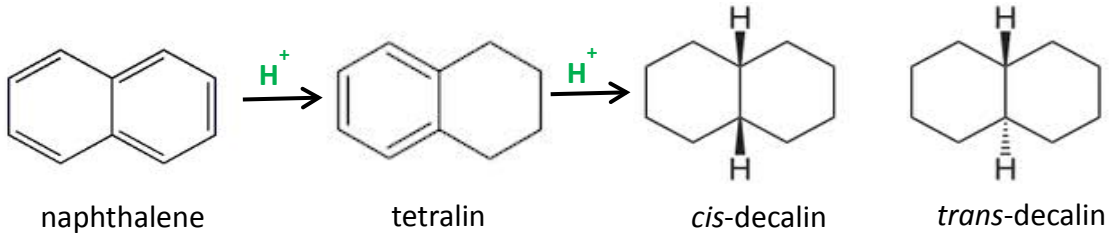

Figure 6.5 Hydrogenation of model compound into fuel-compatible biocrude

Therefore, in this proposed research, the following can be investigated:

- the study of microalgae liquefaction with and without catalysts.
- the effect of adding formate salt as both a hydrogen donor and acid catalyst for a one-pot upgrading of microalgae into biofuel.

- the activation of iron catalyst under reducing conditions.
- a mechanism for hydrodeoxygenation of algal bio-oil in the presence of hydrogen and iron as a catalyst.

6.4 References

1. Ferrari, M.; Bosmans, S.; Maggi, R.; Delmon, B.; Grange, P., CoMo/carbon hydrodeoxygenation catalysts: influence of the hydrogen sulfide partial pressure and of the sulfidation temperature. *Catalysis Today* **2001,** *65* (2-4), 257-264.

2. Gutiérrez, A.; Honkela, M.; Ryymin, E.-M.; Krause, O. In *From sulfided to noble metal catalysts in the hydrodeoxygenation of aliphatic esters*, Integrated Design of catalytic nanomaterials for a sustainable production, France, May 19-24; France, 2009; p 65.

3. Wang, W.; Yang, Y.; Luo, H.; Liu, W., Characterization and hydrodeoxygenation properties of Co promoted Ni–Mo–B amorphous catalysts: influence of Co content. *Reaction Kinetics, Mechanisms and Catalysis* **2010,** *101* (1), 105-115.

4. Karimi, E.; Gomez, A.; Kycia, S. W.; Schlaf, M., Thermal Decomposition of Acetic and Formic Acid Catalyzed by Red Mud -Implications for the Potential Use of Red Mud as a Pyrolysis Bio-Oil Upgrading Catalyst. *Energy & Fuels* **2010,** *24* (4), 2747-2757.

5. Matsui, T.-o.; Nishihara, A.; Ueda, C.; Ohtsuki, M.; Ikenaga, N.-o.; Suzuki, T., Liquefaction of micro-algae with iron catalyst. *Fuel* **1997,** *76* (11), 1043-1048.

6. Glebov, L. S.; Mikaya, A. I.; Yatsenko, A. E.; Zaikin, V. G.; Kliger, G. A.; Loktev, S. M., Effective gas-phase deoxygenation of alcohols and ketones on iron catalyst. *Tetrahedron Letters* **1985,** *26* (28), 3373-3376.

7. Chen, L.; Zhu, Y.; Zheng, H.; Zhang, C.; Zhang, B.; Li, Y., Aqueous-phase hydrodeoxygenation of carboxylic acids to alcohols or alkanes over supported Ru catalysts. *Journal of Molecular Catalysis A: Chemical* **2011,** *351* (0), 217-227.

8. Uchimiya, M.; Klasson, K. T.; Wartelle, L. H.; Lima, I. M., Influence of soil properties on heavy metal sequestration by biochar amendment: 2. Copper desorption isotherms. *Chemosphere* **2011,** *82* (10), 1438-1447.

9. Kwapinski, W.; Byrne, C.; Kryachko, E.; Wolfram, P.; Adley, C.; Leahy, J.; Novotny, E.; Hayes, M., Biochar from Biomass and Waste. *Waste and Biomass Valorization* **2010,** *1* (2), 177-189.

10. Ramsurn, H.; Kumar, S.; Gupta, R. B., Enhancement of Biochar Gasification in Alkali Hydrothermal Medium by Passivation of Inorganic Components Using Ca (OH) $_2$. *Energy & Fuels* **2011**.

11. Azargohar, R.; Dalai, A. K., Biochar As a Precursor of Activated Carbon Twenty-Seventh Symposium on Biotechnology for Fuels and Chemicals. McMillan, J. D.; Adney, W. S.; Mielenz, J. R.; Klasson, K. T., Eds. Humana Press: 2006; pp 762-773.

12. Diao, Y.; Walawender, W. P.; Fan, L. T., Activated carbons prepared from phosphoric acid activation of grain sorghum. *Bioresource technology* **2002,** *81* (1), 45-52.

13. Schröder, E.; Thomauske, K.; Weber, C.; Hornung, A.; Tumiatti, V., Experiments on the generation of activated carbon from biomass. *Journal of Analytical and Applied Pyrolysis* **2007,** *79* (1–2), 106-111.

14. (a) Brown, T. M.; Duan, P.; Savage, P. E., Hydrothermal Liquefaction and Gasification of Nannochloropsis sp. *Energy & Fuels* **2010,** *24* (6), 3639-3646; (b) Patil,

V.; Tran, K.-Q.; Giselrød, H. R., Towards Sustainable Production of Biofuels from Microalgae. *International Journal of Molecular Sciences* **2008,** *9* (7), 1188-1195.

15. Demirbas, A., Use of algae as biofuel sources. *Energy Conversion and Management* **2010,** *51* (12), 2738-2749.

16. (a) Minowa, T.; Yokoyama, S.-y.; Kishimoto, M.; Okakura, T., Oil production from algal cells of Dunaliella tertiolecta by direct thermochemical liquefaction. *Fuel* **1995,** *74* (12), 1735-1738; (b) Yang, Y. F.; Feng, C. P.; Inamori, Y.; Maekawa, T., Analysis of energy conversion characteristics in liquefaction of algae. *Resources, Conservation and Recycling* **2004,** *43* (1), 21-33; (c) Ross, A. B.; Biller, P.; Kubacki, M. L.; Li, H.; Lea-Langton, A.; Jones, J. M., Hydrothermal processing of microalgae using alkali and organic acids. *Fuel* **2010,** *89* (9), 2234-2243; (d) Zhou, D.; Zhang, L.; Zhang, S.; Fu, H.; Chen, J., Hydrothermal Liquefaction of Macroalgae Enteromorpha prolifera to Bio-oil. *Energy & Fuels* **2010,** *24* (7), 4054-4061; (e) Stucki, S.; Vogel, F.; Ludwig, C.; Haiduc, A. G.; Brandenberger, M., Catalytic gasification of algae in supercritical water for biofuel production and carbon capture. *Energy & Environmental Science* **2009,** *2* (5), 535-541.

17. Duan, P.; Savage, P. E., Hydrothermal Liquefaction of a Microalga with Heterogeneous Catalysts. *Industrial & Engineering Chemistry Research* **2010,** *50* (1), 52-61.

18. Song, C.; Schmitz, A. D., Zeolite-Supported Pd and Pt Catalysts for Low-Temperature Hydrogenation of Naphthalene in the Absence and Presence of Benzothiophene. *Energy & Fuels* **1997,** *11* (3), 656-661.

19. Kirumakki, S. R.; Shpeizer, B. G.; Sagar, G. V.; Chary, K. V. R.; Clearfield, A., Hydrogenation of Naphthalene over $NiO/SiO_2–Al_2O_3$ catalysts: Structure–activity correlation. *Journal of Catalysis* **2006,** *242* (2), 319-331.

20. Zhan, X.; Guin, J. A., High-Pressure Hydrogenation of Naphthalene Using a Reduced Iron Catalyst. *Energy & Fuels* **1994,** *8* (6), 1384-1393.

21. Bukur, D. B.; Lang, X.; Ding, Y., Pretreatment effect studies with a precipitated iron Fischer–Tropsch catalyst in a slurry reactor. *Applied Catalysis A: General* **1999,** *186* (1–2), 255-275.

Appendix A

Nanotechnology in Biofuels

A.1 Introduction: Nanotechnology in the Energy Sector

One of the biggest challenges for mankind in this century is to secure a long-term energy supply for sustainable global development.[1] We are increasingly dependent on fossil fuels, our current energy source. Furthermore, the combustion of these fuels causes environmental degradation through air pollution and global warming. Though it will take some decades to come close to a truly sustainable energy system, intensive research is being conducted to find solutions to (1) increase efficiency in production, transmission and utilization of the remaining fossil fuels, (2) reduce negative impacts to the environment, and (3) develop or improve technologies and infrastructure for the smooth transition to the alternative/renewable energy sources (e.g., nuclear power, solar energy, wind power, geothermal energy, biomass and biofuels, hydropower).[2] Nanotechnology, the control of materials and phenomena at scales between 1 to 100 nm, holds the key to many of the technological advancements in the energy sector. It involves the miniaturization as well as the manipulation of atoms and molecules to control their properties which, at this scale, are so different from the bulk properties. For instance, a 100 nm particle has less than 0.2% of atoms on the surface while a 10 nm particle has about 10% on the surface while a 2 nm particle has 90% of its atoms on the surface. Because these surface atoms may have more than one dangling bonds, they are very

active and tend to form bonds with adjacent molecules to become more stable. This translates into more chemical activity, lower melting point and higher solubility.[3] Nanomaterials have been and are being studied for various renewable energy applications. Figure A.1 shows the potential applications of nanotechnology in some key energy processes.

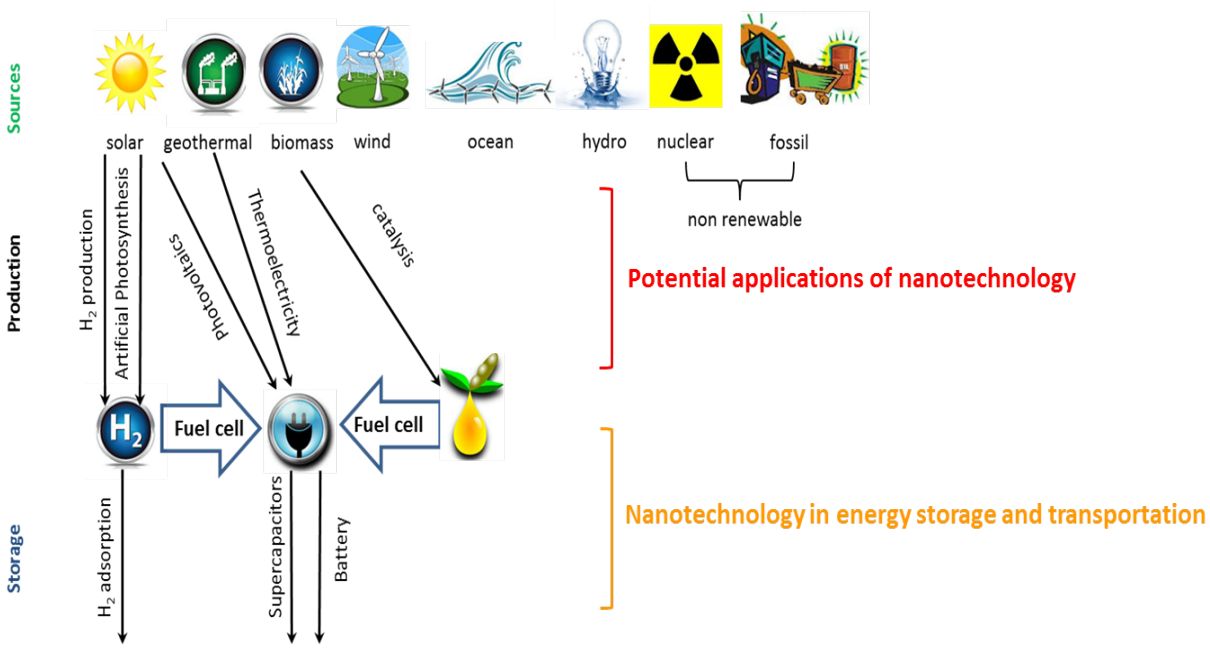

Figure A.1. Most promising applications of nanotechnology for the energy production domain

(*Adapted from* Moniz, E. J.; Garcia-Martinez, J., *Nanotechnology for the energy challenge*. Wiley-VCH: 2010.[2])

This appendix gives an overview on the use of nanotechnology in biofuels including transesterification, gasification and pyrolysis, hydrogenation and reforming. The aim of

this review is an attempt to examine the role of nanotechnology in biofuels and spike the attention of the reader on these current research topics.

A.2 Biofuels and Nanocatalysis

Increased demand in transportation fuels, environmental concerns and depletion of fossil fuel require development of efficient conversion technologies for second-generation biofuels.[4] Furthermore, the Federal Renewable Fuels Standard requires the blending of 36 billion gallons of renewable fuels into transportation fuels by 2022.[5] As of now, only a very small fraction of the demand is met by the renewable fuel.[6] Currently, the demand for renewable fuels is covered by the production of starch-derived ethanol and oil-seed derived biodiesel. Ideally, biomass is regarded as the most sustainable option because it is the largest primary resource, it is clean and has zero net emissions of carbon dioxide.[7] Biomass to biofuel conversion by thermochemical routes can be achieved via direct liquefaction to fuels or by gasification to synthesis gas followed by conversion to diesel via Fischer–Tropsch process.[8] Biomass typically contains 20-30 wt% hemicelluloses, 40-50 wt% cellulose, and 20-30 wt% lignin[9] along with a number of inorganic compounds in small amounts. These constituent biopolymers are composed of long-chain, oxygen-rich molecules and they require different catalysts than the petroleum industry. To this effect, the use of catalysts is needed to facilitate the chemistry by which cellulose- and lignin-derived molecules can be converted to fuels.[1] Most pathways involve the conversion of biomass to syngas or biofuels and the upgrading of the unstable flash pyrolysis or liquefaction products by the use of selective nanocatalysts for reactions like aqueous - phase processing to produce selectively

targeted alkanes from glucose, aldol condensations requiring base catalysts, hydrogenation reactions needing metal catalysts, and bifunctional dehydration/ hydrogenation reactions with metal/acid catalysts. In the following sections, selective processes where nanoparticles (NPs) have been used for the conversion of biomass to biofuels are being presented.

A.3 Transesterification to Produce Biodiesel

Biodiesel (an alternative to fossil diesel) is produced via transesterification of oils as per the following reaction:

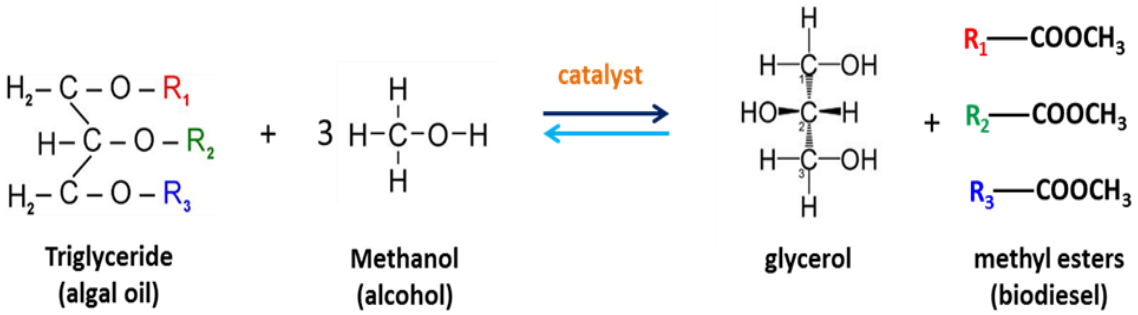

Biodiesel is biodegradable, non-toxic and can be obtained from various renewable sources, among which is algae. Algal biofuels face a number of challenges such as the difficulty to achieve consistent industrial-scale algae production, high production and harvesting costs and energy-intensive lipid extraction processes.[10] The conversion of algae to biofuel can be achieved mainly through anaerobic digestion, supercritical fluid treatment, pyrolysis and gasification. The enzyme-based technologies suffer from low catalytic efficiencies of enzymes, high cost, poor catalysts recovery and a need for high temperatures and strong acids to transform the feedstock produced.[11] Nanoscale materials provide increased surface area for enzyme loading and help to increase the

diffusion rate of substrates to the enzymes, thereby increasing production rates.[12] For example, lipase enzyme from *Candida rugosa* were successfully immobilized in polyvinyl alcohol nanofibrous membranes. Enzyme loading in these bicomponent fibers reached as high as 50%. The lipase-loaded bicomponent fibers exhibited far superior activity than the crude enzyme following exposures to elevated temperatures and humidity. They also possessed far superior stability, i.e., 100, 8, and 3 times longer half-lives than crude lipase following storages at 40, 21 °C and 65% relative humidity, and ambient condition, respectively.[13] Recently, a nanofarming technology has been developed that uses nanoparticles to extract oil from algae without harming the algae (Figure A.2). The extracted oil is then converted to biodiesel by transesterification.[14] Here amine functionalized 10 nm mesoporous silica nanoparticles are used for the selective sequestration of free fatty acids from algae.[15]

For conversion of oil into diesel, several advancements have been made utilizing nanocatalysts. Nano-sized calcium oxide with crystallite size of 20 nm gave 99% conversion of soybean oil to biodiesel while commercial CaO nanoparticles (NPs) of size 43 nm, yielded only 2% biodiesel. The soybean oil/methanol ratio was 1:27 and deactivation was observed after eight cycles. SEM analysis revealed that fresh catalyst consists of numerous crystallites with well-defined edges while the same catalyst, after seven cycles, had formed aggregated polycrystallites with substantially less well-defined edges, hence explaining the deactivation.[16]

In another study, cesium was incorporated in nanocrystalline MgO through co-precipitation under supercritical conditions to generate $Cs_2Mg(CO_3)_2$ nanocrystallites with an enhanced density and strength of surface base sites. This strong synergy between

the two components enhanced the rate of tributyrin transesterification with methanol compared to undoped MgO and homogeneous Cs_2CO_3 catalysts. The nanocatalyst however suffers from poor recyclability due to heavy surface carbon deposition.[17]

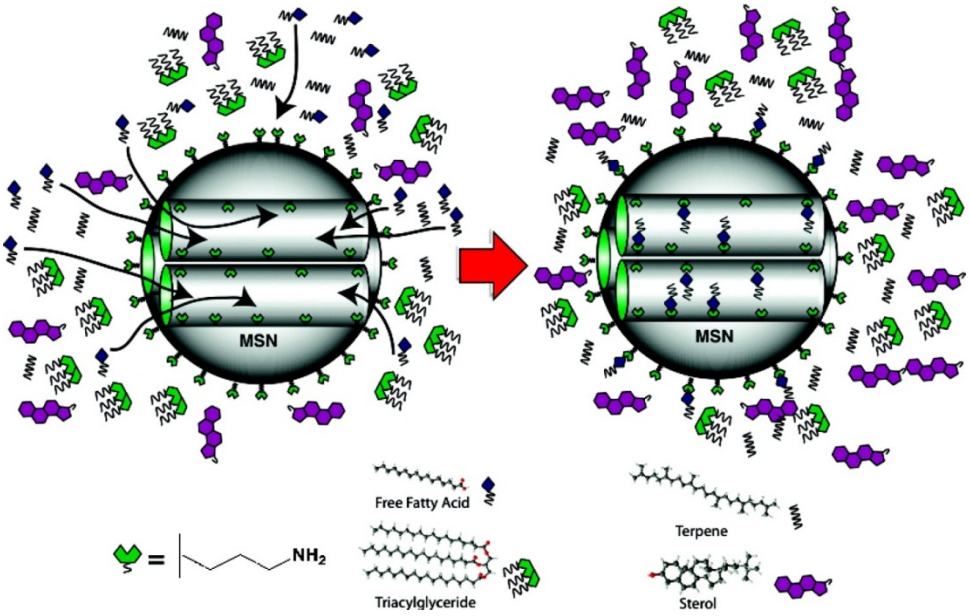

Figure A.2 Selective uptake and sequestration of free fatty acids from a solution of lipids and hydrocarbons found in algal oil[15]

(Valenstein et al., 2012; reproduced with permission of American Chemical Society)

In one study, solid base hydrotalcite-derived nanoparticles with Mg/Al molar ratio of 3/1 were used for the transesterification of *Jatropha* oil in an ultrasonic reactor to obtain a biodiesel yield of 95%. Due to the surface absorption of glycerol byproduct as well as the collapse of the layered structure, the catalyst underwent deactivation.[18] Calcium aluminate-loaded Fe_3O_4 nanoparticles gave a biodiesel yield of 99%. Also, the activity and recovery rate of this catalyst was maintained after 5 cycles of catalysis since having magnetic properties made the catalyst easy to separate.[19]

A.4 Biomass Gasification and Pyrolysis

Nanomaterials can provide particularly high surface area to mass ratio which is desirable for catalysis and control of chemical composition. In fact, specific matching of catalysts with reactor types and processes is one of the other benefits of using nanoscale.[20] Gasification converts carbon-containing feedstock into a synthetic gas comprising of hydrogen, carbon monoxide, etc.[21] Gasification of biomass into fuel gases, such as synthesis gas or producer gas, is a promising route to produce renewable fuels, which is commonly accomplished via partial oxidation of the feedstock using sub-stoichiometric air or oxygen or by indirect heating with or without steam. Hao et al. gasified cellulose and sawdust in supercritical water to produce a gas rich in hydrogen and investigated the use of a suite of nanocatalysts including CeO_2 and $(CeZr)_xO_2$. Increased H_2 production coincided with increase in catalyst's surface area per mass.

Another study[22] investigated methane decomposition reactions to form hydrogen and nano-carbon on a nickel-based nanocatalyst. The catalysts have been designed to stabilize nanoscale metal particles which act as growth tip for the nanocarbons. It was found that temperatures higher than 800 °C render the process more commercially viable due to the amount of hydrogen production. A one-pot synthesis method allowed a metal precursor (nickel acetylacetonate) to reduce directly onto the surface of the carbon nanotube/fiber without the pretreatment of surface functional groups to form carbon nanotube/fiber and aluminosilicate supported Ni catalysts. The catalysts were used for biomass gasification in supercritical water for the production of hydrogen-rich gases. Compared to the two commercially available aluminosilicate supported Ni catalysts, the synthesized catalysts produced similar hydrogen yields (~8 mmol H_2/g biomass) but the

H_2/CH_4 mole ratio for the synthesized catalysts was 3.5 compared to 1.3 for the commercial catalysts.[23]

Pyrolysis, thermal decomposition of materials in the absence of oxygen, is another method to upgrade bioderived feedstocks to fuels.[24] The strategy of impregnating lignocellulosic biomass with aqueous metal salts solutions was investigated for producing H_2-rich gas by pyrolysis of wood (Figure A.3). During the pyrolysis, formation of nickel metal NPs was studied. It was postulated that during the wood impregnation step, the oxygenated groups present in the biomass act as adsorption sites for metal cations in the aqueous medium. This leads to very high metal precursor dispersion into the wood matrix. Subsequently, during pyrolysis, an amorphous $Ni_xO_yH_z$ phase is formed. This phase is then reduced to metallic nickel (Ni^0) by carbon atoms at temperatures below 500 °C, leading to the formation of Ni^0 NPs. The so formed Ni^0 nanocrystallites act as the catalytic active phase for enhancing both H_2 production and tar conversion during the initial stage of biomass pyrolysis.[25]

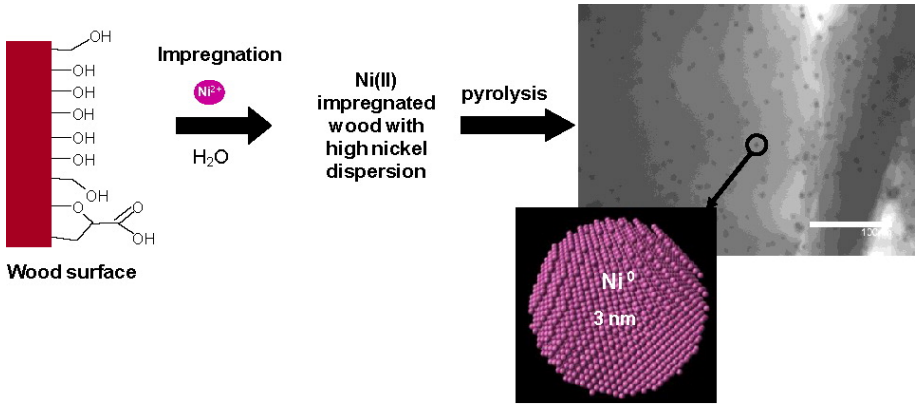

Figure A.3 Ni(II) impregnated wood before pyrolysis[25]

(Richardson et al., 2010; reproduced with permission of Elsevier Science)

During biomass gasification/pyrolysis, along with the generation of useful products (fuel gases, char), many byproducts such as fly ash, NO_x, SO_2 and tar are also formed. Tar is a complex mixture of condensable hydrocarbons, which includes single ring to 5-ring aromatic compounds along with other oxygen-containing hydrocarbons and complex PAH.[26] This so-formed tar will be condensed as temperature is lower than its dew point, then block and foul process equipment like fuel lines, filters, engines and turbines. The tar content in the syngas from an air-blown circulating fluidized bed biomass gasifier was reported to be about 10 g/m^3. Most applications of product gases require a low tar content, of the order 0.05 g/m^3 or less.[27] Hence, tar disposal becomes one of the most necessary and urgent problems during biomass gasification. A novel supported nano-NiO catalyst for tar removal in biomass gasification/pyrolysis was developed so as to significantly enhance the quality of the produced gases.[28]

The supported nano-NiO/γ-Al_2O_3 catalyst was prepared by deposition-precipitation (DP) method. Various analytical methods revealed that the nano-NiO/γ-Al_2O_3 catalysts had a coated structure with a 12 wt% loading of NiO resulting in a higher surface area compared to commercial nickel based catalysts. The active spherical NiO nanoparticles had a size range of 12−18 nm. During biomass pyrolysis, the tar removal efficiency reached to 99% for catalytic pyrolysis at 800 °C with a marked increase in the gas yield. The CO_2 and CH_4 percentages in the product gas after addition of the catalysts were obviously reduced, while those of the valuable H_2 and CO strongly increased. This gas yield increase was attributed to be predominantly through secondary cracking of the pyrolysis vapors on catalyst in the catalytic bed reactor. The NiO/γ-Al_2O_3 catalyst enhanced the cracking of tar in vapor and of hydrocarbons such as CH_4 and C_nH_m to H_2

and CO. The same research group[29] also looked into the use of nano-NiO particles as catalysts in biomass pyrolysis. These spherical nano-NiO particles (mean size of ~7.5 nm and specific surface area of 188 m^2/g) were prepared via precursors, which were obtained by homogeneous precipitation involving an aqueous solution of nickel nitrate hexahydrate and urea.

Pyrolysis of the three biomass components namely cellulose, xylan, and lignin were investigated. Compared to commercial Ni based catalyst, the weight loss of the biomass components occurred at relatively lower temperature, with low residues. It was postulated that the catalyst promoted the devolatilization and thermal degradation of biomass. This could be due to the possible formation of weak bonds between volatiles and the catalyst, causing other bonds in the volatile molecule to be stretched and weakened. This means that the activation energy of biomass-derived components was decreased due to another possible reaction pathway. The nanocatalyst (in particular, particles with a smaller size of ~7.5 nm) also accelerated primary and secondary decomposition reactions of biomass which could then occur at a lower temperature.

A.5 Hydrogenation of Biomass-Derived Compounds

Biomass derived compounds need to be hydrogenated or hydro-deoxygenated in order to produce useful fuels and chemicals and several nanocatalysts have been tested to enhance these reactions. For example, 5-hydromethylfurfural (HMF) has been successfully synthesized from fructose, glucose and cellulose using different catalysts, including nanocatalysts.[30] HMF can be converted to 2,5-dimethylfuran (DMF) via hydrogenation or to levulinic acid (LA) via an acid-catalyzed ring-opening process.[31]

LA is a biomass-derived platform molecule and serves as precursor for liquid fuels like ɣ-valerolactone (gVL).[32] Highly dispersed metal nanoparticulates on metal oxide supports have shown to be efficient for aerobic oxidation of HMF with gold showing marked chemoselectivity. One study[33] reported the remarkable development of an HMF oxidation/esterification process using Au on a TiO_2 support. The reactions were run at 130 °C and 4 bar O_2 in methanol with MeONa as base. A high yield of 98% 2,5-furandimethylcarboxylate (FDMC) was obtained. The authors proposed an oxidation pathway of HMF to FDMC via the hemiacetal intermediates. Another investigation[34] was performed using Au on CeO_2 to catalyze biomass-derived HMF oxidation into FDCA but without a base. The results revealed that the catalytic performance of Au/CeO_2 depends on the particle size of the catalyst. Decreasing the particle size led to an increase in external-to-internal atom ratio resulting in high populations of unsaturations. Unsaturations, as described in the study, are defect sites mainly oxygen vacancies formed in the presence of Ce^{3+}. The increase in the population of defects resulted in enhanced adsorption and redox potential of the catalysts. A number of studies have investigated the use of gold for the oxidation of HMF including using TiO_2 and carbon supported Pt, Pd and Au[35] catalysts, hydrotalcite-supported Au NPs[36] and gold-copper bimetallic nanoparticles[37] over TiO_2.

Two reactions namely the aqueous oxidation of benzyl alcohol and the hydrogenation of furfural in water were tested under microwave irradiation using carbon-supported Pd nanoparticles. The most active nanocatalysts were trioctylphosphine and triphenylphosphine stabilized- Pd NPs on oxidized carbon support. The presence of oxygen groups on the surface of the carbon support, particularly those of acidic character,

improved the Pd NPs immobilization as well as the water affinity, and consequently the catalytic performances of the system.[38] Hydrogenation of succinic acid (SA) in aqueous ethanol under mild reaction conditions was investigated using a variety of highly active, stable and reusable supported metal nanoparticles (SMNPs) including Pt, Pd, Rh and Ru (5% loading) on a mesoporous material derived from biomass (Starbon®–SMNPs).[39] The versatility of the functional groups as well as its stability under aqueous conditions makes Starbon®-300 a good candidate. Ru –Starbon® and Pt–Starbon® catalysts exhibited the highest conversion since they were smaller and evenly dispersed. The selectivity was also significantly different: for Ru–Starbon®, 60-82% tetrahydrofuran (THF) was obtained while Pd, Pt and Rh–Starbon® materials were more selective to 1,4-butanediol (BDO). The reaction conditions could also be tuned to maximize γ-butyrolactone (GBL) production from Pd–Starbon® or Ru–Starbon® (up to 65% selectivity at 45% conversion—10 h reaction—using 5% Pd–Starbon®). Interestingly, the catalysts were found to preserve over 95% of their initial activity even after 5 reaction cycles.

One-step conversion of cellobiose to C6-alcohols was achieved by selectively breaking the C-O-C (glycosidic) bonds (Figure A.4) via hydrogenation using water-soluble transition metals (Ru, Rh, Pd or Pt) nanocluster catalysts under H_2 pressure in ionic liquid. Ru was the only metal that exhibited high stability under the conditions (120 °C and 40 bar of H_2) and gave high activity and selectivity, that is, the cellobiose was quantitatively converted to C6-alcohols. This concept creates new opportunity to transform cellulose into biofuels and other useful value-added chemicals.[40] A continuous process was designed in which two homogeneous phases coexisted with an emulsion in a layered configuration: oil/emulsion/water.[41]

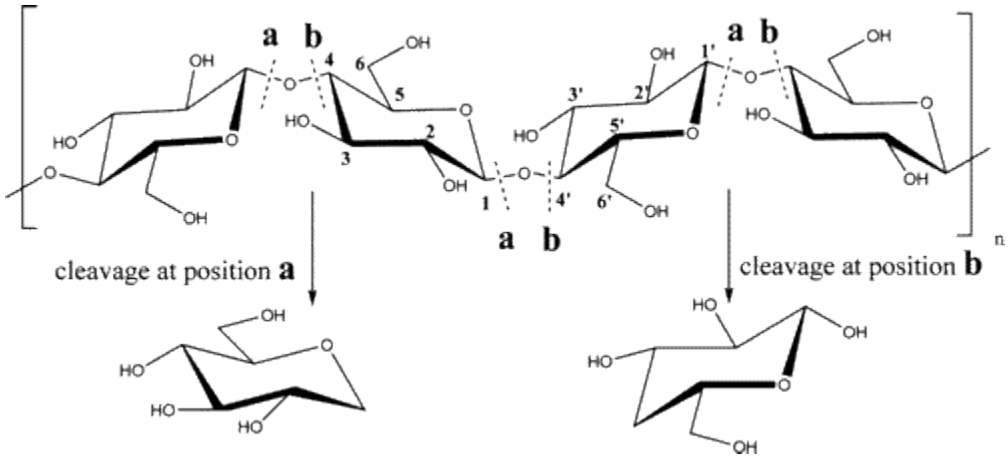

Figure A.4 Cellulose structure and the potential monomers formed following cleavage of the C−O−C bonds at position a or b[40]

(Yan et al., 2006; reproduced with permission of American Chemical Society)

Bearing in mind that carbon nanotubes, being hydrophobic, have been shown to produce emulsions, hybrid nanoparticles were prepared by fusing carbon nanotubes to silica. By tuning their composition, the hydrophilic-hydrophobic balance could be modified. These nanohybrids were studied by incorporating a transition metal, rendering them catalytically active for hydrogenation. The Pd particles still sit in the organic/aqueous interface and the emulsions formed are unaffected. Depositing a metal such as Pd on the hydrophilic face would catalyze aqueous reactions, whereas deposition on the hydrophobic face would favor chemistry in the organic solvent. Full conversion can therefore be achieved on both sides of the emulsion by constant removal of products formed from both the top and bottom layers since the reaction occurs in the emulsion phase.

One of the ways to upgrade biomass derived bio-oil is by hydrodeoxygenation (HDO) through the use of catalysts to remove oxygen (from the oxygenated compounds found in bio-oil) as CO, CO_2 or H_2O. In one study[42], a task-specific ionic liquid (3-methyl-1-butylpyridine dicyanamide) was used as a precursor with silica NPs as a hard template to yield a high-nitrogen-content (12 wt %) mesoporous carbon material. This material could stabilize Pd NPs and the resulting $Pd@CN_{0.132}$ catalyst exhibited a high activity for the hydrodeoxygenation of vanillin, a common component in lignin-derived bio-oil. The reaction conditions were mild with low hydrogen pressure and water as a clean solvent. 100% conversion of vanillin and 100% selectivity for 2-methoxy-4-methylphenol were achieved and the catalyst did not lose its activity after six recycles. The special structure of the catalytic N-doped carbon–metal heterojunction, lead to a very stable and uniform dispersion of Pd NPs and promoted additional electronic activation of the metal NPs as well as a good dispersion of the catalyst in water. The high catalytic performance of $Pd@CN_{0.132}$ reveals a promising potential for the biofuel upgrade process. Simultaneous condensation and hydrogenation of biomass-derived oxygenates in water/oil emulsions stabilized by amphiplilic nanohybrid catalysts was also investigated[43]. The emulsion system led to an enhancement in the mass transfer between phases due to a larger interfacial area. For instance, it was found that the aldol-condensation reaction of furfural and acetone is more effective in an emulsion system than in single aqueous phase. In addition, the presence of the two phases facilitated the separation of the products. Among the different basic oxides employed to grow carbon nanotubes (CNT) on their surface, the nanohybrids supported on MgO have shown to be the most effective for aldol-condensation. Active metals such as Pd or Pt were

incorporated onto the nanohybrids to facilitate the hydrogenation of the aldol-condensation products in the same emulsion system. Increasing the temperature led to the formation of fully deoxygenated long-chain alkanes (tridecane).

One group[44] examined the vapor-phase furfural decarbonylation/hydrogenation reaction network as a function of Pt nanoparticles with various particle sizes (1.5–7.1 nm size range) and shapes (rounded, cubes, octahedral). The Pd NPs were encapsulated in poly(vinylpyrrolidone) (PVP) and dispersed on MCF-17 mesoporous silica. The reaction conditions were ambient pressure in the 443–513 K range. Furfural decarbonylation and hydrogenation reactions yielded mainly furan and furfuryl alcohol (FFA), respectively. In both reactions, the structure of the catalysts brought about changes in product selectivities, turnover rates (TORs), and apparent activation energies (E_A's). Small particles were found to give predominantly furan as a product, via decarbonylation, while larger sized particles yielded both furan and furfuryl alcohol. Octahedral particles were observed to be selective to furfuryl alcohol, while cube shaped particles produced an equal amount of furan and furfuryl alcohol. The differences in selectivity have been attributed to the presence of two different catalytically active sites which change in ratio with NP size and shape.

A.6 Reforming of Biomass-Derived Compounds

Aqueous Phase Reforming (APR) can produce hydrogen and carbon monoxide (synthesis gas) from biomass derived molecules at a mild temperature of 220-320 °C in the liquid phase by utilizing a suitable nanocatalyst (e.g., Pt, Ru, Pt-Ru).[1] This one-pot reaction process can produce hydrogen and reduced sugars simultaneously.[45] For

example, APR was utilized to convert glycerol into 1,2-propanediol (1,2-PDO) using 5 wt.% Ru/Al_2O_3 mixed with 5 wt.% Pt/Al_2O_3 catalyst, without any added hydrogen. A glycerol conversion of 50.1% and a 1,2-PDO selectivity of 47.2% were obtained. When the same reaction was carried out with added hydrogen (41 bar), a lower selectivity to 1,2-PDO (31.9%) was obtained since the excess hydrogen promoted the transformation of CO and CO_2 to methane and other alkanes, adversely affecting the 1,2-PDO selectivity.[46] Aqueous phase reforming of polyol over supported Pt–Re bimetallic catalyst has been attempted and the activity of supported 3 wt% Pt–Re catalysts was found to be as follows: Al_2O_3 < SiO_2 < activated carbon < CMK-3(ordered mesoporous carbon). The reason why CMK-3 supported catalyst exhibited the highest catalytic activity for APR reaction (Figure A.7) is due to its easy accessibility to its metal catalytic active sites, easy escape of product gas and a high metal dispersion. It was observed that both the conversion of carbon to gas and hydrogen yield increased with both temperature and corresponding system pressure. Low weight hourly space velocity also favored hydrogen yield and conversion of carbon to gas without decreasing the selectivity of hydrogen and alkane.[47]

The effect of support properties on catalytic performance for APR of 5 wt% glycerol was studied by loading MgO, Al_2O_3, CeO_2, TiO_2 and SiO_2 catalysts on pre-synthesized Pt colloids on the support. By measuring the conversion of glycerol, rate of hydrogen production and composition of gaseous products, it was found that the overall catalytic activities decreased in the following order: $Pt/MgO > Pt/Al_2O_3 > Pt/CeO_2 > Pt/TiO_2 > Pt/SiO_2$.

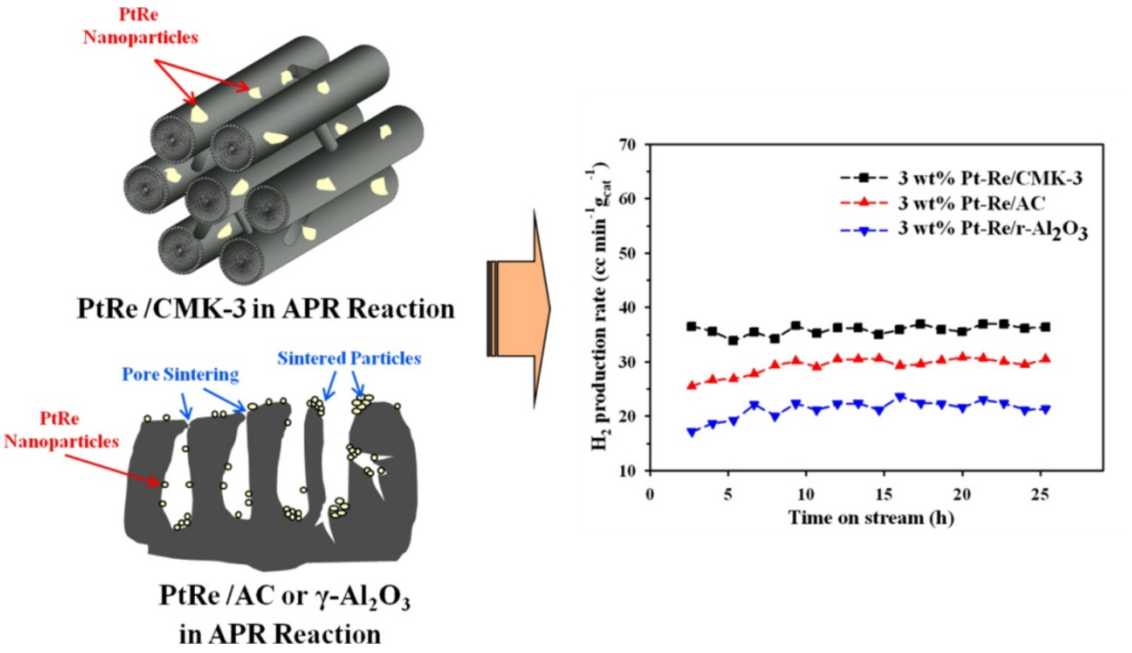

Figure A.5 Hydrogen production rates when using PtRe NPs on different supports[47]

(Kim et al., 2011; reproduced with permission of Elsevier BV)

WGS played a key role in the process of APR since both are related to the surface properties. It was postulated that WGS preferred the basic sites and further enhance the APR.[48] Recently, a carbon supported PtMo catalyst was used for the aqueous phase reforming of glycerol to produce hydrogen. Using X-ray absorption spectroscopy (XAS), it was found that the catalyst consisted of bimetallic nanoparticles with a Pt rich core and a Mo rich surface with approximately 25% of the surface atoms being Pt. The fresh PtMo NPs were about 2 nm and after 30 days of glycerol reforming at 31 bar and 230 °C, they increased in size to about 5 nm.[49] Other types of supported (CMK-3, commercial activated carbon (AC) and alumina) Pt-based bimetallic catalysts (Pt–Re, Pt–Mn, Pt–Fe, Pt–Cs, Pt–Ba, Pt–Ga, Pt–Ag, and Pt–Mo) were tested for hydrogen production via APR of ethylene glycol. The 1:1 Pt:Mn molar ratio significantly enhanced the catalytic

performances because of the interaction between the Pt and Mn species, leading to the Pt–Mn alloys supported on CMK-3. Out of all the supports, the CMK-3 support demonstrated better performance than the commercial AC and alumina. Therefore, it was concluded that the catalytic performance of the APR reaction over Pt–Mn/CMK-3 catalyst depended on the alloy effect as well as the structural properties and nature of the support.[50]

Recently, a new family of surface facet-controlled bimetallic Cu-based nanocatalysts supported on the graphene derivative has been synthesized.[51] Their unique surface configuration show exceptional activity and stability for aqueous phase biomass conversion. Using the graphene derivative as a 2-D template, the directed growth of dominant reactive surface facets of Cu nanocrystals (Cu{111}[43]) was achieved by lattice-match engineering. These Cu-graphene catalysts were used for converting biopolyols (glycerol, xylitol, and sorbitol) to value-added chemicals, such as lactic acid and other useful co-products consisting of diols and linear alcohols. Furthermore, trace amounts of Pd was incorporated to enhance activity and stability so that the hydrogen generated *in situ* from polyols is used for sequential hydrogenolysis of the feedstock. Figure A.6 illustrates how the addition of Pd enhances the stability whereby no significant leaching is found on the spent catalyst (A.6b) whereas Cu has obviously leached in the Cu/rGO catalyst in Figure A.6(a). Steam reforming of biomass-derived oxygenates like ethanol yield hydrogen which can be used as energy source for fuel cell applications. Steam reforming catalysts need to be active, stable and display high selectivity for H_2. One study[52] synthesized Co nanoparticles (~5 nm) on an inert support (graphitized activated carbon, g-AC).

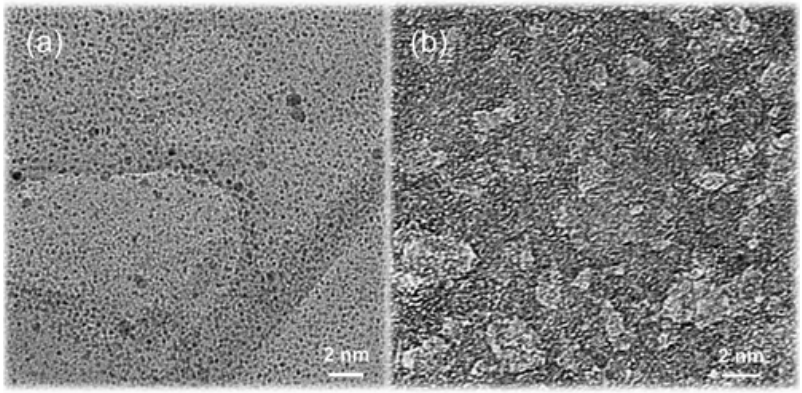

Figure A.6 TEM images of (a) spent Cu/reduced graphene oxide (rGO) (after first run) and (b) CuPd/rGO (after third recycle) catalysts[51]

(Jin et al., 2013; reproduced with permission of American Chemical Society)

Acetone was used as a model compound because it is the intermediate observed in ethanol and acetic acid steam reforming, has characteristic bonds found in biomass-derived oxygenates, and is a key component in butanol derived from fermentation. DFT calculations revealed that the Co nanoparticles served to cleave the C-C bond of acetone while efficiently dissociating H_2O to oxidize CH_x* and C*. The high selectivity of the supported Co NP to H_2 is attributed to facile scission of the C-H bond relative to that of the C-C bond of acetone. The exceptional stability of the catalyst is due to enhanced oxygen mobility by facile water dissociation on the Co nanoparticles and the lack of acid/base sites on the inert support. Therefore, acetone (either as a byproduct or as a reactant) can be selectively steam reformed to produce hydrogen without any catalyst deactivation issues. Fundamental understanding of the nature of nanoparticles is needed to provide further insight into the rational design of catalysts for upgrading of bio-oil.

A.7 Conclusions

Even though nanotechnology, as a new area of technology, still faces many challenges like reliability, safety, lifetime and costs, it has also demonstrated promising results in the field of sustainable energy applications, as pointed out by many examples in this review. The valorization of biomass is still very much an ongoing area of research due to the fact that it has the tremendous potential of being a source of fuel and value-added chemicals. The use of nanocatalysts can help in maximizing yields, minimizing residues, decreasing environmental impacts and obtaining products at low costs. The main challenges remain the complexity of the structure of lignocellulosic biomass. In gasification, for instance, the impurities cause tar formation while in pyrolysis, the bio-oil formed contains a lot of oxygenated compounds. The separation or purification of bio-oil therefore becomes complex. One solution would be to separate the biomass into fractions (hemicellulose, cellulose and lignin) in order to produce specialty chemicals and fuels at higher conversions and selectivities.[1] With the materials we have today, we are not able to provide the solutions at the efficiency and cost required but due to on-going research in nanotechnology around the world, novel materials are being developed using better material science and engineering expertise so that we can contribute to the well-being of the present and future generations.[53]

A.8 References

1. Alonso, D. M.; Wettstein, S. G.; Dumesic, J. A., Bimetallic catalysts for upgrading of biomass to fuels and chemicals. *Chemical Society Reviews* **2012,** *41* (24), 8075-8098.

2. Moniz, E. J.; Garcia-Martinez, J., *Nanotechnology for the energy challenge*. Wiley-VCH: 2010.

3. Mao, S. S.; Chen, X., Selected nanotechnologies for renewable energy applications. *International Journal of Energy Research* **2007,** *31* (6-7), 619-636.

4. Ramsurn, H.; Gupta, R. B., Production of Biocrude from Biomass by Acidic Subcritical Water Followed by Alkaline Supercritical Water Two-Step Liquefaction. *Energy & Fuels* **2012,** *26* (4), 2365-2375.

5. *U.S. Environmental Protection Agency, Renewable Fuel Standard (RFS)*; 2011.

6. *U.S. Department of Energy, Annual Energy Review 2011, report No. DOE/EIA-0384(2011)*; 2012.

7. Gupta, R. B.; Demirbas, A., *Gasoline, diesel and ethanol biofuels from grasses and plants*. Cambridge University Press: 2010.

8. Vertes, A. A.; Qureshi, N.; Blaschek, H. P.; Yukawa, H., *Biomass to Biofuels: Strategies for Global Industries*. 2010.

9. Cheng, S.; D'cruz, I.; Wang, M.; Leitch, M.; Xu, C., Highly Efficient Liquefaction of Woody Biomass in Hot-Compressed Alcohol-Water Co-solvents. *Energy & Fuels* **2010,** *24* (9), 4659-4667.

10. Pattarkine, M.; Pattarkine, V., Nanotechnology for Algal Biofuels. In *The Science of Algal Fuels*, Gordon, R.; Seckbach, J., Eds. Springer Netherlands: 2012; Vol. 25, pp 147-163.

11. (a) Li, C.; Yoshimoto, M.; Fukunaga, K.; Nakao, K., Characterization and immobilization of liposome-bound cellulase for hydrolysis of insoluble cellulose. *Bioresource technology* **2007,** *98* (7), 1366-1372; (b) Moxley, G.; Zhu, Z.; Zhang, Y.-H.

P., Efficient sugar release by the cellulose solvent-based lignocellulose fractionation technology and enzymatic cellulose hydrolysis. *Journal of agricultural and food chemistry* **2008,** *56* (17), 7885-7890.

12. Cruz, J. C.; Pfromm, P. H.; Tomich, J. M.; Rezac, M. E., Conformational changes and catalytic competency of hydrolases adsorbing on fumed silica nanoparticles: I. Tertiary structure. *Colloids and Surfaces B: Biointerfaces* **2010,** *79* (1), 97-104.

13. Wang, Y.; Hsieh, Y. L., Immobilization of lipase enzyme in polyvinyl alcohol (PVA) nanofibrous membranes. *Journal of Membrane Science* **2008,** *309* (1–2), 73-81.

14. Lin, V.; Mahoney, P.; Gibson, K. Nanofarming Technology Extracts Biofuel Oil without harming Algae. http://www.ameslab.gov/news/news-releases/nanofarming-technology-extracts-biofuel-oil-without-harming-algae.

15. Valenstein, J. S.; Kandel, K.; Melcher, F.; Slowing, I. I.; Lin, V. S. Y.; Trewyn, B. G., Functional Mesoporous Silica Nanoparticles for the Selective Sequestration of Free Fatty Acids from Microalgal Oil. *ACS Applied Materials & Interfaces* **2012,** *4* (2), 1003-1009.

16. Venkat Reddy, C. R.; Oshel, R.; Verkade, J. G., Room-temperature conversion of soybean oil and poultry fat to biodiesel catalyzed by nanocrystalline calcium oxides. *Energy & Fuels* **2006,** *20* (3), 1310-1314.

17. Montero, J.; Wilson, K.; Lee, A., Cs Promoted Triglyceride Transesterification Over MgO Nanocatalysts. *Topics in Catalysis* **2010,** *53* (11-12), 737-745.

18. Deng, X.; Fang, Z.; Liu, Y.-h.; Yu, C.-L., Production of biodiesel from Jatropha oil catalyzed by nanosized solid basic catalyst. *Energy* **2011,** *36* (2), 777-784.

19. Tang, S.; Wang, L.; Zhang, Y.; Li, S.; Tian, S.; Wang, B., Study on preparation of $Ca/Al/Fe_3O_4$ magnetic composite solid catalyst and its application in biodiesel transesterification. *Fuel Processing Technology* **2012,** *95*, 84-89.

20. Saunders, J. R.; Benfield, D.; Moussa, W.; Amirfazli, A., Nanotechnology's implications for select systems of renewable energy. *International Journal of Green Energy* **2007,** *4*, 483-503.

21. Abuadala, A.; Dincer, I.; Naterer, G. F., Exergy analysis of hydrogen production from biomass gasification. *International Journal of Hydrogen Energy* **2010,** *35* (10), 4981-4990.

22. Hao, X.; Guo, L.; Zhang, X.; Guan, Y., Hydrogen production from catalytic gasification of cellulose in supercritical water. *Chemical Engineering Journal* **2005,** *110* (1–3), 57-65.

23. Taylor, A. D.; DiLeo, G. J.; Sun, K., Hydrogen production and performance of nickel based catalysts synthesized using supercritical fluids for the gasification of biomass. *Applied Catalysis B: Environmental* **2009,** *93* (1–2), 126-133.

24. Lestari, S.; Mäki-Arvela, P.; Beltramini, J.; Lu, G.; Murzin, D. Y., Transforming triglycerides and fatty acids into biofuels. *Chemsuschem* **2009,** *2* (12), 1109-1119.

25. Richardson, Y.; Blin, J.; Volle, G.; Motuzas, J.; Julbe, A., In situ generation of Ni metal nanoparticles as catalyst for H_2-rich syngas production from biomass gasification. *Applied Catalysis A: General* **2010,** *382* (2), 220-230.

26. Devi, L.; Ptasinski, K. J.; Janssen, F. J. J. G., A review of the primary measures for tar elimination in biomass gasification processes. *Biomass and Bioenergy* **2003,** *24* (2), 125-140.

27. Han, J.; Kim, H., The reduction and control technology of tar during biomass gasification/pyrolysis: An overview. *Renewable and Sustainable Energy Reviews* **2008,** *12* (2), 397-416.

28. Li, J.; Yan, R.; Xiao, B.; Liang, D. T.; Du, L., Development of Nano-NiO/Al_2O_3 Catalyst to be Used for Tar Removal in Biomass Gasification. *Environmental Science & Technology* **2008,** *42* (16), 6224-6229.

29. Li, J.; Yan, R.; Xiao, B.; Liang, D. T.; Lee, D. H., Preparation of Nano-NiO Particles and Evaluation of Their Catalytic Activity in Pyrolyzing Biomass Components. *Energy & Fuels* **2007,** *22* (1), 16-23.

30. (a) De, S.; Dutta, S.; Patra, A. K.; Bhaumik, A.; Saha, B., Self-assembly of mesoporous TiO_2 nanospheres via aspartic acid templating pathway and its catalytic application for 5-hydroxymethyl-furfural synthesis. *Journal of Materials Chemistry* **2011,** *21* (43), 17505-17510; (b) Dutta, S.; De, S.; Patra, A. K.; Sasidharan, M.; Bhaumik, A.; Saha, B., Microwave assisted rapid conversion of carbohydrates into 5-hydroxymethylfurfural catalyzed by mesoporous TiO_2 nanoparticles. *Applied Catalysis A: General* **2011,** *409*, 133-139.

31. Dutta, S.; De, S.; Saha, B., A Brief Summary of the Synthesis of Polyester Building-Block Chemicals and Biofuels from 5-Hydroxymethylfurfural. *ChemPlusChem* **2012,** *77* (4), 259-272.

32. Manzer Leo, E., Biomass Derivatives: A Sustainable Source of Chemicals. In *Feedstocks for the Future,* American Chemical Society: 2006; Vol. 921, pp 40-51.

33. Taarning, E.; Nielsen, I. S.; Egeblad, K.; Madsen, R.; Christensen, C. H., Chemicals from renewables: aerobic oxidation of furfural and hydroxymethylfurfural over gold catalysts. *Chemsuschem* **2008,** *1* (1-2), 75-78.

34. Casanova, O.; Iborra, S.; Corma, A., Biomass into Chemicals: Aerobic Oxidation of 5-Hydroxymethyl-2-furfural into 2, 5-Furandicarboxylic Acid with Gold Nanoparticle Catalysts. *Chemsuschem* **2009,** *2* (12), 1138-1144.

35. Davis, S. E.; Houk, L. R.; Tamargo, E. C.; Datye, A. K.; Davis, R. J., Oxidation of 5-hydroxymethylfurfural over supported Pt, Pd and Au catalysts. *Catalysis Today* **2011,** *160* (1), 55-60.

36. Gupta, N. K.; Nishimura, S.; Takagaki, A.; Ebitani, K., Hydrotalcite-supported gold-nanoparticle-catalyzed highly efficient base-free aqueous oxidation of 5-hydroxymethylfurfural into 2,5-furandicarboxylic acid under atmospheric oxygen pressure. *Green Chemistry* **2011,** *13* (4), 824-827.

37. Pasini, T.; Piccinini, M.; Blosi, M.; Bonelli, R.; Albonetti, S.; Dimitratos, N.; Lopez-Sanchez, J. A.; Sankar, M.; He, Q.; Kiely, C. J., Selective oxidation of 5-hydroxymethyl-2-furfural using supported gold–copper nanoparticles. *Green Chemistry* **2011,** *13* (8), 2091-2099.

38. Garcia-Suarez, E. J.; Balu, A. M.; Tristany, M.; Garcia, A. B.; Philippot, K.; Luque, R., Versatile dual hydrogenation-oxidation nanocatalysts for the aqueous transformation of biomass-derived platform molecules. *Green Chemistry* **2012,** *14*, 1434-1439.

39. Clark, J. H.; Yoshida, K.; Gai, P. L., Efficient aqueous hydrogenation of biomass platform molecules using supported metal nanoparticles on Starbons®. *Chemical Communications* **2009,** (35), 5305-5307.

40. Yan, N.; Zhao, C.; Luo, C.; Dyson, P. J.; Liu, H.; Kou, Y., One-Step Conversion of Cellobiose to C_6-Alcohols Using a Ruthenium Nanocluster Catalyst. *Journal of the American Chemical Society* **2006,** *128* (27), 8714-8715.

41. Crossley, S.; Faria, J.; Shen, M.; Resasco, D. E., Solid Nanoparticles that Catalyze Biofuel Upgrade Reactions at the Water/Oil Interface. *Science* **2010,** *327* (5961), 68-72.

42. Xu, X.; Li, Y.; Gong, Y.; Zhang, P.; Li, H.; Wang, Y., Synthesis of Palladium Nanoparticles Supported on Mesoporous N-Doped Carbon and Their Catalytic Ability for Biofuel Upgrade. *Journal of the American Chemical Society* **2012,** *134* (41), 16987-16990.

43. Zapata, P. A.; Faria, J.; Ruiz, M. P.; Resasco, D. E., Condensation/Hydrogenation of Biomass-Derived Oxygenates in Water/Oil Emulsions Stabilized by Nanohybrid Catalysts. *Topics in Catalysis* **2012,** *55* (1-2), 38-52.

44. Pushkarev, V. V.; Musselwhite, N.; An, K.; Alayoglu, S.; Somorjai, G. A., High Structure Sensitivity of Vapor-Phase Furfural Decarbonylation/Hydrogenation Reaction Network as a Function of Size and Shape of Pt Nanoparticles. *Nano Letters* **2012,** *12* (10), 5196-5201.

45. Chang, A. C. C.; Louh, R. F.; Wong, D.; Tseng, J.; Lee, Y. S., Hydrogen production by aqueous-phase biomass reforming over carbon textile supported Pt–Ru bimetallic catalysts. *International Journal of Hydrogen Energy* **2011,** *36* (14), 8794-8799.

46. Roy, D.; Subramaniam, B.; Chaudhari, R. V., Aqueous phase hydrogenolysis of glycerol to 1,2-propanediol without external hydrogen addition. *Catalysis Today* **2010,** *156* (1–2), 31-37.

47. Kim, H.-D.; Park, H. J.; Kim, T.-W.; Jeong, K.-E.; Chae, H.-J.; Jeong, S.-Y.; Lee, C.-H.; Kim, C.-U., The effect of support and reaction conditions on aqueous phase reforming of polyol over supported Pt–Re bimetallic catalysts. *Catalysis Today* **2012,** *185* (1), 73-80.

48. Guo, Y.; Azmat, M. U.; Liu, X.; Wang, Y.; Lu, G., Effect of support's basic properties on hydrogen production in aqueous-phase reforming of glycerol and correlation between WGS and APR. *Applied Energy* **2012,** *92*, 218-223.

49. Dietrich, P.; Lobo-Lapidus, R.; Wu, T.; Sumer, A.; Akatay, M. C.; Fingland, B.; Guo, N.; Dumesic, J.; Marshall, C.; Stach, E.; Jellinek, J.; Delgass, W. N.; Ribeiro, F.; Miller, J., Aqueous Phase Glycerol Reforming by PtMo Bimetallic Nano-Particle Catalyst: Product Selectivity and Structural Characterization. *Topics in Catalysis* **2012,** *55* (1-2), 53-69.

50. Kim, H.-D.; Park, H. J.; Kim, T.-W.; Jeong, K.-E.; Chae, H.-J.; Jeong, S.-Y.; Lee, C.-H.; Kim, C.-U., Hydrogen production through the aqueous phase reforming of ethylene glycol over supported Pt-based bimetallic catalysts. *International Journal of Hydrogen Energy* **2012,** *37* (10), 8310-8317.

51. Jin, X.; Dang, L.; Lohrman, J.; Subramaniam, B.; Ren, S.; Chaudhari, R. V., Lattice-Matched Bimetallic CuPd-Graphene Nanocatalysts for Facile Conversion of Biomass-Derived Polyols to Chemicals. *ACS Nano* **2013**.

52. Sun, J.; Mei, D.; Karim, A. M.; Datye, A. K.; Wang, Y., Minimizing the Formation of Coke and Methane on Co Nanoparticles in Steam Reforming of Biomass-Derived Oxygenates. *ChemCatChem* **2013,** *5*.

53. Serrano, E.; Rus, G.; García-Martínez, J., Nanotechnology for sustainable energy. *Renewable and Sustainable Energy Reviews* **2009,** *13* (9), 2373-2384.

Appendix B

Peer-Reviewed Publications

1. **Ramsurn, H**.; Gupta, R. B., Deoxy-Liquefaction of Switchgrass in Supercritical Water with Calcium Formate as an *in-situ* Hydrogen Donor. *Submitted to Bioresource Technology, April 2013.*
2. **Ramsurn, H**.; Gupta, R. B., Nanotechnology in Solar and Bio fuels. *Invited paper. Submitted to a special issue of the ACS Sustainable Chemistry and Engineering Journal. February 2013.*
3. **Ramsurn, H**.; Gupta, R. B., Production of Biocrude from Biomass by Acidic Subcritical Water Followed by Alkaline Supercritical Water Two-Step Liquefaction. *Energy & Fuels* **2012**, *26* (4), 2365-2375.
4. **Ramsurn, H**.; Kumar, S.; Gupta, R. B., Enhancement of Biochar Gasification in Alkali Hydrothermal Medium by Passivation of Inorganic Components Using $Ca(OH)_2$. *Energy & Fuels* **2011,** *25* (5), 2389-2398.
5. Byrd, A. J.; Kumar, S.; Kong, L**.; Ramsurn, H.**; Gupta, R. B., Hydrogen production from catalytic gasification of switchgrass biocrude in supercritical water. *International Journal of Hydrogen Energy* **2011,** *36* (5), 3426-3433.

Book Chapter (in press)

Ramsurn Hema and Gupta Ram, Hydrogenation by Nanoparticles. A chapter in New and Future Developments in Catalysis. Catalysis by Nanoparticles, 1st edition, edited by Suib Steven.(Elsevier, 2013)

Appendix C

Conference Presentations and Posters

1. **Ramsurn, H**.; Kumar, S.; Gupta, R.B. *Supercritical-Water Gasification of Switchgrass biochar: Effect of K_2CO_3 catalysis and $Ca(OH)_2$ passivation.* (poster) AIChE National Meeting, Salt Lake City, UT, United States, 2010
2. **Ramsurn, H**.; Kumar, S.; Gupta, R.B. *Enhancement of Biochar Gasification in Alkali Hydrothermal Medium by Passivation of Inorganic Components Using $Ca(OH)_2$*. Graduate School Council Symposium, Auburn University, April 2011
3. **Ramsurn, H**.; Gupta, R.B. *Production of Biocrude from Biomass by Acidic Subcritical Water Followed by Alkaline Supercritical Water Two-Step Liquefaction.* Research Week, Auburn University, April 2012
4. **Ramsurn, H.;** Gupta, R.B. *Two-Step Biomass Hydrothermal Liquefaction Process through Acidic Subcritical- followed by Alkaline Supercritical-Water Treatment.* 10th International Symposium on Supercritical Fluids, San Francisco, CA, United States, May 2012.
5. **Ramsurn, H**.; Gupta, R.B. *Two-Step Biomass Hydrothermal Liquefaction Process through Acidic Subcritical- followed by Alkaline Supercritical-Water Treatment.(*poster) Lignocellulosic Biofuels Workshop, Auburn, AL, United States, June 2012.

6. **Ramsurn, H**. *Efficient Conversion of Biomass to Petroleum-Compatible Biocrude, Syngas and Char.* (poster) AIChE Annual Meeting, Pittsburg, PA, United States, October 2012.
7. **Ramsurn, H**.; Gupta, R.B. *A Two-Step Biomass Hydrothermal Liquefaction Process: (i) Acidic Subcritical, followed by (ii) Alkaline Supercritical-Water Treatment.* AIChE Annual Meeting, Pittsburg, PA, United States, October 2012.
8. **Ramsurn, H**.; Gupta, R.B. *Nanotechnology in Sustainable Energy.* First Sustainable Nanotechnology Organization Conference, Arlington VA, United States, November 2012.
9. Román, A.; **Ramsurn, H**.; Gupta, R.B.; Mosjidis, J. *Subcritical Water Extraction of Proteins from Sunn Hemp*. (poster- third prize) 2012 SHPE Conference, Fort Worth, TX, United States, November 2012